

## A DDFV METHOD FOR A CAHN–HILLIARD/STOKES PHASE FIELD MODEL WITH DYNAMIC BOUNDARY CONDITIONS

FRANCK BOYER<sup>1</sup> AND FLORE NABET<sup>2,3</sup>

**Abstract.** In this paper we propose a “Discrete Duality Finite Volume” method (DDFV for short) for the diffuse interface modelling of incompressible two-phase flows. This numerical method is, conservative, robust and is able to handle general geometries and meshes. The model we study couples the Cahn–Hilliard equation and the unsteady Stokes equation and is endowed with particular nonlinear boundary conditions called dynamic boundary conditions. To implement the scheme for this model we have to derive new discrete consistent DDFV operators that allows an energy stable coupling between both discrete equations. We are thus able to obtain the existence of a family of solutions satisfying a suitable energy inequality, even in the case where a first order time-splitting method between the two subsystems is used. We illustrate various properties of such a model with some numerical results.

**Mathematics Subject Classification.** 35K55, 65M08, 65M12, 76D07, 76M12, 76T10.

Received December 31, 2015. Revised August 3, 2016. Accepted November 12, 2016.

### 1. INTRODUCTION

The aim of this paper is to derive and analyse a finite volume scheme for a phase-field model of two-phase incompressible flows with surface tension effects and contact-line dynamics on the walls. We propose a numerical method that falls into the Discrete Duality Finite Volume framework (DDFV for short); this choice is guided by the capability of the method to deal with very general meshes (distorted, non conforming, locally refined, ...) while ensuring good robustness, stability and accuracy properties.

#### 1.1. Presentation of the phase-field model and related discretization issues

The diffuse interface two-phase flow model under study couples the Cahn–Hilliard and the Stokes (or Navier–Stokes) equations. The main feature of such a model is to allow the presence of diffuse interfaces of prescribed width  $\varepsilon$  in the system while being able to describe surface tension effects in the hydrodynamics,

---

*Keywords and phrases.* Cahn–Hilliard/Stokes model, dynamic boundary conditions, contact angle dynamics, finite volume method.

<sup>1</sup> Université Toulouse 3 – Paul Sabatier, CNRS, Institut de Mathématiques de Toulouse, UMR 5129, 31062 Toulouse, France. [franck.boyer@math.univ-toulouse.fr](mailto:franck.boyer@math.univ-toulouse.fr)

<sup>2</sup> CMAP, Ecole polytechnique, CNRS, Université Paris-Saclay, 91128, Palaiseau, France. [flore.nabet@polytechnique.edu](mailto:flore.nabet@polytechnique.edu)

<sup>3</sup> Team RAPSODI, Inria Lille – Nord Europe, 40 av. Halley, 59650 Villeneuve d’Ascq, France

through a suitable capillary force term in the momentum equation. The main unknown of this equation, the order parameter  $c$ , is a smooth function which is equal to 1 in one of the two phases, 0 in the other one and which varies continuously between 0 and 1 across the interface.

Here, wall effects are modelled through a nonlinear dynamic boundary condition for the order parameter. Usually this kind of model is studied with the homogeneous Neumann boundary condition on the order parameter (see for example [1–3, 7, 10, 25, 27, 31] and the references therein), which implies that the contact angle between the diphasic interface and the wall is imposed to be equal to the static contact angle  $\frac{\pi}{2}$ . However for some physical systems, this condition may not be realistic for at least two reasons:

- the static contact angle may be different from  $\pi/2$  due to wetting effects depending on the nature of the two fluids and the material of the container,
- the influence of the hydrodynamics on the system near the wall implies that the dynamic contact angle is not equal to the static contact angle; a time relaxation phenomenon may occur at the contact line.

In order to take into account the contact angle dynamics, it is proposed in [26] to use a dynamic boundary condition for the order parameter (see also [40]). To our knowledge, there is only few available contributions concerning the discretization of the Cahn–Hilliard/Navier–Stokes phase field model with dynamic boundary conditions. From a computational point of view, some recent works propose numerical schemes for such kind of models and give various simulations (see [12, 16, 17, 32, 43, 44] and the references therein), but without precise mathematical analysis. We also mention [42] which is concerned with a slightly different model but gives a thorough stability analysis for a conforming finite element discretization.

We would like here to develop a finite volume strategy in order to compute approximate solutions of our model. The main motivation for that is twofold:

- First, those methods are naturally conservative and flux consistent, which is an important feature due to the normal derivative term in the boundary condition (1.1g).
- Second, those methods are, by construction, able to deal with much more general grids than usual conforming triangulations.

Here, in the DDFV framework, we are particularly concerned with the difficulties that are induced by the nonlinear boundary terms and by the coupling terms. Those issues are the price to pay for the fact that the numerical method is, by nature, applicable on very general families of meshes as mentioned above. We will describe in details how to build all the coupling terms combined with a time splitting scheme for this model for which we can show nonlinear stability estimates.

Since they are not our main concern here, we have chosen to neglect the issues related to the nonlinear inertia term in the Navier–Stokes equations (those difficulties can be treated as in [22] for instance), thus the system we will eventually study is the coupling between the Cahn–Hilliard equation and the unsteady Stokes problem with dynamic boundary conditions, in the context of the Boussinesq approximation for the buoyancy term. Finally, for simplicity, we concentrate on the 2D case but we emphasise that 3D versions of the DDFV schemes are available and were analysed for instance in [4, 30].

## 1.2. The Cahn–Hilliard/Stokes system with dynamic boundary condition

### 1.2.1. Presentation of the system of equations

Let  $\Omega \subset \mathbb{R}^2$  be a connected and bounded polygonal domain. For a given final time  $T > 0$  the problem we are interested in is the following: To find the order parameter  $c : (0, T) \times \Omega \rightarrow \mathbb{R}$ , the generalised chemical potential

$\mu : (0, T) \times \Omega \rightarrow \mathbb{R}$ , the velocity  $\mathbf{u} : (0, T) \times \Omega \rightarrow \mathbb{R}^2$  and the pressure  $p : (0, T) \times \Omega \rightarrow \mathbb{R}$  satisfying

$$\begin{cases} \partial_t c + \mathbf{u} \cdot \nabla c = \Gamma_b \Delta \mu, & \text{in } (0, T) \times \Omega; & (1.1a) \\ \mu = -\frac{3}{2} \varepsilon \sigma_b \Delta c + \frac{12}{\varepsilon} \sigma_b f'_b(c), & \text{in } (0, T) \times \Omega; & (1.1b) \\ \rho^* \left( \partial_t \mathbf{u} - \frac{1}{\mathcal{R}_e} \Delta \mathbf{u} \right) + \nabla p = \mu \nabla c + \rho(c) \mathbf{g}, & \text{in } (0, T) \times \Omega; & (1.1c) \\ \operatorname{div} \mathbf{u} = 0, & \text{in } (0, T) \times \Omega; & (1.1d) \\ \mathbf{u} = \mathbf{u}_b, & \text{on } (0, T) \times \Gamma; & (1.1e) \\ \partial_n \mu = 0, & \text{on } (0, T) \times \Gamma; & (1.1f) \\ \frac{3}{2} \varepsilon \sigma_b D_s \partial_t c_{|\Gamma} = -f'_s(c_{|\Gamma}) - \frac{3}{2} \varepsilon \sigma_b \partial_n c, & \text{on } (0, T) \times \Gamma; & (1.1g) \end{cases}$$

where  $c_{|\Gamma}$  is the trace of  $c$  on  $\Gamma = \partial\Omega$ , as well as suitable initial data for  $c$  and  $\mathbf{u}$ . We assume that the boundary velocity data satisfies

$$\mathbf{u}_b \in (H^{1/2}(\Gamma))^2, \text{ is time-independent and satisfies } \mathbf{u}_b \cdot \vec{\mathbf{n}} = 0, \text{ on } \Gamma. \quad (1.2)$$

Several physical parameters appear in the model:

- In the Cahn–Hilliard equation,  $\varepsilon > 0$  stands for the interface thickness (see Fig. 1b),  $\sigma_b > 0$  is the binary surface tension between the two components and  $\Gamma_b > 0$  is a diffusion coefficient called the mobility. Moreover, in the dynamic boundary condition,  $D_s > 0$  is a relaxation coefficient.
- In the Stokes problem,  $\mathcal{R}_e > 0$  is the Reynolds number,  $\rho^*$  the reference density (the one of the heavier fluid),  $c \mapsto \rho(c)$  represents the density variations of the mixture (in practice it is chosen as a regularised heaviside step function such that  $\max \rho = \rho^*$ ), and  $\mathbf{g}$  the gravity vector.

In order to simplify the presentation, in Sections 2, 3 and 4 of the paper all the coefficients in the equations will be taken equal to one. The functions  $f_b$  and  $f_s$  are nonlinear functions called respectively bulk and surface Cahn–Hilliard potential that satisfy the following dissipativity assumption

$$\liminf_{|c| \rightarrow \infty} f'_b(c) > 0, \quad (1.3)$$

as well as the following polynomial growth condition

$$|f'_b(c)| + |f'_s(c)| \leq C(1 + |c|^p), \quad \forall c \in \mathbb{R}, \quad (1.4)$$

for some  $C > 0$  and  $p \in [1, +\infty[$ . We additionally assume that there exists  $\alpha_1 > 0$  such that

$$f_b(c) \geq \alpha_1 c^2 \quad \text{and} \quad f_s(c) \geq 0, \quad \forall c \in \mathbb{R}. \quad (1.5)$$

Since adding constants to  $f_b$  and  $f_s$  does not change the equations, the first assumption above is actually a consequence of (1.3) whereas the second one is equivalent to say that  $f_s$  is bounded from below.

A typical choice for the bulk Cahn–Hilliard potential is the double-well function  $f_b(c) = c^2(1 - c)^2$  (see Fig. 1a).

Let us recall that the dynamic boundary condition has been initially introduced in [26] to describe the contact-line dynamics. For this purpose, we define the total Cahn–Hilliard energy as the sum of the bulk free energy,

$$\mathcal{F}_b(c) := \int_{\Omega} \left( \frac{3}{4} \varepsilon \sigma_b |\nabla c|^2 + \frac{12}{\varepsilon} \sigma_b f_b(c) \right), \quad (1.6)$$

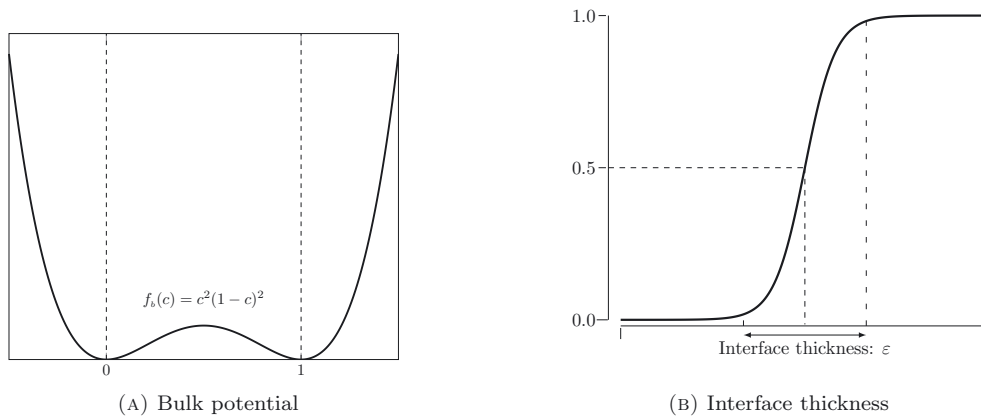


FIGURE 1. Double-well structure of  $f_b$  and definition of the interface thickness.

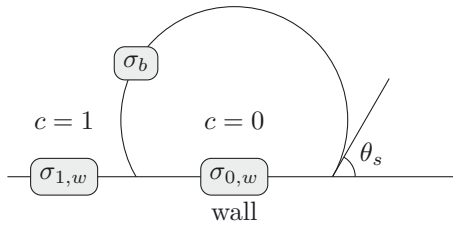


FIGURE 2. Definition of the contact angle  $\theta_s$ , case  $\sigma_{0,w} > \sigma_{1,w}$ .

and a surface free energy  $\mathcal{F}_s$  defined as follows,

$$\mathcal{F}_s(c) := \int_{\Gamma} f_s(c_{\Gamma}) \tag{1.7}$$

with

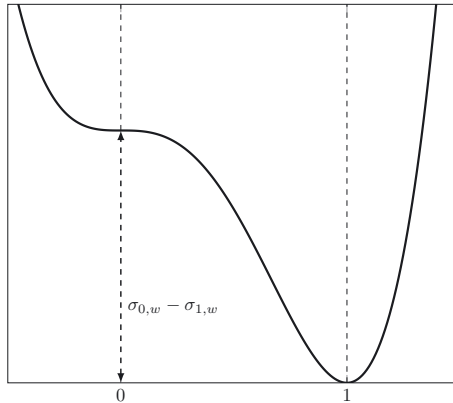
$$f_s(c_{\Gamma}) := \begin{cases} (\sigma_{0,w} - \sigma_{1,w})c_{\Gamma}^3(3c_{\Gamma} - 4) + \sigma_{0,w} & \text{if } \sigma_{0,w} \geq \sigma_{1,w}, \\ (\sigma_{0,w} - \sigma_{1,w})(3c_{\Gamma} + 1)(1 - c_{\Gamma})^3 + \sigma_{1,w} & \text{if } \sigma_{1,w} \geq \sigma_{0,w}, \end{cases} \tag{1.8}$$

where  $\sigma_{1,w}$  is the surface tension between the phase  $c = 1$  and the wall,  $\sigma_{0,w}$  is the surface tension between the phase  $c = 0$  and the wall. We say that the phase  $c = 1$  is wetting if  $\sigma_{1,w} < \sigma_{0,w}$ . Those formulas (see Fig. 3) are chosen in a such a way that  $c = 0$  and  $c = 1$  are critical points of  $f_s$  with  $f_s(1) = \sigma_{1,w}$  and  $f_s(0) = \sigma_{0,w}$  and such that the condition (1.5) is fulfilled.

Following Young’s law, the static contact-angle  $\theta_s$  (see Fig. 2) associated with those surface tension parameters is given by the relation

$$\cos(\theta_s) = \frac{\sigma_{0,w} - \sigma_{1,w}}{\sigma_b}.$$

Observe that this choice of surface potential is not exactly the same as the one in [12, 16, 17, 26, 43, 44] where a cubic surface potential is considered (and thus assumption (1.5) is not satisfied). As explained above, our construction retains the main qualitative properties required for  $f_s$  so that it gives satisfactory numerical results (see Sect. 5) while allowing a complete mathematical analysis, which is not the case for a cubic surface potential.

FIGURE 3. Degenerate double-well structure of  $f_s$ .

### 1.2.2. Formal energy estimate

The previous system is built upon thermodynamical consistency assumptions that ensure that we have dissipation of the total energy (at least without source terms). This is a fundamental property from a mathematical analysis point of view as well as for ensuring stability of related numerical schemes.

Let us describe here the formal computations that lead to this estimate. One of the main achievements of this work will be to be able to satisfy such an estimate at the discrete level.

- We multiply equation (1.1a) by  $\mu$  and we integrate over  $\Omega$ . Since  $\partial_n \mu = 0$  on  $\Gamma$  the Stokes formula gives,

$$\int_{\Omega} (\mu \partial_t c + \mathbf{u} \cdot (\mu \nabla c) + \Gamma_b |\nabla \mu|^2) = 0.$$

- We multiply equation (1.1b) by  $\partial_t c$  and we integrate over  $\Omega$  we have,

$$\int_{\Omega} \mu \partial_t c = \int_{\Omega} \partial_t \left( \frac{3}{4} \varepsilon \sigma_b |\nabla c|^2 + \frac{12}{\varepsilon} \sigma_b f_b(c) \right) - \frac{3}{2} \varepsilon \sigma_b \int_{\Gamma} \partial_t c \partial_n c.$$

- For standard Neumann boundary conditions on  $c$ , the boundary term  $\int_{\Gamma} \partial_t c \partial_n c$  just cancels whereas, in our case, the term contributes to the energy balance. Indeed, by multiplying (1.1g) by  $\partial_t c|_{\Gamma}$  and integrating on  $\Gamma$  we get

$$\frac{d}{dt} \int_{\Gamma} f_s(c|_{\Gamma}) + \frac{3}{2} \varepsilon \sigma_b D_s \int_{\Gamma} |\partial_t c|_{\Gamma}|^2 + \frac{3}{2} \varepsilon \sigma_b \int_{\Gamma} \partial_t c \partial_n c = 0.$$

- Let  $(\mathbf{w}, p_0) \in (H^1(\Omega))^2 \times L_0^2(\Omega)$  be a solution to the Stokes problem:

$$\begin{cases} -\frac{\rho^*}{\mathcal{R}_e} \Delta \mathbf{w} + \nabla p_0 = 0, & \text{in } \Omega; \\ \operatorname{div} \mathbf{w} = 0, & \text{in } \Omega; \\ \mathbf{w} = \mathbf{u}_b, & \text{on } \Gamma. \end{cases}$$

There exists  $C_1 > 0$  such that  $\|\mathbf{w}\|_{H^1(\Omega)} \leq C_1 \|\mathbf{u}_b\|_{H^{1/2}(\Gamma)}$ .

Then, we multiply equation (1.1c) by  $\mathbf{u} - \mathbf{w}$  and we integrate over  $\Omega$ . Since  $\operatorname{div} \mathbf{u} = \operatorname{div} \mathbf{w} = 0$  in  $\Omega$  and  $\mathbf{u} - \mathbf{w} = 0$  on  $\Gamma$  we get,

$$\int_{\Omega} (\mu \nabla c) \cdot (\mathbf{u} - \mathbf{w}) = \int_{\Omega} \left( \frac{\rho^*}{2} \partial_t |\mathbf{u} - \mathbf{w}|^2 + \frac{\rho^*}{\mathcal{R}_e} |\nabla(\mathbf{u} - \mathbf{w})|^2 \right) - \int_{\Omega} \rho(c) \mathbf{g} \cdot (\mathbf{u} - \mathbf{w}).$$

- Summing the previous four identities, and using that the convective term and the capillary term cancel each other

$$\int_{\Omega} \mathbf{u} \cdot (\mu \nabla c) = \int_{\Omega} \mu (\mathbf{u} \cdot \nabla c), \quad (1.9)$$

we finally obtain

$$\begin{aligned} \frac{d}{dt} \int_{\Omega} \left( \mathcal{F}_b(c) + \mathcal{F}_s(c) + \frac{\rho^*}{2} |\mathbf{u} - \mathbf{w}|^2 \right) &= -\Gamma_b \int_{\Omega} |\nabla \mu|^2 - \frac{\rho^*}{\mathcal{R}_e} \int_{\Omega} |\nabla(\mathbf{u} - \mathbf{w})|^2 \\ &\quad - \frac{3}{2} \varepsilon \sigma_b D_s \int_{\Gamma} |\partial_t c_{1\Gamma}|^2 - \int_{\Omega} (\mu \nabla c) \cdot \mathbf{w} + \int_{\Omega} \rho(c) \mathbf{g} \cdot (\mathbf{u} - \mathbf{w}). \end{aligned}$$

To conclude to the stability estimate, we have to deal with the term due to the lifting  $\mathbf{w}$  of the non-homogeneous Dirichlet boundary condition  $\mathbf{u}_b$  by writing

$$\left| \int_{\Omega} (\mu \nabla c) \cdot \mathbf{w} \right| \leq \frac{\Gamma_b}{2} \|\nabla \mu\|_{L^2(\Omega)}^2 + C \|\mathbf{u}_b\|_{H^{1/2}(\Gamma)}^2 \|\nabla c\|_{L^2(\Omega)}^2.$$

The claim follows by Gronwall's lemma and (1.5).

### 1.3. Outline and main contributions

Since this paper is devoted to the construction and analysis of a DDFV scheme for the previous system we shall begin in Section 2 by a presentation of the DDFV framework we will use along the paper: the main notation and assumptions on the meshes, the associated discrete operators and the available functional inequalities used in this work.

In Section 3, we present the DDFV discretizations chosen for the main two ingredients in (1.1) that is, the one for the (un-)steady Stokes problem with non-homogeneous Dirichlet boundary condition (Sect. 3.1 and Appendix A) and the one for the Cahn–Hilliard equation with dynamic boundary condition (Sect. 3.2).

Section 4, which is the main part of this work, is dedicated to the analysis of the DDFV discretization for the complete problem. As explained in Section 1.2.2, it is crucial to propose a discretization of the coupling terms that ensures that the dissipation of the discrete total energy estimate will hold. Therefore, the first step to obtain a suitable DDFV scheme for the Cahn–Hilliard/Stokes phase field problem, is to define DDFV operators that discretize these terms (see Sect. 4.1) and for which, at least in a weak sense, the suitable cancellation properties hold. We will show how to deal with this problem when considering a standard fully-coupled time-stepping discretization.

However, from a computational point of view it can be demanding to solve a complete steady Cahn–Hilliard/Stokes problem at each time step since we have a very strong coupling between the two sets of equations. Additionally, even if it is not considered in this paper, it could be useful to use an incremental projection method (or any of its variant) for solving the Stokes part of the system and therefore we need a more flexible time stepping method.

That's the reason why we choose to present an alternative time splitting approach to discretize the complete problem. The price to pay is that, even if we build discrete operators which satisfy a discrete form of (1.9), we cannot directly prove dissipation of the energy because of the splitting error of the time discretization. Some additional work is thus needed and is presented in Section 4.2 where we prove existence and stability properties for the solution of the fully discretized problem under some weak condition on the time step.

We conclude by presenting in Section 5 some numerical results that illustrate the good behaviour of the numerical method and the influence of the dynamic nonlinear boundary condition on the global behaviour of some typical diphasic flows.

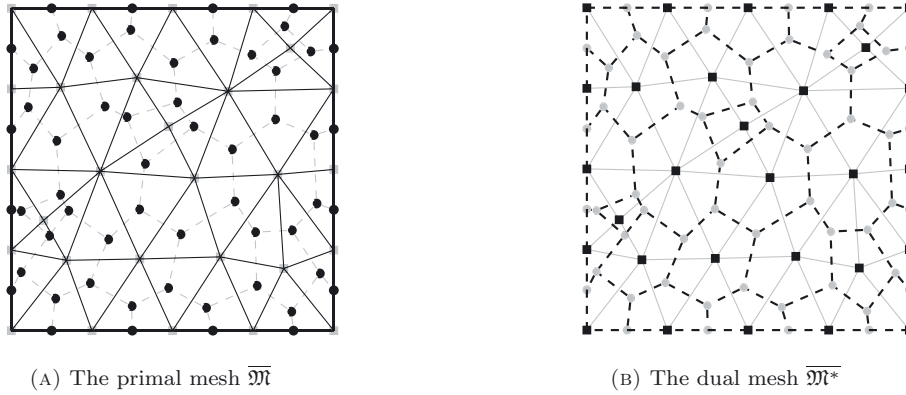


FIGURE 4. A DDFV mesh  $\mathcal{T}$  made of conforming triangles.

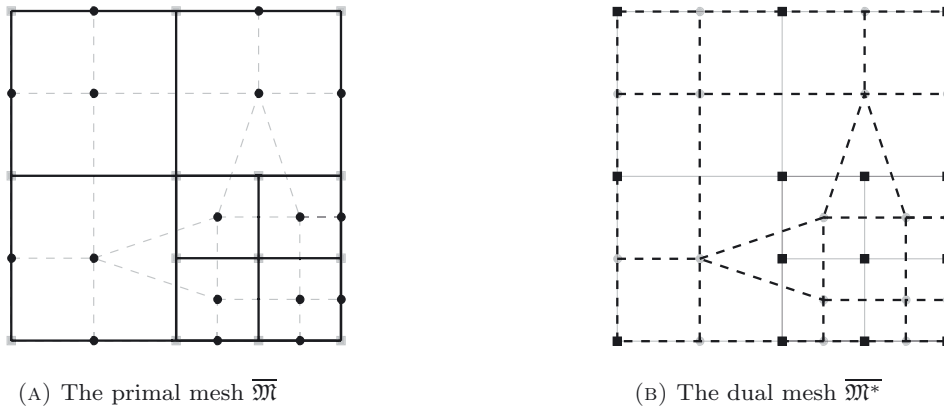


FIGURE 5. A DDFV mesh  $\mathcal{T}$  made of non-conforming quadrangles.

## 2. DDFV FRAMEWORK

### 2.1. The DDFV meshes and notations

We recall here the main notations and definitions taken from [5]. A DDFV mesh  $\mathcal{T}$  is constituted by a primal mesh  $\overline{\mathfrak{M}}$  and a dual mesh  $\overline{\mathfrak{M}^*}$ . We denote by  $\partial\mathcal{T}$  the boundary mesh  $\partial\mathfrak{M} \cup \partial\mathfrak{M}^*$  (see Figs. 4 and 5 for examples of conforming or non conforming meshes).

The (interior) primal mesh  $\mathfrak{M}$  is a set of disjoint open polygonal control volumes  $\kappa \subset \Omega$  such that  $\cup \overline{\kappa} = \overline{\Omega}$ . We denote by  $\partial\mathfrak{M}$  the set of edges of the control volumes in  $\mathfrak{M}$  included in  $\Gamma$ , which we consider as degenerate control volumes.

- To each control volume  $\kappa \in \mathfrak{M}$ , we associate a point  $x_\kappa$ . Even though many choices are possible, in this paper, we always assume  $x_\kappa$  to be the mass center of  $\kappa$ .
- To each degenerate control volume  $\mathcal{L} \in \partial\mathfrak{M}$ , we associate the point  $x_\mathcal{L}$  that we choose here equal to the midpoint of the control volume  $\mathcal{L}$ .

At any vertex of the primal control volume in  $\mathfrak{M}$ , denoted by  $x_{\kappa^*}$ , we associate the dual control volume  $\kappa^* \in \overline{\mathfrak{M}^*}$  which is defined as the polygon obtained by joining all the centers of the surrounding primal control volumes. We define  $\mathfrak{M}^*$  (resp.  $\partial\mathfrak{M}^*$ ) as the set of all the dual control volume such that  $x_{\kappa^*} \notin \Gamma$  (resp.  $x_{\kappa^*} \in \Gamma$ ).

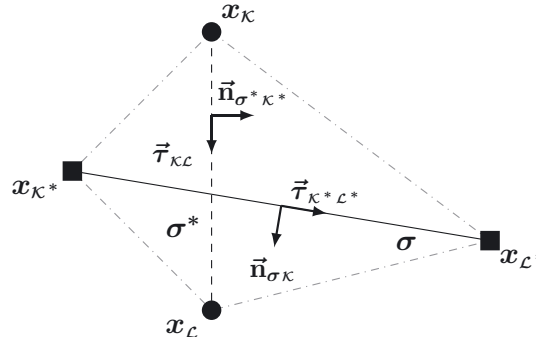


FIGURE 6. Notations in a diamond cell  $\mathcal{D}$ .

We also assume, even though it is not strictly necessary, that any  $\kappa \in \mathfrak{M}$  (resp.  $\kappa^* \in \overline{\mathfrak{M}^*}$ ) is star-shaped with respect to  $x_\kappa$  (resp.  $x_{\kappa^*}$ ).

For all control volumes  $\kappa$  and  $\mathcal{L}$ , we assume that  $\partial\kappa \cap \partial\mathcal{L}$  is either empty or a common vertex or an edge of the primal mesh denoted by  $\sigma = \kappa|\mathcal{L}$ . We note by  $\mathcal{E}$  the set of such edges. We also note  $\sigma^* = \kappa^*|\mathcal{L}^*$  and  $\mathcal{E}^*$  for the corresponding dual definitions.

Given the primal and dual control volumes, we define the diamond cells  $\mathcal{D}_\sigma$  being the quadrangles whose diagonals are a primal edge  $\sigma = \kappa|\mathcal{L} = (x_{\kappa^*}, x_{\mathcal{L}^*})$  and a corresponding dual edge  $\sigma^* = \kappa^*|\mathcal{L}^* = (x_\kappa, x_\mathcal{L})$ , (see Fig. 6). Note that the diamond cells are not necessarily convex. If  $\sigma \in \mathcal{E} \cap \partial\overline{\Omega}$ , the quadrangle  $\mathcal{D}_\sigma$  degenerate into a triangle. The set of the diamond cells is denoted by  $\mathfrak{D}$  and we have  $\overline{\Omega} = \bigcup_{\mathcal{D} \in \mathfrak{D}} \overline{\mathcal{D}}$ .

For any primal control volume  $\kappa \in \overline{\mathfrak{M}}$ , we note:

- $m_\kappa$  its Lebesgue measure,
- $\mathcal{E}_\kappa$  the set of its edges (if  $\kappa \in \mathfrak{M}$ ), or the one-element set  $\{\kappa\}$  if  $\kappa \in \partial\mathfrak{M}$ .
- $\mathfrak{D}_\kappa = \{\mathcal{D}_\sigma \in \mathfrak{D}, \sigma \in \mathcal{E}_\kappa\}$ ,

We will also use corresponding dual notations:  $m_{\kappa^*}$ ,  $\mathcal{E}_{\kappa^*}$  and  $\mathfrak{D}_{\kappa^*}$ .

For any  $\kappa^* \in \partial\mathfrak{M}^*$  we introduce the edge  $\sigma_{\Gamma}^{\kappa^*} = \partial\kappa^* \cap \Gamma$  and we denote  $m_{\sigma_{\Gamma}^{\kappa^*}}$  its length.

For a diamond cell  $\mathcal{D}$  whose vertices are  $(x_\kappa, x_{\kappa^*}, x_\mathcal{L}, x_{\mathcal{L}^*})$  (see Fig 6), we note

- $m_\sigma$  (resp.  $m_{\sigma^*}$ ) the length of the primal edge  $\sigma = [x_{\kappa^*}, x_{\mathcal{L}^*}]$  (resp. the dual edge  $\sigma^* = [x_\kappa, x_\mathcal{L}]$ ),
- $\vec{n}_{\sigma\kappa}$  the unit vector normal to  $\sigma$  going from  $x_\kappa$  to  $x_\mathcal{L}$ ,
- $\vec{n}_{\sigma^*\kappa^*}$  the unit vector normal to  $\sigma^*$  going from  $x_{\kappa^*}$  to  $x_{\mathcal{L}^*}$ ,
- $\vec{\tau}_{\kappa\mathcal{L}}$  the unit tangent vector to  $\sigma^*$  oriented from  $x_\kappa$  to  $x_\mathcal{L}$ ,
- $\vec{\tau}_{\kappa^*\mathcal{L}^*}$  the unit tangent vector to  $\sigma$  oriented from  $x_{\kappa^*}$  to  $x_{\mathcal{L}^*}$ ,
- $m_{\mathcal{D}}$  the Lebesgue measure of  $\mathcal{D}$ .

Let us note that the following relations hold:

$$\vec{n}_{\kappa\mathcal{L}} \cdot \vec{\tau}_{\kappa\mathcal{L}} = \vec{n}_{\kappa^*\mathcal{L}^*} \cdot \vec{\tau}_{\kappa^*\mathcal{L}^*} = \frac{2m_{\mathcal{D}}}{m_\sigma m_{\sigma^*}} \quad \text{and} \quad \vec{n}_{\kappa\mathcal{L}} \cdot \vec{\tau}_{\kappa^*\mathcal{L}^*} = \vec{n}_{\kappa^*\mathcal{L}^*} \cdot \vec{\tau}_{\kappa\mathcal{L}} = 0. \tag{2.1}$$

We define the set of boundary diamond cells  $\mathfrak{D}_{\text{ext}}$  as the set of diamond cells which possess one side included in  $\partial\Omega$ ; the set of interior diamond cells is thus  $\mathfrak{D}_{\text{int}} = \mathfrak{D} \setminus \mathfrak{D}_{\text{ext}}$ .

Let  $\text{size}(\mathcal{T})$  be the maximum of the diameters of the diamond cells in  $\mathfrak{D}$ . We introduce a positive number  $\text{reg}(\mathcal{T})$  that measures the regularity of a given mesh and is useful to perform the convergence analysis of finite



volume schemes:

$$\text{reg}(\mathcal{T}) := \max \left( \mathcal{N}, \mathcal{N}^*, \max_{\kappa^* \in \mathfrak{M}^*} \frac{\text{diam}(\kappa^*)}{\sqrt{m_{\kappa^*}}}, \max_{\kappa \in \mathfrak{M}} \frac{\text{diam}(\kappa)}{\sqrt{m_{\kappa}}}, \right. \\ \left. \max_{\mathcal{D} \in \mathfrak{D}} \frac{\text{diam}(\mathcal{D})}{\sqrt{m_{\mathcal{D}}}}, \max_{\mathcal{D} \in \mathfrak{D}} \frac{m_{\sigma} m_{\sigma^*}}{m_{\mathcal{D}}}, \max_{\substack{\kappa \in \mathfrak{M} \\ \mathcal{D} \in \mathfrak{D}_{\kappa}}} \frac{\text{diam}(\kappa)}{\text{diam}(\mathcal{D})}, \max_{\substack{\kappa^* \in \mathfrak{M}^* \\ \mathcal{D} \in \mathfrak{D}_{\kappa^*}}} \frac{\text{diam}(\kappa^*)}{\text{diam}(\mathcal{D})} \right), \quad (2.2)$$

where  $\mathcal{N}$  and  $\mathcal{N}^*$  are the maximum of edges of each primal cell and the maximum of edges incident to any vertex. The number  $\text{reg}(\mathcal{T})$  should be uniformly bounded when  $\text{size}(\mathcal{T}) \rightarrow 0$  for the convergence results to hold.

In order to simplify the presentation of the DDFV scheme, we shall adopt the following convention: for any quantity  $F^{\mathcal{T}}$  that is defined on  $\mathcal{T}$  (that is which belongs to  $\mathbb{R}^{\mathcal{T}}$  or  $(\mathbb{R}^2)^{\mathcal{T}}$ ), we shall write

$$F^{\mathcal{T}} := (F^{\mathfrak{M}}, F^{\partial \mathfrak{M}}, F^{\mathfrak{M}^*}, F^{\partial \mathfrak{M}^*}), \quad (2.3)$$

to identify the contributions of the different submeshes (primal/dual, interior/boundary). In the same way we shall denote by  $F^{\partial \mathcal{T}} := (F^{\partial \mathfrak{M}}, F^{\partial \mathfrak{M}^*})$  the boundary values.

*Projections onto the mesh.*

Let us define now the mean-value projection  $\mathbb{P}_{\mathbf{m}}^{\mathcal{T}}$  whose goal is to give a suitable DDFV discretization of initial conditions and source terms to be used in our numerical scheme. In order to deal with non-homogeneous boundary data for the velocity, we shall also need a variant  $\tilde{\mathbb{P}}_{\mathbf{m}}^{\mathcal{T}}$  of this projection with a specific choice for boundary terms on corners of the domain.

**Definition 2.1.** For any smooth enough real- or vector-valued function  $v$  on  $\Omega$  we define the mean-value projection  $\mathbb{P}_{\mathbf{m}}^{\mathcal{T}}$  as follows

$$\mathbb{P}_{\mathbf{m}}^{\mathfrak{M}} v := \left( \left( \frac{1}{m_{\kappa}} \int_{\kappa} v \right)_{\kappa \in \mathfrak{M}} \right) \quad \text{and} \quad \mathbb{P}_{\mathbf{m}}^{\mathfrak{M}^*} v := \left( \left( \frac{1}{m_{\kappa^*}} \int_{\kappa^*} v \right)_{\kappa^* \in \mathfrak{M}^*} \right), \\ \mathbb{P}_{\mathbf{m}}^{\partial \mathfrak{M}} v := \left( \left( \frac{1}{m_{\sigma}} \int_{\sigma} v \right)_{\sigma \in \mathfrak{M}} \right) \quad \text{and} \quad \mathbb{P}_{\mathbf{m}}^{\partial \mathfrak{M}^*} v := \left( \left( \frac{1}{m_{\sigma_F}^{\kappa^*}} \int_{\sigma_F^{\kappa^*}} v \right)_{\kappa^* \in \partial \mathfrak{M}^*} \right).$$

We also define  $\tilde{\mathbb{P}}_{\mathbf{m}}^{\mathcal{T}} v$  to be equal to  $\mathbb{P}_{\mathbf{m}}^{\mathcal{T}} v$ , excepted for all boundary dual unknowns where we set for  $\kappa^* \in \partial \mathfrak{M}^*$ ,

$$\tilde{\mathbb{P}}_{\mathbf{m}}^{\kappa^*} v := \begin{cases} 0, & \text{if } x_{\kappa^*} \text{ is a corner point of } \Gamma = \partial \Omega \\ \mathbb{P}_{\mathbf{m}}^{\kappa^*} v, & \text{otherwise.} \end{cases}$$

We can now introduce the two subsets of  $(\mathbb{R}^2)^{\mathcal{T}}$  needed to take into account the homogeneous or non-homogeneous Dirichlet boundary conditions in the Stokes problem

$$\mathbb{E}_0 := \left\{ \mathbf{u}_{\mathcal{T}} \in (\mathbb{R}^2)^{\mathcal{T}} \text{ such that } \mathbf{u}_{\partial \mathcal{T}} = 0 \right\} \\ \text{and } \mathbb{E}_{\mathbf{u}_b} := \left\{ \mathbf{u}_{\mathcal{T}} \in (\mathbb{R}^2)^{\mathcal{T}} \text{ such that } \mathbf{u}_{\partial \mathcal{T}} = \tilde{\mathbb{P}}_{\mathbf{m}}^{\partial \mathcal{T}} \mathbf{u}_b \right\}, \quad (2.4)$$

where  $\mathbf{u}_b$  satisfies (1.2). Observe that we use the projection  $\tilde{\mathbb{P}}_{\mathbf{m}}^{\partial \mathcal{T}}$  here, so that all the corner dual unknowns in  $\mathbb{E}_{\mathbf{u}_b}$  are set to zero, by definition.

## 2.2. Discrete operators

In this subsection, we define the discrete operators which are needed in order to write and analyse the DDFV scheme.

*Operators from primal/dual meshes into the diamond mesh.*

**Definition 2.2** (Discrete gradient). We define the discrete gradient operator  $\nabla^{\mathfrak{D}}$  that maps vector fields of  $(\mathbb{R}^2)^{\mathcal{T}}$  (resp. scalar fields of  $\mathbb{R}^{\mathcal{T}}$ ) into matrix fields of  $(\mathcal{M}_2(\mathbb{R}))^{\mathfrak{D}}$  (resp. vector fields of  $(\mathbb{R}^2)^{\mathfrak{D}}$ ), as follows: for any diamond  $\mathfrak{D} \in \mathfrak{D}$ , we set

$$\begin{aligned}\nabla^{\mathfrak{D}} \mathbf{u}_{\mathcal{T}} &:= \frac{1}{2m_{\mathfrak{D}}} [m_{\sigma}(\mathbf{u}_{\mathcal{L}} - \mathbf{u}_{\mathcal{K}}) \otimes \bar{\mathbf{n}}_{\sigma\mathcal{K}} + m_{\sigma^*}(\mathbf{u}_{\mathcal{L}^*} - \mathbf{u}_{\mathcal{K}^*}) \otimes \bar{\mathbf{n}}_{\sigma^*\mathcal{K}^*}], \quad \forall \mathbf{u}_{\mathcal{T}} \in (\mathbb{R}^2)^{\mathcal{T}}, \\ \nabla^{\mathfrak{D}} u_{\mathcal{T}} &:= \frac{1}{2m_{\mathfrak{D}}} [m_{\sigma}(u_{\mathcal{L}} - u_{\mathcal{K}})\bar{\mathbf{n}}_{\sigma\mathcal{K}} + m_{\sigma^*}(u_{\mathcal{L}^*} - u_{\mathcal{K}^*})\bar{\mathbf{n}}_{\sigma^*\mathcal{K}^*}], \quad \forall u_{\mathcal{T}} \in \mathbb{R}^{\mathcal{T}}.\end{aligned}$$

In this definition we used the usual notation for the tensor product of two vectors  $\mathbf{a}, \mathbf{b} \in \mathbb{R}^2$ , defined by  $\mathbf{a} \otimes \mathbf{b} = \mathbf{a} {}^t \mathbf{b} \in \mathcal{M}_2(\mathbb{R})$ ,  ${}^t \mathbf{b}$  being the transpose of  $\mathbf{b}$ .

**Definition 2.3** (Discrete divergence of vector fields). We define the discrete divergence operator  $\text{div}^{\mathfrak{D}}$  mapping vector fields of  $(\mathbb{R}^2)^{\mathcal{T}}$  into scalar fields in  $\mathbb{R}^{\mathfrak{D}}$ , as follows. For any  $\mathfrak{D} \in \mathfrak{D}$ , we set

$$\begin{aligned}\text{div}^{\mathfrak{D}} \mathbf{u}_{\mathcal{T}} &:= \text{Tr}(\nabla^{\mathfrak{D}} \mathbf{u}_{\mathcal{T}}) \\ &= \frac{1}{2m_{\mathfrak{D}}} [m_{\sigma}(\mathbf{u}_{\mathcal{L}} - \mathbf{u}_{\mathcal{K}}) \cdot \bar{\mathbf{n}}_{\sigma\mathcal{K}} + m_{\sigma^*}(\mathbf{u}_{\mathcal{L}^*} - \mathbf{u}_{\mathcal{K}^*}) \cdot \bar{\mathbf{n}}_{\sigma^*\mathcal{K}^*}], \quad \forall \mathbf{u}_{\mathcal{T}} \in (\mathbb{R}^2)^{\mathcal{T}}.\end{aligned}$$

*Operators from the diamond mesh into the primal/dual meshes.*

**Definition 2.4** (Discrete divergence of matrix fields). We define the discrete divergence operator  $\mathbf{div}^{\mathcal{T}}$  mapping matrix fields in  $(\mathcal{M}_2(\mathbb{R}))^{\mathfrak{D}}$  into vector fields in  $(\mathbb{R}^2)^{\mathcal{T}}$ , as follows. For any  $\xi_{\mathfrak{D}} \in (\mathcal{M}_2(\mathbb{R}))^{\mathfrak{D}}$ , we set  $\mathbf{div}^{\mathfrak{D}} \xi_{\mathfrak{D}} = 0$  and

$$\left\{ \begin{array}{l} \mathbf{div}^{\mathcal{K}} \xi_{\mathfrak{D}} := \frac{1}{m_{\mathcal{K}}} \sum_{\sigma \in \partial \mathcal{K}} m_{\sigma} \xi_{\mathfrak{D}} \cdot \bar{\mathbf{n}}_{\sigma\mathcal{K}}, \quad \forall \mathcal{K} \in \mathfrak{M}, \\ \mathbf{div}^{\mathcal{K}^*} \xi_{\mathfrak{D}} := \frac{1}{m_{\mathcal{K}^*}} \sum_{\sigma^* \in \partial \mathcal{K}^*} m_{\sigma^*} \xi_{\mathfrak{D}} \cdot \bar{\mathbf{n}}_{\sigma^*\mathcal{K}^*}, \quad \forall \mathcal{K}^* \in \mathfrak{M}^*, \\ \mathbf{div}^{\mathcal{K}^*} \xi_{\mathfrak{D}} := \frac{1}{m_{\mathcal{K}^*}} \left( \sum_{\mathfrak{D}_{\sigma, \sigma^*} \in \mathfrak{D}_{\mathcal{K}^*}} m_{\sigma^*} \xi_{\mathfrak{D}} \cdot \bar{\mathbf{n}}_{\sigma^*\mathcal{K}^*} + \sum_{\mathfrak{D} \in \mathfrak{D}_{\mathcal{K}^*} \cap \mathfrak{D}_{\text{ext}}} d_{\mathcal{K}^*, \mathcal{L}} \xi_{\mathfrak{D}} \cdot \bar{\mathbf{n}}_{\sigma\mathcal{K}} \right), \quad \forall \mathcal{K}^* \in \partial \mathfrak{M}^*, \end{array} \right.$$

where  $d_{\mathcal{K}^*, \mathcal{L}}$  is the distance between  $x_{\mathcal{K}^*}$  and  $x_{\mathcal{L}}$ .

We can also define a discrete divergence for vector fields as follows (see [5, 8] for more details).

**Definition 2.5** (Discrete divergence of vector fields). We define the discrete divergence operator  $\text{div}^{\mathcal{T}}$  mapping vector fields of  $(\mathbb{R}^2)^{\mathfrak{D}}$  into scalar fields of  $\mathbb{R}^{\mathcal{T}}$ , as follows

$$\text{div}^{\mathcal{T}} \xi_{\mathfrak{D}} := \left( \mathbf{div}^{\mathcal{T}} \begin{pmatrix} {}^t \xi_{\mathfrak{D}} \\ 0 \end{pmatrix} \right) \cdot \begin{pmatrix} 1 \\ 0 \end{pmatrix}, \quad \forall \xi_{\mathfrak{D}} \in (\mathbb{R}^2)^{\mathfrak{D}}.$$

**Definition 2.6** (Discrete pressure gradient). We define the discrete gradient operator  $\nabla^{\mathcal{T}}$  mapping scalar fields of  $\mathbb{R}^{\mathfrak{D}}$  into vector fields in  $(\mathbb{R}^2)^{\mathcal{T}}$  as follows

$$\nabla^{\mathcal{T}} p_{\mathfrak{D}} := \mathbf{div}^{\mathcal{T}}(p_{\mathfrak{D}} \text{Id}), \quad \forall p_{\mathfrak{D}} \in \mathbb{R}^{\mathfrak{D}}.$$

### 2.3. Discrete Green/Stokes formulas

First of all, we define the following bilinear forms. For  $d \in \{1, 2\}$  and for any  $u_T, v_T \in (\mathbb{R}^d)^T$ ,  $p_D, q_D \in (\mathbb{R}^d)^D$  we set

$$\begin{aligned} \llbracket u_T, v_T \rrbracket_T &:= \frac{1}{2} \left( \sum_{\kappa \in \mathfrak{M}} m_\kappa (u_\kappa, v_\kappa)_{\mathbb{R}^d} + \sum_{\kappa^* \in \mathfrak{M}^*} m_{\kappa^*} (u_{\kappa^*}, v_{\kappa^*})_{\mathbb{R}^d} \right), \\ (p_D, q_D)_D &:= \sum_{D \in \mathfrak{D}} m_D (p_D, q_D)_{\mathbb{R}^d}. \end{aligned}$$

Since the primal boundary values of  $u_T$  and  $v_T$  does not enter the definition of  $\llbracket \cdot, \cdot \rrbracket_T$ , it is a semi-inner product whereas  $(\cdot, \cdot)_D$  is actually an inner product. We denote by  $\|\cdot\|_T$  and  $\|\cdot\|_D$  the associated (semi-)norms. For any  $q \geq 1$  we also define

$$\begin{aligned} \|\mathbf{u}_T\|_{q,T} &:= \left( \frac{1}{2} \sum_{\kappa \in \mathfrak{M}} m_\kappa |\mathbf{u}_\kappa|^q + \frac{1}{2} \sum_{\kappa^* \in \mathfrak{M}^*} m_{\kappa^*} |\mathbf{u}_{\kappa^*}|^q \right)^{\frac{1}{q}}, \\ \|\mathbf{u}_T\|_{\infty,T} &:= \max \left( \max_{\mathfrak{M}} |\mathbf{u}_\kappa|, \max_{\mathfrak{M}^*} |\mathbf{u}_{\kappa^*}| \right). \end{aligned}$$

We also define two other inner products

$$\begin{aligned} \llbracket u_{\partial T}, v_{\partial T} \rrbracket_{\partial T} &:= \frac{1}{2} \left( \sum_{\mathcal{L} \in \partial \mathfrak{M}} m_\sigma u_\mathcal{L} v_\mathcal{L} + \sum_{\kappa^* \in \partial \mathfrak{M}^*} m_{\sigma_{\kappa^*}} u_{\kappa^*} v_{\kappa^*} \right), \quad \forall u_{\partial T}, v_{\partial T} \in \mathbb{R}^{\partial T}, \\ (\xi_D : \phi_D)_D &:= \sum_{D \in \mathfrak{D}} m_D (\xi_D : \phi_D) \quad \forall \xi_D, \phi_D \in (\mathcal{M}_2(\mathbb{R}))^D, \end{aligned}$$

and we denote by  $\|\cdot\|_{\partial T}$  and  $\|\cdot\|_D$  the associated norms. For any  $q \geq 1$ , we also set

$$\|u_{\partial T}\|_{q,\partial T} := \left( \frac{1}{2} \sum_{\mathcal{L} \in \partial \mathfrak{M}} m_\sigma |u_\mathcal{L}|^q + \frac{1}{2} \sum_{\kappa^* \in \partial \mathfrak{M}^*} m_{\sigma_{\kappa^*}} |u_{\kappa^*}|^q \right)^{\frac{1}{q}}, \quad \forall u_{\partial T} \in \mathbb{R}^{\partial T}.$$

In order to state the DDFV Green formulas, we shall also use the following bilinear form

$$(\phi_D, v_{\partial \mathfrak{M}})_{\partial \Omega} := \sum_{D \in \mathfrak{D}_{\text{ext}}} m_\sigma \phi_D v_\mathcal{L}, \quad \forall \phi_D \in \mathbb{R}^{2 \times \text{ext}}, v_{\partial \mathfrak{M}} \in \mathbb{R}^{\partial \mathfrak{M}},$$

and the following trace operators:

- a trace operator for scalar fields of  $\mathbb{R}^T$  defined by  $\gamma^T : u_T \mapsto (\gamma^\mathcal{L}(u_T))_{\mathcal{L} \in \partial \mathfrak{M}} \in \mathbb{R}^{\partial \mathfrak{M}}$  with

$$\gamma^\mathcal{L}(u_T) := \frac{d_{\kappa^*, \mathcal{L}} u_{\kappa^*} + d_{\mathcal{L}^*, \mathcal{L}} u_{\mathcal{L}^*} + m_\sigma u_\mathcal{L}}{2m_\sigma}, \quad \forall \mathcal{L} = [x_{\kappa^*}, x_{\mathcal{L}^*}] \in \partial \mathfrak{M};$$

- a trace operator for vector fields of  $(\mathbb{R}^2)^D$  defined as follows,

$$\gamma^D : \phi_D \in (\mathbb{R}^2)^D \mapsto (\phi_D)_{D \in \mathfrak{D}_{\text{ext}}} \in (\mathbb{R}^2)^{2 \times \text{ext}}.$$

We can now state the following discrete Green formulas that give its name to the Discrete Duality Method (see for instance, [5, 15] for the proofs).

**Theorem 2.7** (Green formulas). *For any  $(\xi_D, \mathbf{u}_T) \in (\mathcal{M}_2(\mathbb{R}))^D \times \mathbb{E}_0$  and for any  $(\mathbf{g}_D, v_T) \in (\mathbb{R}^2)^D \times \mathbb{R}^T$ , the following equalities hold,*

$$\llbracket \text{div}^T \xi_D, \mathbf{u}_T \rrbracket_T = - (\xi_D : \nabla^D \mathbf{u}_T)_D, \quad (2.5a)$$

$$\llbracket \text{div}^T \mathbf{g}_D, v_T \rrbracket_T = - (\mathbf{g}_D, \nabla^D v_T)_D + (\gamma^D(\mathbf{g}_D) \cdot \bar{\mathbf{n}}_T, \gamma^T(v_T))_{\partial \Omega}, \quad (2.5b)$$

with  $\bar{\mathbf{n}}_T = ((\bar{\mathbf{n}}_{\kappa \mathcal{L}})_{\mathcal{L} \in \partial \mathfrak{M}}) \in (\mathbb{R}^2)^{2 \times \text{ext}}$ .

### 2.4. Discrete functional inequalities

In this section we gather without proofs some discrete functional inequalities available in the literature and that we will use all along the paper. We assume that a DDFV mesh  $\mathcal{T}$  of  $\Omega$  is fixed.

**Theorem 2.8** (Discrete Poincaré–Sobolev inequality, ([6], Thm. 5.1)). *Let  $q \geq 1$ , there exists  $C_2 > 0$  depending only on  $\Omega$  and  $q$  such that*

$$\|\mathbf{u}_{\mathcal{T}}\|_{q,\mathcal{T}} \leq C_2 (\|\mathbf{u}_{\mathcal{T}}\|_{\mathcal{T}} + \|\|\nabla^{\mathfrak{D}} \mathbf{u}_{\mathcal{T}}\|\|_{\mathfrak{D}}), \quad \forall \mathbf{u}_{\mathcal{T}} \in (\mathbb{R}^2)^{\mathcal{T}}.$$

**Theorem 2.9** (Discrete Poincaré inequality, ([5], Lem. 3.2)). *There exists  $C_3 > 0$ , depending only on the diameter of  $\Omega$  and on  $\text{reg}(\mathcal{T})$ , such that*

$$\|\mathbf{u}_{\mathcal{T}}\|_{\mathcal{T}} \leq C_3 \|\|\nabla^{\mathfrak{D}} \mathbf{u}_{\mathcal{T}}\|\|_{\mathfrak{D}}, \quad \forall \mathbf{u}_{\mathcal{T}} \in \mathbb{E}_0.$$

**Definition 2.10** (Quasi-uniform mesh family). We define the number  $\text{reg}_{\text{unif}}(\mathcal{T})$  as follows

$$\text{reg}_{\text{unif}}(\mathcal{T}) := \sup \left( \text{reg}(\mathcal{T}), \sup_{\kappa \in \mathfrak{M}} \frac{\text{size}(\mathcal{T})^2}{m_{\kappa}}, \sup_{\kappa^* \in \mathfrak{M}^*} \frac{\text{size}(\mathcal{T})^2}{m_{\kappa^*}} \right).$$

We say that a family of DDFV meshes  $(\mathcal{T}^{(m)})_{m \in \mathbb{N}}$  is quasi-uniform if  $\text{reg}_{\text{unif}}(\mathcal{T}^{(m)})$  is bounded.

**Proposition 2.11.** *For any  $q \geq 1$ , there exists a constant  $C_4 > 0$  (depending on  $q$  and  $\text{reg}_{\text{unif}}(\mathcal{T})$ ) such that,*

$$\|u_{\mathcal{T}}\|_{\infty,\mathcal{T}} \leq \frac{C_4}{\text{size}(\mathcal{T})^{2/q}} \|u_{\mathcal{T}}\|_{q,\mathcal{T}}, \quad \forall u_{\mathcal{T}} \in \mathbb{R}^{\mathcal{T}}. \tag{2.6}$$

We define the primal and dual mean-values of a function  $\mu_{\mathcal{T}} \in \mathbb{R}^{\mathcal{T}}$  as follows,

$$M_{\mathfrak{M}}(\mu_{\mathcal{T}}) := \sum_{\kappa \in \mathfrak{M}} m_{\kappa} \mu_{\kappa} \quad \text{and} \quad M_{\mathfrak{M}^*}(\mu_{\mathcal{T}}) := \sum_{\kappa^* \in \mathfrak{M}^*} m_{\kappa^*} \mu_{\kappa^*}.$$

Observe that the primal boundary values of  $\mu_{\mathcal{T}}$  does not appear in those definition. This is due to the fact that boundary primal control volumes are degenerate.

The following result is proved in ([6], Thms. 5.1 and 5.3).

**Theorem 2.12.** *For any  $q \geq 1$  there exists  $C_5 > 0$  depending only on  $q$ ,  $\Omega$  and on  $\text{reg}(\mathcal{T})$  such that*

$$\|\mu_{\mathcal{T}}\|_{q,\mathcal{T}} \leq C_5 \|\|\nabla^{\mathfrak{D}} \mu_{\mathcal{T}}\|\|_{\mathfrak{D}}, \quad \forall \mu_{\mathcal{T}} \in \mathbb{R}^{\mathcal{T}}, \quad \text{with } M_{\mathfrak{M}}(\mu_{\mathcal{T}}) = M_{\mathfrak{M}^*}(\mu_{\mathcal{T}}) = 0. \tag{2.7}$$

Finally, using the fact that the trace operator is continuous from  $BV(\Omega)$  into  $L^1(\Gamma)$ , we can use similar techniques as that in ([6], Thm. 5.1) to obtain the following discrete trace theorem.

**Theorem 2.13** (Trace inequality). *For any  $q \geq 1$ , there exists  $C_6 > 0$  depending only on  $q$ ,  $\Omega$ , and  $\text{reg}(\mathcal{T})$  such that*

$$\|u_{\partial\mathcal{T}}\|_{q,\partial\mathcal{T}} \leq C_6 (\|u_{\mathcal{T}}\|_{\mathcal{T}} + \|\|\nabla^{\mathfrak{D}} u_{\mathcal{T}}\|\|_{\mathfrak{D}}), \quad \forall u_{\mathcal{T}} \in \mathbb{R}^{\mathcal{T}}. \tag{2.8}$$

### 2.5. Stability estimates

We can finally prove the stability of the projections introduced in Definition 2.1.

**Proposition 2.14.** *There exists  $C_7 > 0$  depending on  $\text{reg}(\mathcal{T})$  such that*

- For any  $v \in H^1(\Omega)$ , we have

$$\|\mathbb{P}_{\mathbf{m}}^{\mathcal{T}} v\|_{\mathcal{T}} + \|\|\nabla^{\mathfrak{D}} \mathbb{P}_{\mathbf{m}}^{\mathcal{T}} v\|\|_{\mathfrak{D}} \leq C_7 \|v\|_{H^1(\Omega)}. \tag{2.9}$$

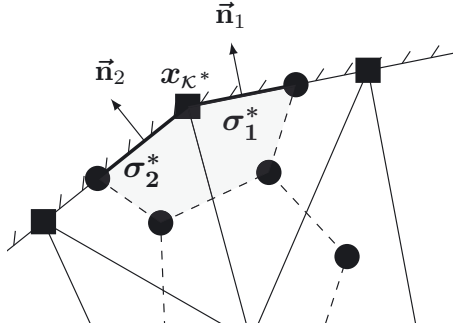


FIGURE 7. Case where  $x_{\kappa^*}$  is a corner point of  $\Omega$ .

- For any  $\mathbf{v} \in (H^1(\Omega))^2$  such that  $\mathbf{v} \cdot \vec{\mathbf{n}} = 0$  on  $\Gamma$ , we have

$$\left\| \widetilde{\mathbb{P}}_{\mathbf{m}}^{\mathcal{T}} \mathbf{v} \right\|_{\mathcal{T}} + \left\| \nabla^{\mathcal{D}} \widetilde{\mathbb{P}}_{\mathbf{m}}^{\mathcal{T}} \mathbf{v} \right\|_{\mathcal{D}} \leq C_7 \|\mathbf{v}\|_{H^1(\Omega)}. \tag{2.10}$$

*Proof.* We first choose if necessary a lifting of  $v$  (resp.  $\mathbf{v}$ ) in  $H^1(\mathbb{R}^2)$  (resp.  $(H^1(\mathbb{R}^2))^2$ ).

The proof of the first point is now quite standard, see for instance [5]. It is based on the following inequality (see [5] and [18], Lem. 3.4): there exists a universal  $C_8 > 0$  such that for any non degenerate polygonal domain  $A$  and  $\sigma$  one of its edge we have

$$\left| \frac{1}{m_A} \int_A v - \frac{1}{m_{\sigma}} \int_{\sigma} v \right|^2 \leq C_8 \frac{\text{diam}(A)^3}{m_{\sigma} m_A} \int_{\widehat{A}} |\nabla v|^2, \quad \forall v \in H^1(\mathbb{R}^2), \tag{2.11}$$

where  $\widehat{A}$  is the convex hull of  $A$ .

We just focus on the fact that even the discrete  $L^2$  estimate in (2.9) needs a complete  $H^1$  norm in the right-hand side, since we have chosen here the dual boundary values of  $\mathbb{P}_{\mathbf{m}}^{\mathcal{T}} v$  to be defined as mean-values of the trace on  $\Gamma$  of the function  $v$  (this is a small difference with [5, 18] that can be handled without difficulties).

For the estimate (2.10), we observe that the difference  $\mathbf{w}_{\mathcal{T}} = \mathbb{P}_{\mathbf{m}}^{\mathcal{T}} \mathbf{v} - \widetilde{\mathbb{P}}_{\mathbf{m}}^{\mathcal{T}} \mathbf{v}$  is non-zero only on corner points of  $\Gamma$  (and there is only a finite number of such points) and we want to evaluate  $\left\| \nabla^{\mathcal{D}} \mathbf{w}_{\mathcal{T}} \right\|_{\mathcal{D}}^2$ .

Let  $\kappa^* \in \partial \mathfrak{M}^*$  such that  $x_{\kappa^*}$  is a corner point of  $\Gamma$ , see Fig 7. We denote by  $\sigma_1, \sigma_2 \in \mathcal{E}_{\text{ext}} = \partial \mathfrak{M}$  the only two exterior edges such that  $\partial \kappa^* \cap \sigma_i \neq \emptyset$  and we set  $\sigma_i^* = \sigma_i \cap \partial \kappa^*$ ,  $i = 1, 2$ . Thanks to (2.11) we have for  $i = 1, 2$

$$\begin{aligned} \left| \frac{1}{m_{\kappa^*}} \int_{\kappa^*} \mathbf{v} - \frac{1}{m_{\sigma_i^*}} \int_{\sigma_i^*} \mathbf{v} \right|^2 &\leq C_8 \frac{\text{diam}(\widehat{\kappa}^*)^3}{m_{\sigma_i^*} m_{\kappa^*}} \int_{\widehat{\kappa}^*} |\nabla \mathbf{v}|^2 \\ &\leq C(\text{reg}(\mathcal{T})) \int_{\widehat{\kappa}^*} |\nabla \mathbf{v}|^2. \end{aligned} \tag{2.12}$$

Since by assumption we have  $\mathbf{v} \cdot \vec{\mathbf{n}}_i = 0$  on  $\sigma_i^*$ , we have  $\int_{\sigma_i^*} \mathbf{v} \cdot \vec{\mathbf{n}}_i = 0$  so that we get

$$\left| \frac{1}{m_{\kappa^*}} \int_{\kappa^*} \mathbf{v} \cdot \vec{\mathbf{n}}_i \right|^2 \leq C(\text{reg}(\mathcal{T})) \int_{\widehat{\kappa}^*} |\nabla \mathbf{v}|^2, \quad \text{for } i = 1, 2.$$

Since the unit vectors  $\vec{\mathbf{n}}_1$  and  $\vec{\mathbf{n}}_2$  are not colinear (because  $x_{\kappa^*}$  is a corner point of  $\Gamma$ ), we conclude that

$$\left| \frac{1}{m_{\kappa^*}} \int_{\kappa^*} \mathbf{v} \right|^2 \leq C(\text{reg}(\mathcal{T})) \int_{\widehat{\kappa}^*} |\nabla \mathbf{v}|^2.$$

Coming back to (2.12), we finally obtain that for  $i = 1, 2$  we have

$$\left| \frac{1}{m_{\sigma_i^*}} \int_{\sigma_i^*} \mathbf{v} \right|^2 \leq C(\text{reg}(\mathcal{T})) \int_{\widehat{\mathcal{K}}^*} |\nabla \mathbf{v}|^2.$$

Finally, we have that  $\sigma_r^{\mathcal{K}^*} = \sigma_1^* \cup \sigma_2^*$  so that  $\mathbf{w}_{\mathcal{K}^*}$  is a convex combination of  $\frac{1}{m_{\sigma_1^*}} \int_{\sigma_1^*} \mathbf{v}$  and  $\frac{1}{m_{\sigma_2^*}} \int_{\sigma_2^*} \mathbf{v}$ . It follows that

$$|\mathbf{w}_{\mathcal{K}^*}|^2 \leq C(\text{reg}(\mathcal{T})) \int_{\widehat{\mathcal{K}}^*} |\nabla \mathbf{v}|^2.$$

The contribution of  $\mathbf{w}_{\mathcal{K}^*}$  in  $\|\nabla^{\mathcal{D}} \mathbf{w}_{\mathcal{T}}\|_{\mathcal{D}}^2$  is thus bounded as follows

$$\frac{m_{\sigma}^2}{4m_{\mathcal{D}}} |\mathbf{w}_{\mathcal{K}^*}|^2 \leq C(\text{reg}(\mathcal{T})) \int_{\widehat{\mathcal{K}}^*} |\nabla \mathbf{v}|^2 \leq C(\text{reg}(\mathcal{T})) \|\mathbf{v}\|_{H^1}^2.$$

The same estimate holds for each corner point of  $\Gamma$  which gives the claim by summing all of them (there is only a finite and fixed number of such exceptional points). □

### 3. SEPARATE ANALYSIS OF THE STOKES AND OF THE CAHN–HILLIARD DDFV SCHEMES

In this section, before the study of the full coupled system, we present separately the DDFV scheme for the steady Stokes problem in a first part and for the Cahn–Hilliard equation with dynamic boundary condition in a second part.

#### 3.1. The steady Stokes problem

The aim of this section is to investigate the DDFV discretization of the non-homogeneous 2D incompressible steady Stokes problem: Find a velocity field  $\mathbf{u} : \Omega \rightarrow \mathbb{R}^2$  and a pressure field  $p : \Omega \rightarrow \mathbb{R}$ ,

$$\begin{cases} -\Delta \mathbf{u} + \nabla p = \mathbf{f}, & \text{in } \Omega, \\ \text{div} \mathbf{u} = 0, & \text{in } \Omega, \\ \mathbf{u} = \mathbf{u}_{\mathbf{b}}, & \text{on } \Gamma, \\ m(p) = 0, \end{cases} \tag{3.1}$$

where  $\mathbf{f}$  is a function in  $(L^2(\Omega))^2$ ,  $\mathbf{u}_{\mathbf{b}}$  satisfies (1.2) and  $m(p) := \frac{1}{|\Omega|} \int_{\Omega} p$  is the average of  $p$ .

In the case of homogeneous boundary condition (that is if  $\mathbf{u}_{\mathbf{b}} = 0$ ) the DDFV discretization of the problem (in this primal form) was for instance studied in [9, 29] (see also [30] for the 3D case). We would like here to recall those results and to generalise some of them to the non-homogeneous Dirichlet boundary data.

The DDFV method for the Stokes problem requires staggered unknowns. For the velocity field, it associates to any primal cell  $\kappa \in \overline{\mathcal{M}}$  an unknown value  $\mathbf{u}_{\kappa} \in \mathbb{R}^2$  and to any dual cell  $\kappa^* \in \overline{\mathcal{M}}^*$  an unknown value  $\mathbf{u}_{\kappa^*} \in \mathbb{R}^2$ . For the pressure field, we consider one unknown value  $p_{\mathcal{D}} \in \mathbb{R}$  for each diamond cell  $\mathcal{D} \in \mathcal{D}$ . These unknowns are collected in two vectors  $\mathbf{u}_{\mathcal{T}} \in (\mathbb{R}^2)^{\mathcal{T}}$ , and,  $p_{\mathcal{D}} \in \mathbb{R}^{\mathcal{D}}$ .

The DDFV scheme for problem (3.1) then reads as follows: Find  $\mathbf{u}_{\mathcal{T}} \in \mathbb{E}_{\mathbf{u}_{\mathbf{b}}}$  and  $p_{\mathcal{D}} \in \mathbb{R}^{\mathcal{D}}$  such that

$$\begin{cases} \text{div}^{\mathcal{M}}(-\nabla^{\mathcal{D}} \mathbf{u}_{\mathcal{T}} + p_{\mathcal{D}} \text{Id}) = \mathbb{P}_m^{\mathcal{M}} \mathbf{f}, \\ \text{div}^{\mathcal{M}^*}(-\nabla^{\mathcal{D}} \mathbf{u}_{\mathcal{T}} + p_{\mathcal{D}} \text{Id}) = \mathbb{P}_m^{\mathcal{M}^*} \mathbf{f}, \\ \text{div}^{\mathcal{D}} \mathbf{u}_{\mathcal{T}} = 0, \\ m(p_{\mathcal{D}}) := \sum_{\mathcal{D} \in \mathcal{D}} m_{\mathcal{D}} p_{\mathcal{D}} = 0. \end{cases} \tag{3.2}$$

This scheme is formally obtained by replacing the continuous gradient and divergence operators by the discrete DDFV operators defined previously. It amounts to integrating the mass (resp. momentum) balance equation on the diamond mesh  $\mathfrak{D}$  (resp. on the primal and interior dual meshes  $\mathfrak{M}$  and  $\mathfrak{M}^*$ ), and then to approximate the fluxes by using the DDFV gradient operator. Therefore, even though it is not clear at first sight in this compact operator-oriented presentation, this scheme is indeed a finite volume method. The non-homogeneous Dirichlet boundary conditions are specified on  $\partial\mathfrak{M}$  and on  $\partial\mathfrak{M}^*$  through the definition of the space  $\mathbb{E}_{\mathbf{u}_b}$  (see (2.4)).

The practical implementation of the scheme is straightforward: it simply consists in making a loop over the diamond cells and to compute for each of them the contribution of the momentum flux across primal and dual cells. Those fluxes only depend on the four velocity unknowns and of the pressure unknown related to the current diamond cell. The source term and the boundary data then appears in the right-hand side member of the resulting square linear system.

For a given mesh  $\mathcal{T}$ , the discrete Inf-Sup (LBB) constant associated with this problem is defined in a standard way as follows

$$\beta_{\mathcal{T}} := \inf_{p_{\mathfrak{D}} \in \mathbb{R}^{\mathfrak{D}}} \left( \sup_{\mathbf{v}_{\mathcal{T}} \in \mathbb{E}_0} \frac{\left( \operatorname{div}^{\mathfrak{D}} \mathbf{v}_{\mathcal{T}}, p_{\mathfrak{D}} \right)_{\mathfrak{D}}}{\|\nabla^{\mathfrak{D}} \mathbf{v}_{\mathcal{T}}\|_{\mathfrak{D}} \|p_{\mathfrak{D}} - m(p_{\mathfrak{D}})\|_{\mathfrak{D}}} \right). \quad (3.3)$$

In this paper, we assume that all the DDFV meshes considered satisfy the Inf-Sup condition  $\beta_{\mathcal{T}} > 0$ , which amounts to say that the kernel of the pressure gradient operator  $\nabla^{\mathfrak{T}}$  only contains constants. For such meshes, it is a standard fact to prove that the discrete Stokes problem (3.2) is well-posed. However, the stability and convergence of such method depends on the uniform Inf-Sup condition, that is to say that  $\beta_{\mathcal{T}}$  must remain away from 0 when the mesh is refined.

In [9] the Inf-Sup stability of such DDFV scheme with homogeneous Dirichlet boundary condition was thoroughly investigated. In particular, it is proved that for many kind of meshes, including non-conforming Cartesian meshes or conforming triangle meshes the Inf-Sup stability property holds, at least up to a single unstable pressure mode in some cases.

As for the continuous case (see Sect. 1.2.2), in order to deal with the non-homogeneous Dirichlet boundary condition in the discrete energy estimate of the fully Cahn–Hilliard/Stokes coupled problem, we need to introduce a suitable lifting of the boundary data. In order to simplify the computations, we will define such a lifting as a solution to the Stokes problem without source term.

**Theorem 3.1.** *There exists a unique  $(\mathbf{w}_{\mathcal{T}}, q_{\mathfrak{D}}) \in \mathbb{E}_{\mathbf{u}_b} \times \mathbb{R}^{\mathfrak{D}}$  solution to the following Stokes problem:*

$$\begin{cases} \operatorname{div}^{\mathfrak{M}}(-\nabla^{\mathfrak{D}} \mathbf{w}_{\mathcal{T}} + q_{\mathfrak{D}} \operatorname{Id}) = 0, \\ \operatorname{div}^{\mathfrak{M}^*}(-\nabla^{\mathfrak{D}} \mathbf{w}_{\mathcal{T}} + q_{\mathfrak{D}} \operatorname{Id}) = 0, \\ \operatorname{div}^{\mathfrak{D}} \mathbf{w}_{\mathcal{T}} = 0, \\ m(q_{\mathfrak{D}}) = 0. \end{cases} \quad (3.4)$$

Moreover, there exists  $C_9 > 0$  depending on  $\Omega$ ,  $\beta_{\mathcal{T}}$ ,  $\operatorname{reg}(\mathcal{T})$  such that

$$\|\mathbf{w}_{\mathcal{T}}\|_{\mathcal{T}} \leq C_9 \|\mathbf{u}_b\|_{H^{1/2}(\Gamma)} \quad \text{and} \quad \|\nabla^{\mathfrak{D}} \mathbf{w}_{\mathcal{T}}\|_{\mathfrak{D}} \leq C_9 \|\mathbf{u}_b\|_{H^{1/2}(\Gamma)}.$$

This result is classical in the continuous setting but its proof do not seem to be available in the literature in the DDFV framework. We propose a complete proof in the Appendix A.

### 3.2. The Cahn–Hilliard DDFV scheme

In this section, we describe the DDFV scheme associated with the following Cahn–Hilliard equation with dynamic boundary conditions: Find the concentration  $c$  and the chemical potential  $\mu$  such that

$$\begin{cases} \partial_t c = \Delta \mu, & \text{in } (0, T) \times \Omega; \\ \mu = -\Delta c + f'_b(c), & \text{in } (0, T) \times \Omega; \\ \partial_n \mu = 0, & \text{on } (0, T) \times \Gamma; \\ \partial_t c_{\Gamma} = -f'_s(c_{\Gamma}) - \partial_n c, & \text{on } (0, T) \times \Gamma, \end{cases} \quad (3.5)$$

with the initial condition  $c(0) = c_0$ .

From a theoretical point of view, the questions such as existence, uniqueness and regularity of solutions, existence of attractors and convergence to stationary states have been treated (see [14, 35, 39, 41, 45] and the references therein). From a numerical point of view, finite-difference methods have been implemented in [20, 21, 28] where the authors give various numerical illustrations, without proof of stability or convergence. Convergence results and optimal error estimates for the space semi-discrete scheme, with a finite-element discretization, are proved in [13] when the domain is a slab with periodic conditions in the longitudinal direction. Concerning finite-volume methods on unstructured grids, in [37, 38] the author proposes and analyses finite-volume schemes based on a two point flux approximation which is posed on a possibly smooth non-polygonal domain. However, up to our knowledge, there is no DDFV scheme available yet for this kind of problem. Our interest for this particular method comes from its capability to handle very general grids (even non conforming) and its very good robustness properties (as illustrated in the benchmarks [19, 23] for instance).

For the space discretization, all the discrete unknowns are located on the primal and dual meshes (namely on the centers and the vertices). For the time discretization, we set  $N \in \mathbb{N}^*$  and  $\Delta t = \frac{T}{N}$ . For any  $n \in \{1, \dots, N\}$ , we define  $t^n = n\Delta t$ . Then, the approximation at time  $t^n$  is denoted by

$$c_{\mathcal{T}}^n = \begin{pmatrix} (c_{\kappa}^n)_{\kappa \in \overline{\mathfrak{M}}} \\ (c_{\kappa^*}^n)_{\kappa^* \in \overline{\mathfrak{M}^*}} \end{pmatrix} \in \mathbb{R}^{\mathcal{T}} \quad \text{and} \quad \mu_{\mathcal{T}}^n = \begin{pmatrix} (\mu_{\kappa}^n)_{\kappa \in \overline{\mathfrak{M}}} \\ (\mu_{\kappa^*}^n)_{\kappa^* \in \overline{\mathfrak{M}^*}} \end{pmatrix} \in \mathbb{R}^{\mathcal{T}}.$$

Contrary to the velocity/pressure unknowns for the Stokes problem here the unknowns  $c_{\mathcal{T}}$  and  $\mu_{\mathcal{T}}$  are colocalized scalar fields.

To derive a DDFV scheme for the Cahn–Hilliard equation with dynamic boundary conditions (3.5), we first adopt a semi-discrete time discretization, then we formally replace the differential operators in the system by the discrete operators defined in Section 2.2. Here also, it amounts to integrate the two equations on the primal and dual meshes and to use discrete gradient operators to define the required numerical fluxes.

The additional delicate point here is the approximation of the dynamic boundary condition on the boundary dual control volumes. Indeed, these control volumes have a specific role because they are considered both as interior unknowns in the equation on the chemical potential and as boundary unknowns in the dynamic boundary condition. Let us remark that this is not the case for boundary primal control volumes because they only play a role here in the discretization on the dynamic boundary condition, since those control volume are in fact degenerate (they are edges of interior control volumes).

To obtain the DDFV approximation for the boundary dual mesh  $\partial\mathfrak{M}^*$ , we integrate the equation on the chemical potential on all boundary dual cells  $\kappa^* \in \partial\mathfrak{M}^*$  and the dynamic boundary condition on  $\sigma_{\Gamma}^{\kappa^*} = \partial\kappa^* \cap \Gamma$ .



In summary, the DDFV scheme we propose then reads, for a given initial data  $c_T^0 \in \mathbb{R}^T$ : for any  $n$ , find  $(c_T^{n+1}, \mu_T^{n+1}) \in \mathbb{R}^T \times \mathbb{R}^T$  such that,

$$\left\{ \begin{array}{l} \frac{c_{T_0}^{n+1} - c_{T_0}^n}{\Delta t} = \operatorname{div}^T (\nabla^{\mathfrak{D}} \mu_T^{n+1}), \\ \gamma^{\mathfrak{D}} (\nabla^{\mathfrak{D}} \mu_T^{n+1}) \cdot \vec{\mathbf{n}}_T = 0, \\ \mu_{\mathfrak{M}}^{n+1} = -\operatorname{div}^{\mathfrak{M}} (\nabla^{\mathfrak{D}} c_T^{n+1}) + d^{f_b}(c_{\mathfrak{M}}^n, c_{\mathfrak{M}}^{n+1}), \\ \mu_{\mathfrak{M}^*}^{n+1} = -\operatorname{div}^{\mathfrak{M}^*} (\nabla^{\mathfrak{D}} c_T^{n+1}) + d^{f_b}(c_{\mathfrak{M}^*}^n, c_{\mathfrak{M}^*}^{n+1}), \\ m_{\mathcal{K}^*} \mu_{\mathcal{K}^*}^{n+1} = - \sum_{\mathcal{D}_{\sigma, \sigma^*} \in \mathfrak{D}_{\mathcal{K}^*}} m_{\sigma^*} \nabla^{\mathfrak{D}} c_T^{n+1} \cdot \vec{\mathbf{n}}_{\sigma^* \mathcal{K}^*} + m_{\mathcal{K}^*} d^{f_b}(c_{\mathcal{K}^*}^n, c_{\mathcal{K}^*}^{n+1}) \\ \quad + m_{\sigma_{\mathcal{K}^*}} \frac{c_{\mathcal{K}^*}^{n+1} - c_{\mathcal{K}^*}^n}{\Delta t} + m_{\sigma_{\mathcal{K}^*}} d^{f_s}(c_{\mathcal{K}^*}^n, c_{\mathcal{K}^*}^{n+1}), \quad \forall \mathcal{K}^* \in \partial \mathfrak{M}^*, \\ \frac{c_{\partial \mathfrak{M}}^{n+1} - c_{\partial \mathfrak{M}}^n}{\Delta t} = -d^{f_s}(c_{\partial \mathfrak{M}}^n, c_{\partial \mathfrak{M}}^{n+1}) - \gamma^{\mathfrak{D}} (\nabla^{\mathfrak{D}} c_T^{n+1}) \cdot \vec{\mathbf{n}}_T. \end{array} \right. \quad (3.6)$$

Observe that, since the evolution equation for  $c$  is not discretized on the boundary primal mesh  $\partial \mathfrak{M}$  (due to the Neumann boundary condition on  $\mu$ ), we needed to use here the following notation  $c_{T_0} = \begin{pmatrix} c_{\mathfrak{M}} \\ 0 \\ c_{\mathfrak{M}^*} \end{pmatrix}$ , for any  $c_T \in \mathbb{R}^T$ , which is compatible with the fact that we have conventionally set  $\operatorname{div}^{\partial \mathfrak{M}} = 0$  (see Def. 2.5).

In the previous scheme we have denoted by  $d^{f_b}$  (resp.  $d^{f_s}$ ) the semi-discrete approximation of the nonlinear terms  $f'_b$  (resp.  $f'_s$ ). Many choices are possible for those terms (see [11, 37]) but we decided here to consider the following one

$$d^{f_b}(x, y) := \frac{f_b(y) - f_b(x)}{y - x} \quad \text{and} \quad d^{f_s}(x, y) := \frac{f_s(y) - f_s(x)}{y - x}, \quad \forall x, y, x \neq y, \quad (3.7)$$

which ensures automatically the stability property. In practice, the potentials  $f_b$  and  $f_s$  we use are polynomial functions, thus the terms  $d^{f_b}$  and  $d^{f_s}$  are also polynomial functions in the two variables  $x$  and  $y$ . Therefore, there is no need to make divisions in their computation, thus avoiding numerical accuracy issues. Using the assumption (1.4), we easily prove that  $d^{f_b}$  and  $d^{f_s}$  satisfy, for some  $C > 0$ ,

$$|d^{f_b}(x, y)| + |d^{f_s}(x, y)| \leq C(1 + |x|^p + |y|^p), \quad \forall x, y \in \mathbb{R}. \quad (3.8)$$

Recall that the continuous total free energy is the sum of a bulk energy and a surface energy (see Defs. 1.6 and 1.7). Similarly, the discrete free energy associated with the numerical scheme under study is defined as follows. For any  $c_T \in \mathbb{R}^T$ ,

$$\mathcal{F}_T(c_T) := \underbrace{\frac{1}{2} \|\nabla^{\mathfrak{D}} c_T\|_{\mathfrak{D}}^2 + \llbracket f_b(c_T), 1_T \rrbracket_T}_{:= \mathcal{F}_{b, T}(c_T)} + \underbrace{\llbracket f_s(c_{\partial T}), 1_{\partial T} \rrbracket_{\partial T}}_{:= \mathcal{F}_{s, \partial \mathfrak{M}}(c_{\partial T})}, \quad (3.9)$$

where  $1_{\partial T} \in \mathbb{R}^{\partial T}$  is the constant function equal to 1 on all the boundary control volumes and 0 elsewhere.

**Proposition 3.2** (Properties of the Cahn–Hilliard DDFV scheme). *Let  $c_T^n \in \mathbb{R}^T$ . Assuming that there exists a solution  $(c_T^{n+1}, \mu_T^{n+1}) \in \mathbb{R}^T \times \mathbb{R}^T$  to problem (3.6) then the following properties hold:*

- *Volume conservation:*

$$M_{\mathfrak{M}}(c_T^{n+1}) = M_{\mathfrak{M}}(c_T^n), \quad \text{and} \quad M_{\mathfrak{M}^*}(c_T^{n+1}) = M_{\mathfrak{M}^*}(c_T^n),$$

- *Energy equality:*

$$\mathcal{F}_\tau(c_\tau^{n+1}) - \mathcal{F}_\tau(c_\tau^n) + \Delta t \|\nabla^{\mathcal{D}} \mu_\tau^{n+1}\|_{\mathfrak{D}}^2 + \frac{1}{2} \|\nabla^{\mathcal{D}}(c_\tau^{n+1} - c_\tau^n)\|_{\mathfrak{D}}^2 + \frac{1}{\Delta t} \|c_{\partial\tau}^{n+1} - c_{\partial\tau}^n\|_{\partial\tau}^2 = 0.$$

We do not give the proof here because it is very similar to the proof of Proposition 4.9 that we detail below.

Let us remark that the right hand-side of the energy equality is exactly equal to 0 because we choose the discretization (3.7) for the nonlinear terms. As a consequence, the dissipation of the discrete total energy is valid for all time step  $\Delta t$ . This property leads to the existence of a solution to problem (3.6). We do not give the details since the proof can be done in a similar (even simpler) way as the one of our main result (Thm. 4.11) that concerns the complete coupled system.

#### 4. COUPLING BETWEEN THE CAHN–HILLIARD EQUATION AND THE UNSTEADY STOKES PROBLEM

We can now enter the heart of the paper, that is to propose and analyse a DDFV scheme for the phase-field coupled problem (1.1).

##### 4.1. Definition of discrete coupling operators

In Sections 3.1 and 3.2 we have introduced all the notation and tools necessary to study DDFV schemes. We also described the corresponding discretizations of the steady Stokes problem in the one hand and of the Cahn–Hilliard equation with dynamic boundary condition in the other hand.

The main new difficulty is to describe a suitable discretization of the coupling terms that is of the advection term  $\mathbf{u} \cdot \nabla c$  in the Cahn–Hilliard equation and of the capillary forces term  $\mu \nabla c$  in the momentum equation.

Let us summarise the issues that we need to deal with.

- **Convection term:**

The velocity unknowns are located on the primal and the dual meshes but the discrete gradient of the concentration  $c$  is naturally defined on diamond cells. Thus, we cannot discretize the term  $\mathbf{u} \cdot \nabla c$  by simply writing  $\mathbf{u}_\tau \cdot \nabla^{\mathcal{D}} c_\tau$  which is meaningless.

The first idea, in order to ensure mass conservation, is to discretize this term in conservative form  $\text{div}(c\mathbf{u})$ . The Stokes formula gives

$$\int_{\mathcal{K}} \text{div}(c\mathbf{u}) = \sum_{\sigma \in \mathcal{E}_{\mathcal{K}}} \int_{\sigma} c \mathbf{u} \cdot \mathbf{n}_{\sigma\mathcal{K}}, \quad \int_{\mathcal{K}^*} \text{div}(c\mathbf{u}) = \sum_{\sigma^* \in \mathcal{E}_{\mathcal{K}^*}} \int_{\sigma^*} c \mathbf{u} \cdot \mathbf{n}_{\sigma^*\mathcal{K}^*},$$

and we propose to discretize those balance equations as follows

$$\begin{cases} \text{div}_{\pi}^{\mathcal{K}}(\mathbf{u}_{\tau}, c_{\tau}) := \frac{1}{m_{\mathcal{K}}} \sum_{\sigma \in \mathcal{E}_{\mathcal{K}}} c_{\sigma} F_{\sigma, \mathcal{K}}^{\pi}(\mathbf{u}_{\tau}), \quad \forall \mathcal{K} \in \mathfrak{M}, \\ \text{div}_{\pi}^{\mathcal{K}^*}(\mathbf{u}_{\tau}, c_{\tau}) := \frac{1}{m_{\mathcal{K}^*}} \sum_{\sigma^* \in \mathcal{E}_{\mathcal{K}^*}} c_{\sigma^*} F_{\sigma^*, \mathcal{K}^*}^{\pi}(\mathbf{u}_{\tau}), \quad \forall \mathcal{K}^* \in \overline{\mathfrak{M}^*}, \end{cases} \tag{4.1}$$

where  $c_{\sigma}$  (resp.  $c_{\sigma^*}$ ) is a primal (resp. dual) edge approximations of  $c$  defined from the main unknowns  $c_{\tau}$  as follows

$$c_{\sigma} := \frac{c_{\mathcal{K}} + c_{\mathcal{L}}}{2}, \quad c_{\sigma^*} := \frac{c_{\mathcal{K}^*} + c_{\mathcal{L}^*}}{2}, \tag{4.2}$$

and  $F_{\sigma,\kappa}^\pi(\mathbf{u}_T)$  (resp.  $F_{\sigma^*,\kappa^*}^\pi(\mathbf{u}_T)$ ) is an approximation of the flux  $\int_\sigma \mathbf{u} \cdot \vec{\mathbf{n}}_{\sigma\kappa}$ , (resp.  $\int_{\sigma^*} \mathbf{u} \cdot \vec{\mathbf{n}}_{\sigma^*\kappa^*}$ ). Those new fluxes have to satisfy the following conditions:

(1) Conservativity:

$$\begin{cases} F_{\sigma,\kappa}^\pi(\mathbf{u}_T) = -F_{\sigma,\mathcal{L}}^\pi(\mathbf{u}_T), & \text{if } \sigma = \kappa|\mathcal{L}, \\ F_{\sigma^*,\kappa^*}^\pi(\mathbf{u}_T) = -F_{\sigma^*,\mathcal{L}^*}^\pi(\mathbf{u}_T), & \text{if } \sigma^* = \kappa^*|\mathcal{L}^*. \end{cases} \tag{4.3}$$

(2) Divergence-free condition:

$$\begin{cases} \operatorname{div}_\pi^\kappa(\mathbf{u}_T, 1) = 0, & \forall \kappa \in \mathfrak{M}, \\ \operatorname{div}_\pi^{\kappa^*}(\mathbf{u}_T, 1) = 0, & \forall \kappa^* \in \overline{\mathfrak{M}^*}. \end{cases} \tag{4.4}$$

Those properties imply the mass conservation property as well as the fact that the constant pure states  $c \equiv 0$ ,  $c \equiv 1$  will be particular solutions of the convected Cahn–Hilliard equation. This is an important requirement to ensure that the bulk phases will be suitably computed by the coupled model.

• **Capillary forces term:**

Similarly we cannot simply write  $\mu_T \nabla^D c_T$ , which is meaningless, to discretize the capillary forces term in the momentum equation. We shall build in the sequel an adapted discretization of this term denoted by  $\mathcal{G}^T(c_T, \mu_T)$ .

We will base our construction on the fact that, at the continuous level, this term  $\mu \nabla c$  can be interpreted as the local volume force exerted through the interface which exactly compensate the local free energy creation due to the convective term in the Cahn–Hilliard equation.

In other words, we will try to mimic at the discrete level the following identity

$$\int_\Omega (\mathbf{u} \cdot \nabla c) \mu = \int_\Omega (\mu \nabla c) \cdot \mathbf{u},$$

that is to say, with the DDFV notation,

$$\llbracket \operatorname{div}_\pi^T(\mathbf{u}_T, c_T), \mu_T \rrbracket_T = \llbracket \mathcal{G}^T(c_T, \mu_T), \mathbf{u}_T \rrbracket_T, \quad \forall \mathbf{u}_T \in \mathbb{E}_{\mathbf{u}_b}, \forall c_T, \mu_T \in \mathbb{R}^T. \tag{4.5}$$

The construction of the fluxes  $F_{\sigma,\kappa}^\pi(\mathbf{u}_T)$  and of the operator  $\mathcal{G}^T$  satisfying those properties is now given in the following two subsections.

4.1.1. *Construction of primal and dual mass fluxes*

In this section, we shall give a precise definition of the mass fluxes  $F_{\sigma,\kappa}^\pi(\mathbf{u}_T)$ ,  $F_{\sigma^*,\kappa^*}^\pi(\mathbf{u}_T)$  in such a way that (4.3) and (4.4) are fulfilled. The construction is mainly inspired by the one in [22], even though we adopt a slightly different point of view.

We begin with some additional notation related to diamond cells. Let  $\mathcal{D} \in \mathfrak{D}$  be the diamond cell whose vertices are  $x_\kappa, x_\mathcal{L}, x_{\kappa^*}, x_{\mathcal{L}^*}$  (see Fig. 8).

- We use the letter  $\mathfrak{s}$  to refer to the sides of the diamond  $\mathcal{D}$ . More precisely,  $\mathfrak{s}_{\kappa\kappa^*} \subset \partial\mathcal{D}$  is the side  $\mathcal{D}$  whose ends are  $x_\kappa$  and  $x_{\kappa^*}$ . We use similar notations for the three other sides of  $\mathcal{D}$ :  $\mathfrak{s}_{\kappa\mathcal{L}^*}$ ,  $\mathfrak{s}_{\mathcal{L}\kappa^*}$  and  $\mathfrak{s}_{\mathcal{L}\mathcal{L}^*}$ .
- The set of all the sides of all the diamond cells in  $\mathfrak{D}$  is denoted by  $\mathfrak{S}$ .
- We note  $m_\mathfrak{s}$  the length of any side  $\mathfrak{s} \in \mathfrak{S}$  and  $\vec{\mathbf{n}}_{\mathfrak{s},\mathcal{D}}$  the unit normal vector of  $\mathfrak{s}$  outward to  $\mathcal{D}$ .

For any  $\mathbf{u}_T \in (\mathbb{R}^2)^T$  and any side  $\mathfrak{s} = [x_\mathcal{P}, x_{\mathcal{P}^*}]$  of the diamond cell, with  $\mathcal{P} \in \{\kappa, \mathcal{L}\}$  and  $\mathcal{P}^* \in \{\kappa^*, \mathcal{L}^*\}$ , we define the flux across  $\mathfrak{s}$  to be

$$F_{\mathfrak{s},\mathcal{D}}^\pi(\mathbf{u}_T) := m_\mathfrak{s} \frac{\mathbf{u}_\mathcal{P} + \mathbf{u}_{\mathcal{P}^*}}{2} \cdot \vec{\mathbf{n}}_{\mathfrak{s},\mathcal{D}}. \tag{4.6}$$

Thanks to the following geometric formulas valid in each half diamond

$$\begin{aligned} m_\sigma \vec{\mathbf{n}}_{\kappa\mathcal{L}} &= -m_{\mathfrak{s}_{\kappa\kappa^*}} \vec{\mathbf{n}}_{\mathfrak{s}_{\kappa\kappa^*},\mathcal{D}} - m_{\mathfrak{s}_{\kappa\mathcal{L}^*}} \vec{\mathbf{n}}_{\mathfrak{s}_{\kappa\mathcal{L}^*},\mathcal{D}} = m_{\mathfrak{s}_{\mathcal{L}\kappa^*}} \vec{\mathbf{n}}_{\mathfrak{s}_{\mathcal{L}\kappa^*},\mathcal{D}} + m_{\mathfrak{s}_{\mathcal{L}\mathcal{L}^*}} \vec{\mathbf{n}}_{\mathfrak{s}_{\mathcal{L}\mathcal{L}^*},\mathcal{D}}, \\ m_{\sigma^*} \vec{\mathbf{n}}_{\kappa^*\mathcal{L}^*} &= -m_{\mathfrak{s}_{\kappa\kappa^*}} \vec{\mathbf{n}}_{\mathfrak{s}_{\kappa\kappa^*},\mathcal{D}} - m_{\mathfrak{s}_{\mathcal{L}\kappa^*}} \vec{\mathbf{n}}_{\mathfrak{s}_{\mathcal{L}\kappa^*},\mathcal{D}} = m_{\mathfrak{s}_{\kappa\mathcal{L}^*}} \vec{\mathbf{n}}_{\mathfrak{s}_{\kappa\mathcal{L}^*},\mathcal{D}} + m_{\mathfrak{s}_{\mathcal{L}\mathcal{L}^*}} \vec{\mathbf{n}}_{\mathfrak{s}_{\mathcal{L}\mathcal{L}^*},\mathcal{D}}, \end{aligned}$$

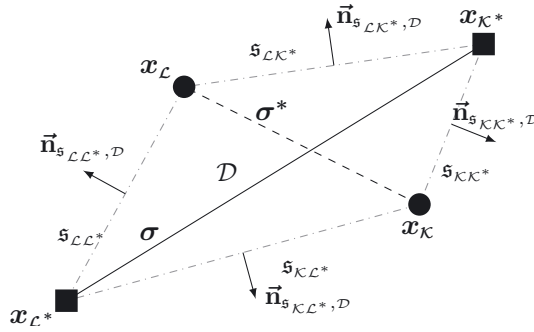


FIGURE 8. Definitions in a diamond cell  $\mathcal{D} \in \mathfrak{D}$ .

and to the definition of the discrete divergence operator (see Def. 2.3), we observe that

$$\operatorname{div}^{\mathcal{D}} \mathbf{u}_{\mathcal{T}} = \frac{1}{m_{\mathcal{D}}} \sum_{s \subset \partial \mathcal{D}} F_{s,\mathcal{D}}^{\pi}(\mathbf{u}_{\mathcal{T}}). \tag{4.7}$$

We observe now that, for a divergence-free vector field  $\mathbf{u}$ , the Stokes formula gives

$$\int_{\sigma} \mathbf{u} \cdot \vec{\mathbf{n}}_{\sigma\mathcal{K}} + \int_{s_{\mathcal{K}\mathcal{K}^*}} \mathbf{u} \cdot \vec{\mathbf{n}}_{s_{\mathcal{K}\mathcal{K}^*},\mathcal{D}} + \int_{s_{\mathcal{K}\mathcal{L}^*}} \mathbf{u} \cdot \vec{\mathbf{n}}_{s_{\mathcal{K}\mathcal{L}^*},\mathcal{D}} = 0.$$

We use this property (and similar ones for dual cells), at the discrete level, to define the following fluxes

$$\begin{cases} F_{\sigma,\mathcal{K}}^{\pi}(\mathbf{u}_{\mathcal{T}}) = - \left( F_{s_{\mathcal{K}\mathcal{K}^*},\mathcal{D}}^{\pi}(\mathbf{u}_{\mathcal{T}}) + F_{s_{\mathcal{K}\mathcal{L}^*},\mathcal{D}}^{\pi}(\mathbf{u}_{\mathcal{T}}) \right) \\ F_{\sigma^*,\mathcal{K}^*}^{\pi}(\mathbf{u}_{\mathcal{T}}) = - \left( F_{s_{\mathcal{K}\mathcal{K}^*},\mathcal{D}}^{\pi}(\mathbf{u}_{\mathcal{T}}) + F_{s_{\mathcal{L}^*\mathcal{K}^*},\mathcal{D}}^{\pi}(\mathbf{u}_{\mathcal{T}}) \right). \end{cases} \tag{4.8}$$

**Proposition 4.1.** *Let  $\mathbf{u}_{\mathbf{b}}$  satisfying (1.2) and  $\mathbf{u}_{\mathcal{T}} \in \mathbb{E}_{\mathbf{u}_{\mathbf{b}}}$ , such that  $\operatorname{div}^{\mathcal{D}} \mathbf{u}_{\mathcal{T}} = 0$ .*

*Then, the primal and dual fluxes defined in (4.8) satisfy the properties (4.3) and (4.4).*

*Moreover, for any  $\sigma \in \mathcal{E}_{\text{ext}}$ , if we denote by  $\mathcal{D} \in \mathfrak{D}_{\text{ext}}$  the associated boundary diamond, we have*

$$F_{\sigma,\mathcal{K}}^{\pi}(\mathbf{u}_{\mathcal{T}}) = 0, \text{ and } \begin{cases} F_{\sigma^*,\mathcal{K}^*}^{\pi}(\mathbf{u}_{\mathcal{T}}) = -F_{s_{\mathcal{K}\mathcal{K}^*},\mathcal{D}}^{\pi}(\mathbf{u}_{\mathcal{T}}), \\ F_{\sigma^*,\mathcal{L}^*}^{\pi}(\mathbf{u}_{\mathcal{T}}) = -F_{s_{\mathcal{K}\mathcal{L}^*},\mathcal{D}}^{\pi}(\mathbf{u}_{\mathcal{T}}). \end{cases}$$

We particularly emphasise the fact that, the boundary dual fluxes in the last formula are not zero in general for, at least, two reasons: first, the normals  $\vec{\mathbf{n}}_{s_{\mathcal{K}\mathcal{K}^*},\mathcal{D}}$  and  $\vec{\mathbf{n}}_{s_{\mathcal{K}\mathcal{L}^*},\mathcal{D}}$  are not parallel to the outward normal to the domain, and second the interior unknown  $\mathbf{u}_{\mathcal{K}}$  are no reason to have its normal component to be zero. However, those terms will compensate each other in the forthcoming conservativity and stability computations.

*Proof.*

- For a divergence-free discrete vector field, the formula (4.7) implies

$$F_{s_{\mathcal{K}\mathcal{K}^*},\mathcal{D}}^{\pi}(\mathbf{u}_{\mathcal{T}}) + F_{s_{\mathcal{K}\mathcal{L}^*},\mathcal{D}}^{\pi}(\mathbf{u}_{\mathcal{T}}) + F_{s_{\mathcal{L}^*\mathcal{K}^*},\mathcal{D}}^{\pi}(\mathbf{u}_{\mathcal{T}}) + F_{s_{\mathcal{L}^*\mathcal{L}^*},\mathcal{D}}^{\pi}(\mathbf{u}_{\mathcal{T}}) = 0, \tag{4.9}$$

that we can rewrite as follows

$$F_{\sigma,\mathcal{K}}^{\pi}(\mathbf{u}_{\mathcal{T}}) + F_{\sigma,\mathcal{L}}^{\pi}(\mathbf{u}_{\mathcal{T}}) = 0,$$

but also as follows

$$F_{\sigma^*,\mathcal{K}^*}^{\pi}(\mathbf{u}_{\mathcal{T}}) + F_{\sigma^*,\mathcal{L}^*}^{\pi}(\mathbf{u}_{\mathcal{T}}) = 0.$$

This is exactly the conservativity property we wanted to show.

- Let us consider a primal control volume  $\mathcal{K}$ . From (4.1), proving the property (4.4), is equivalent to show that

$$\sum_{\sigma \in \mathcal{E}_{\mathcal{K}}} F_{\sigma, \mathcal{K}}^{\pi}(\mathbf{u}_{\mathcal{T}}) = 0.$$

Using the definition (4.8) of those fluxes, we arrive to

$$\sum_{\sigma \in \mathcal{E}_{\mathcal{K}}} F_{\sigma, \mathcal{K}}^{\pi}(\mathbf{u}_{\mathcal{T}}) = - \sum_{\sigma \in \mathcal{E}_{\mathcal{K}}} \left( F_{\mathfrak{s}_{\mathcal{K}\mathcal{K}^*}, \mathcal{D}}^{\pi}(\mathbf{u}_{\mathcal{T}}) + F_{\mathfrak{s}_{\mathcal{K}\mathcal{L}^*}, \mathcal{D}}^{\pi}(\mathbf{u}_{\mathcal{T}}) \right),$$

where, in this sum, the diamond  $\mathcal{D}$  is the one associated with the edge  $\sigma$ . We observe now that, for each vertex  $x_{\mathcal{K}^*}$  of the control volume  $\mathcal{K}$ , the side  $\mathfrak{s}_{\mathcal{K}\mathcal{K}^*}$  in this sum appears exactly twice. More precisely, we have

$$\sum_{\sigma \in \mathcal{E}_{\mathcal{K}}} F_{\sigma, \mathcal{K}}^{\pi}(\mathbf{u}_{\mathcal{T}}) = - \sum_{\substack{\mathcal{K}^* \in \overline{\mathfrak{M}}^* \\ \text{s.t. } \mathfrak{s}_{\mathcal{K}\mathcal{K}^*} \in \mathfrak{S}}} \left( F_{\mathfrak{s}_{\mathcal{K}\mathcal{K}^*}, \mathcal{D}}^{\pi}(\mathbf{u}_{\mathcal{T}}) + F_{\mathfrak{s}_{\mathcal{K}\mathcal{K}^*}, \mathcal{D}'}^{\pi}(\mathbf{u}_{\mathcal{T}}) \right),$$

where in this sum  $\mathcal{D}$  and  $\mathcal{D}'$  are the two diamond cells sharing the common side  $\mathfrak{s}_{\mathcal{K}\mathcal{K}^*}$ . Due to opposite normal orientations, we deduce from (4.6) that the two corresponding fluxes above exactly cancels, and the claim is proved for primal control volumes. The same computation can be made on dual control volumes, by using Proposition 4.1.

- Assume now that  $\mathcal{D} \in \mathfrak{D}_{\text{ext}}$ . In that case, the diamond cell degenerates into a triangle. It means that, in Figure 8, the point  $x_{\mathcal{L}}$  belongs to  $\sigma = [x_{\mathcal{K}^*}, x_{\mathcal{L}^*}]$ . Consequently,  $\mathfrak{s}_{\mathcal{L}\mathcal{L}^*}$  and  $\mathfrak{s}_{\mathcal{L}\mathcal{K}^*}$  are included in the edge  $\sigma$ , which is itself included in the boundary of  $\Omega$ . By the definition of  $\mathbb{E}_{\mathbf{u}_b}$ , of the projection  $\widetilde{\mathbb{P}}_{\mathbf{m}}^{\mathcal{T}}$  (see Def. 2.1) and the assumption (1.2), we deduce that  $F_{\mathfrak{s}_{\mathcal{L}\mathcal{K}^*}, \mathcal{D}}^{\pi}(\mathbf{u}_{\mathcal{T}}) = F_{\mathfrak{s}_{\mathcal{L}\mathcal{L}^*}, \mathcal{D}}^{\pi}(\mathbf{u}_{\mathcal{T}}) = 0$ . By (4.8) and the conservativity property (4.3), we obtain the last claim of the proposition.  $\square$

To sum up, we can gather the construction of the convection operator in the following definition.

**Definition 4.2** (Definition of the discrete operator  $\text{div}_{\pi}^{\mathcal{T}}$ ). We define the operator  $\text{div}_{\pi}^{\mathcal{T}} : (\mathbb{R}^2)^{\mathcal{T}} \times \mathbb{R}^{\mathcal{T}} \rightarrow \mathbb{R}^{\mathcal{T}}$  as follows. Let  $\mathbf{u}_{\mathcal{T}} \in (\mathbb{R}^2)^{\mathcal{T}}$  and  $c_{\mathcal{T}} \in \mathbb{R}^{\mathcal{T}}$ , then we set  $\text{div}_{\pi}^{\text{om}}(\mathbf{u}_{\mathcal{T}}, c_{\mathcal{T}}) = 0$  and the other terms are defined in (4.1), with the fluxes definition (4.2), (4.6) and (4.8).

#### 4.1.2. Definition and properties of the operator $\mathcal{G}^{\mathcal{T}}$

We are now in position to define the discrete operator  $\mathcal{G}^{\mathcal{T}} : \mathbb{R}^{\mathcal{T}} \times \mathbb{R}^{\mathcal{T}} \rightarrow (\mathbb{R}^2)^{\mathcal{T}}$ . We recall that it is supposed to approximate the continuous operator  $(c, \mu) \mapsto \mu \nabla c$ , while ensuring the compatibility condition (4.5) that is crucial to prove energy estimates (see Sect. 4.2).

For any  $\kappa \in \mathfrak{M}$  and  $\kappa^* \in \overline{\mathfrak{M}}^*$  such that  $x_{\mathcal{K}^*}$  is a vertex of  $\mathcal{K}$ , we consider the segment  $\mathfrak{s} = [x_{\mathcal{K}}, x_{\mathcal{K}^*}]$  which, by construction is a common side of exactly two diamonds  $\mathcal{D}_1$  and  $\mathcal{D}_2$ . Let  $\vec{\mathbf{n}}_{\mathcal{D}_1, \mathcal{D}_2}$  the unit normal across  $\mathfrak{s}$  oriented from  $\mathcal{D}_1$  to  $\mathcal{D}_2$  and  $x_{\mathcal{L}_1}, x_{\mathcal{L}_1^*}$  (resp.  $x_{\mathcal{L}_2}, x_{\mathcal{L}_2^*}$ ) the other vertices of  $\mathcal{D}_1$  (resp.  $\mathcal{D}_2$ ). With those notations, the primal (resp. dual) edge of  $\mathcal{D}_i$  is  $\sigma_i = [x_{\mathcal{K}^*}, x_{\mathcal{L}_i^*}]$  (resp.  $\sigma_i^* = [x_{\mathcal{K}}, x_{\mathcal{L}_i}]$ ), see Figure 9.

For any  $c_{\mathcal{T}} \in \mathbb{R}^{\mathcal{T}}$ , we define

$$g_{\mathfrak{s}}(c_{\mathcal{T}}) := \frac{m_{\mathfrak{s}}}{2}(c_{\sigma_2} - c_{\sigma_1})\vec{\mathbf{n}}_{\mathcal{D}_1, \mathcal{D}_2}, \quad \text{and} \quad g_{\mathfrak{s}}^*(c_{\mathcal{T}}) := \frac{m_{\mathfrak{s}}}{2}(c_{\sigma_2^*} - c_{\sigma_1^*})\vec{\mathbf{n}}_{\mathcal{D}_1, \mathcal{D}_2}. \quad (4.10)$$

We recall that we choose to define the edge approximation of  $c$  by (4.2), so that we can rewrite the terms above as follows

$$g_{\mathfrak{s}}(c_{\mathcal{T}}) = \frac{m_{\mathfrak{s}}}{4}(c_{\mathcal{L}_2} - c_{\mathcal{L}_1})\vec{\mathbf{n}}_{\mathcal{D}_1, \mathcal{D}_2}, \quad g_{\mathfrak{s}}^*(c_{\mathcal{T}}) = \frac{m_{\mathfrak{s}}}{4}(c_{\mathcal{L}_2^*} - c_{\mathcal{L}_1^*})\vec{\mathbf{n}}_{\mathcal{D}_1, \mathcal{D}_2},$$

but (4.10) has the advantage that each term can be computed diamond cell by diamond cell, just like the all the other terms in the assembly process. Moreover (4.10) can be used with any other approximation of the terms  $c_{\sigma}$  and  $c_{\sigma^*}$  (with some unwinding for instance).

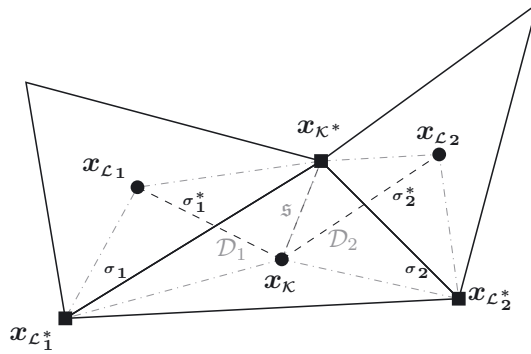


FIGURE 9. Notations for the construction of  $\mathcal{G}^T$ .

**Definition 4.3** (Definition of the discrete operator  $\mathcal{G}^T$ ). For any  $c_T, \mu_T \in \mathbb{R}^T$ , we set  $\mathcal{G}^{\partial \mathfrak{M}}(c_T, \mu_T) := 0$  and

$$\mathcal{G}^\kappa(c_T, \mu_T) := \frac{1}{m_\kappa} \sum_{\substack{\kappa^* \in \overline{\mathfrak{M}^*} \\ \text{s.t. } \mathfrak{s}_{\kappa\kappa^*} \in \mathfrak{S}}} g_{\mathfrak{s}_{\kappa\kappa^*}}(c_T) \mu_\kappa + g_{\mathfrak{s}_{\kappa\kappa^*}}^*(c_T) \mu_{\kappa^*}, \quad \forall \kappa \in \mathfrak{M}$$

$$\mathcal{G}^{\kappa^*}(c_T, \mu_T) := \frac{1}{m_{\kappa^*}} \sum_{\substack{\kappa \in \mathfrak{M} \\ \text{s.t. } \mathfrak{s}_{\kappa\kappa^*} \in \mathfrak{S}}} g_{\mathfrak{s}_{\kappa\kappa^*}}(c_T) \mu_\kappa + g_{\mathfrak{s}_{\kappa\kappa^*}}^*(c_T) \mu_{\kappa^*}, \quad \forall \kappa^* \in \overline{\mathfrak{M}^*}.$$

**Proposition 4.4.** The operators  $\text{div}_\pi^T$  and  $\mathcal{G}^T$  defined above, satisfy the compatibility property (4.5).

*Proof.* From (4.1) and (4.8) we have

$$m_\kappa \text{div}_\pi^\kappa(\mathbf{u}_T, c_T) = \sum_{\sigma \in \mathcal{E}_\kappa} c_\sigma F_{\sigma, \kappa}^\pi(\mathbf{u}_T) = \sum_{\substack{\kappa^* \in \overline{\mathfrak{M}^*} \\ \text{s.t. } \mathfrak{s}_{\kappa\kappa^*} \in \mathfrak{S}}} g_{\mathfrak{s}_{\kappa\kappa^*}}(c_T) \cdot (\mathbf{u}_\kappa + \mathbf{u}_{\kappa^*}),$$

$$m_{\kappa^*} \text{div}_\pi^{\kappa^*}(\mathbf{u}_T, c_T) = \sum_{\sigma^* \in \mathcal{E}_{\kappa^*}} c_{\sigma^*} F_{\sigma^*, \kappa^*}^\pi(\mathbf{u}_T) = \sum_{\substack{\kappa \in \mathfrak{M} \\ \text{s.t. } \mathfrak{s}_{\kappa\kappa^*} \in \mathfrak{S}}} g_{\mathfrak{s}_{\kappa\kappa^*}}^*(c_T) \cdot (\mathbf{u}_\kappa + \mathbf{u}_{\kappa^*}).$$

Multiplying by  $\mu_\kappa$  and  $\mu_{\kappa^*}$  respectively, and summing the results we exactly obtain

$$\llbracket \text{div}_\pi^T(\mathbf{u}_T, c_T), \mu_T \rrbracket_T = \frac{1}{2} \sum_{\kappa \in \mathfrak{M}} m_\kappa \mathbf{u}_\kappa \cdot \mathcal{G}^\kappa(c_T, \mu_T) + \frac{1}{2} \sum_{\kappa^* \in \overline{\mathfrak{M}^*}} m_{\kappa^*} \mathbf{u}_{\kappa^*} \cdot \mathcal{G}^{\kappa^*}(c_T, \mu_T), \quad (4.11)$$

which proves the claim. □

We prove now some properties of the operator  $\mathcal{G}^T$  that will be useful in the stability analysis of our numerical method. We first observe that, provided that  $\mathbf{u}_T$  is divergence-free, adding constants to  $\mu_T$  does not change the value of  $\llbracket \mathcal{G}^T(c_T, \mu_T), \mathbf{u}_T \rrbracket_T$ . More precisely, we have

**Lemma 4.5.** For any  $\mathbf{u}_T \in \mathbb{E}_{\mathbf{u}_b}$  such that  $\text{div}^\mathfrak{D}(\mathbf{u}_T) = 0$  and for any  $\mu_T, c_T \in \mathbb{R}^T$  and  $\alpha, \beta \in \mathbb{R}$  we have,

$$\llbracket \mathcal{G}^T(c_T, \widetilde{\mu}_T), \mathbf{u}_T \rrbracket_T = \llbracket \mathcal{G}^T(c_T, \mu_T), \mathbf{u}_T \rrbracket_T,$$

where we define  $\widetilde{\mu}_T \in \mathbb{R}^T$  as follows,

$$\begin{aligned} \widetilde{\mu}_\kappa &:= \mu_\kappa + \alpha, \quad \forall \kappa \in \mathfrak{M} \\ \text{and } \widetilde{\mu}_{\kappa^*} &:= \mu_{\kappa^*} + \beta, \quad \forall \kappa^* \in \overline{\mathfrak{M}^*}. \end{aligned} \quad (4.12)$$

*Proof.* Thanks to Proposition 4.4 and to the bilinearity of  $\mathcal{G}^\mathcal{T}$ , we have

$$\llbracket \mathcal{G}^\mathcal{T}(c_\mathcal{T}, \widetilde{\mu}_\mathcal{T}), \mathbf{u}_\mathcal{T} \rrbracket_\mathcal{T} = \llbracket \mathcal{G}^\mathcal{T}(c_\mathcal{T}, \mu_\mathcal{T}), \mathbf{u}_\mathcal{T} \rrbracket_\mathcal{T} + \llbracket \operatorname{div}_\pi^\mathcal{T}(\mathbf{u}_\mathcal{T}, c_\mathcal{T}), \widetilde{\mu}_\mathcal{T} - \mu_\mathcal{T} \rrbracket_\mathcal{T}.$$

It remains to prove that the last term in the right hand side of this equality is zero. The definition of  $\widetilde{\mu}_\mathcal{T}$  and the one of  $\operatorname{div}_\pi^\mathcal{T}$  (see (4.1)) give

$$\llbracket \operatorname{div}_\pi^\mathcal{T}(\mathbf{u}_\mathcal{T}, c_\mathcal{T}), \widetilde{\mu}_\mathcal{T} - \mu_\mathcal{T} \rrbracket_\mathcal{T} = \frac{\alpha}{2} \sum_{\kappa \in \mathfrak{M}} \sum_{\sigma \in \mathcal{E}_\kappa} c_\sigma F_{\sigma, \kappa}^\pi(\mathbf{u}_\mathcal{T}) + \frac{\beta}{2} \sum_{\kappa^* \in \overline{\mathfrak{M}}^*} \sum_{\sigma^* \in \mathcal{E}_{\kappa^*}} c_{\sigma^*} F_{\sigma^*, \kappa^*}^\pi(\mathbf{u}_\mathcal{T}).$$

By using the conservativity property (4.3) as well as the boundary conditions for  $\mathbf{u}_\mathcal{T}$  (see Prop. 4.1), we get

$$\sum_{\kappa \in \mathfrak{M}} \sum_{\sigma \in \mathcal{E}_\kappa} c_\sigma F_{\sigma, \kappa}^\pi(\mathbf{u}_\mathcal{T}) = \sum_{\sigma = \kappa | \mathcal{L} \in \mathcal{E}_{\text{int}}} c_\sigma (F_{\sigma, \kappa}^\pi(\mathbf{u}_\mathcal{T}) + F_{\sigma, \mathcal{L}}^\pi(\mathbf{u}_\mathcal{T})) + \sum_{\sigma = \mathcal{L} \in \mathcal{E}_{\text{ext}}} c_\sigma F_{\sigma, \kappa}^\pi(\mathbf{u}_\mathcal{T}) = 0.$$

Similarly, the definition of the fluxes  $F_{\sigma^*, \kappa^*}^\pi$  and the conservativity property leads to

$$\sum_{\kappa^* \in \overline{\mathfrak{M}}^*} \sum_{\sigma^* \in \mathcal{E}_{\kappa^*}} c_{\sigma^*} F_{\sigma^*, \kappa^*}^\pi(\mathbf{u}_\mathcal{T}) = \sum_{\mathcal{D} \in \mathfrak{D}} c_{\sigma^*} (F_{\sigma^*, \kappa^*}^\pi(\mathbf{u}_\mathcal{T}) + F_{\sigma^*, \mathcal{L}^*}^\pi(\mathbf{u}_\mathcal{T})) = 0.$$

The claim is proved.  $\square$

**Proposition 4.6.** *Let  $\mathcal{T}$  be a DDFV mesh of  $\Omega$ , and  $q \in [2, +\infty]$ . Let  $p \in [1, 2]$  be such that*

$$\frac{1}{p} = \frac{1}{2} + \frac{1}{q}.$$

*There exists  $C_{10} > 0$  depending only on  $\operatorname{reg}(\mathcal{T})$  and  $q$ , such that*

$$\|\mathcal{G}^\mathcal{T}(c_\mathcal{T}, \mu_\mathcal{T})\|_{p, \mathcal{T}} \leq C_{10} \|\nabla^\mathfrak{D} c_\mathcal{T}\|_\mathfrak{D} \|\mu_\mathcal{T}\|_{q, \mathcal{T}}, \quad \forall c_\mathcal{T}, \mu \in \mathbb{R}^\mathcal{T}.$$

*Proof.* We assume that  $q < +\infty$ ; the case  $q = +\infty$  is a straightforward adaptation of this case.

Thanks to the definitions (4.2) of  $c_\sigma$  and  $c_{\sigma^*}$  and Definition 2.2 of the discrete DDFV gradient we can write, using the notation of Figure 9, the following formulas

$$g_\mathfrak{s}(c_\mathcal{T}) = \frac{m_\mathfrak{s}}{4} (m_{\sigma_2^*} \nabla^{\mathcal{D}_2} c_\mathcal{T} \cdot \vec{\tau}_{\kappa \mathcal{L}_2} - m_{\sigma_1^*} \nabla^{\mathcal{D}_1} c_\mathcal{T} \cdot \vec{\tau}_{\kappa \mathcal{L}_1}) \vec{\mathbf{n}}_{\mathcal{D}_1, \mathcal{D}_2},$$

$$g_\mathfrak{s}^*(c_\mathcal{T}) = \frac{m_\mathfrak{s}}{4} (m_{\sigma_2} \nabla^{\mathcal{D}_2} c_\mathcal{T} \cdot \vec{\tau}_{\kappa^* \mathcal{L}^* 2} - m_{\sigma_1} \nabla^{\mathcal{D}_1} c_\mathcal{T} \cdot \vec{\tau}_{\kappa^* \mathcal{L}^* 1}) \vec{\mathbf{n}}_{\mathcal{D}_1, \mathcal{D}_2}.$$

It follows that

$$\max(|g_\mathfrak{s}(c_\mathcal{T})|, |g_\mathfrak{s}^*(c_\mathcal{T})|) \leq C(\operatorname{reg}(\mathcal{T})) (m_{\mathcal{D}_1} |\nabla^{\mathcal{D}_1} c_\mathcal{T}| + m_{\mathcal{D}_2} |\nabla^{\mathcal{D}_2} c_\mathcal{T}|),$$

and thus, by definition of  $\mathcal{G}^\mathcal{T}$  we have

$$|\mathcal{G}^\mathcal{T}(c_\mathcal{T}, \mu_\mathcal{T})| \leq C(\operatorname{reg}(\mathcal{T})) \frac{1}{m_\kappa} \sum_{\substack{\kappa^* \in \overline{\mathfrak{M}}^* \\ \text{s.t. } \mathfrak{s}_{\kappa \kappa^*} \in \mathfrak{S}}} (m_{\mathcal{D}_1} |\nabla^{\mathcal{D}_1} c_\mathcal{T}| + m_{\mathcal{D}_2} |\nabla^{\mathcal{D}_2} c_\mathcal{T}|) (|\mu_\kappa| + |\mu_{\kappa^*}|).$$

By using the definition of  $\operatorname{reg}(\mathcal{T})$  we see that

$$\sum_{\mathcal{D} \in \mathfrak{D}_\kappa} m_\mathcal{D} \leq C(\operatorname{reg}(\mathcal{T})) m_\kappa, \quad \forall \kappa \in \mathfrak{M},$$

and therefore, the Hölder inequality with the exponents  $2, q, p/(p-1)$  gives

$$|\mathcal{G}^\mathcal{T}(c_\mathcal{T}, \mu_\mathcal{T})| \leq C(\operatorname{reg}(\mathcal{T})) \frac{m_\kappa^{1-\frac{1}{p}}}{m_\kappa} \left( \sum_{\mathcal{D} \in \mathfrak{D}_\kappa} m_\mathcal{D} |\nabla^\mathcal{D} c_\mathcal{T}|^2 \right)^{\frac{1}{2}} \left( m_\kappa |\mu_\kappa|^q + \sum_{\substack{\kappa^* \in \overline{\mathfrak{M}}^* \\ \text{s.t. } \mathfrak{s}_{\kappa \kappa^*} \in \mathfrak{S}}} m_{\kappa^*} |\mu_{\kappa^*}|^q \right)^{\frac{1}{q}}.$$

It follows

$$m_\kappa |\mathcal{G}^\kappa(c_\mathcal{T}, \mu_\mathcal{T})|^p \leq C(\text{reg}(\mathcal{T})) \left( \sum_{\mathcal{D} \in \mathfrak{D}_\kappa} m_\mathcal{D} |\nabla^\mathcal{D} c_\mathcal{T}|^2 \right)^{\frac{p}{2}} \left( m_\kappa |\mu_\kappa|^q + \sum_{\substack{\kappa^* \in \overline{\mathfrak{M}^*} \\ \text{s.t. } \mathfrak{S}_{\kappa\kappa^*} \in \mathfrak{S}}} m_{\kappa^*} |\mu_{\kappa^*}|^q \right)^{\frac{p}{q}}.$$

Summing those inequalities for  $\kappa \in \mathfrak{M}$  and using once again the Hölder inequality with exponents  $2/p$  and  $q/p$  we obtain the claim.

A similar computation on the dual term  $\mathcal{G}^{\kappa^*}(c_\mathcal{T}, \mu_\mathcal{T})$  concludes the proof. □

By combining Propositions 4.6, 2.11 and Theorem 2.12, we easily obtain the following corollary.

**Corollary 4.7** (Estimate of the operator  $\mathcal{G}^\mathcal{T}$  in the quasi-uniform case). *Let  $\mathcal{T}$  be a DDFV mesh associated with  $\Omega$ , for any  $\alpha > 0$  there exists  $C_{11} > 0$  depending only on the uniform regularity of the mesh  $\text{reg}_{\text{unif}}(\mathcal{T})$  (see Def. 2.10),  $\Omega$  and  $\alpha$  such that for any  $c_\mathcal{T} \in \mathbb{R}^\mathcal{T}$ ,  $\mu_\mathcal{T} \in \mathbb{R}^\mathcal{T}$  satisfying  $M_{\mathfrak{M}}(\mu_\mathcal{T}) = M_{\overline{\mathfrak{M}^*}}(\mu_\mathcal{T}) = 0$  the following inequality holds,*

$$\|\mathcal{G}^\mathcal{T}(c_\mathcal{T}, \mu_\mathcal{T})\|_\mathcal{T} \leq \frac{C_{11}}{\text{size}(\mathcal{T})^\alpha} \|\nabla^\mathfrak{D} c_\mathcal{T}\|_\mathfrak{D} \|\nabla^\mathfrak{D} \mu_\mathcal{T}\|_\mathfrak{D}.$$

#### 4.1.3. Consistency study

It is possible to perform a consistency analysis for the two coupling operators that we have built before. Since we shall not detail the error analysis in this paper, we only give below without proof (see [36]) the main result in this direction.

**Theorem 4.8** (Weak consistency of the operator  $\mathcal{G}^\mathcal{T}$ ). *Let  $\mathbf{u} : \Omega \rightarrow \mathbb{R}^2$  and  $c, \mu : \Omega \rightarrow \mathbb{R}$  be smooth functions such that  $\mathbf{u} \cdot \vec{\mathbf{n}} = 0$  on  $\Gamma$  and  $\text{div} \mathbf{u} = 0$ , then there exists  $C_{12} > 0$  such that,*

$$\|[\mathcal{G}^\mathcal{T}(c_\mathcal{T}^{ex}, \mu_\mathcal{T}^{ex}), \mathbf{u}_\mathcal{T}^{ex}]\|_\mathcal{T} - \langle \mu \cdot \nabla c, \mathbf{u} \rangle \leq C_{12} \text{size}(\mathcal{T}),$$

where  $c_\mathcal{T}^{ex}, \mu_\mathcal{T}^{ex}$  and  $\mathbf{u}_\mathcal{T}^{ex}$  are the discrete functions obtained by taking the value of  $c, \mu$  and  $\mathbf{u}$  respectively at the centers and vertices of the mesh.

## 4.2. DDFV approximation of the uncoupled scheme

A similar derivation as the one given in Sections 3.1 and 3.2 and the definitions of the discrete coupling operators given in Section 4.1 allows us to give the DDFV scheme associated with problem (1.1).

However, we want to use a time splitting algorithm that let us solve successively the Cahn–Hilliard and the Stokes part of the system. This is an important requirement since it allows the use of efficient and specific solvers for each of the two systems (we can think of the incremental projection method for the Stokes part of the system for instance [33, 34]).

Here is the uncoupled numerical scheme that we propose to analyse in the sequel of the paper:

**Step 1.** Resolution of the convected Cahn–Hilliard equation with an explicit velocity field: Let  $(c_\mathcal{T}^n, \mathbf{u}_\mathcal{T}^n) \in \mathbb{R}^\mathcal{T} \times \mathbb{E}_{\mathbf{u}_b}$  be given, find  $(c_\mathcal{T}^{n+1}, \mu_\mathcal{T}^{n+1}) \in \mathbb{R}^\mathcal{T} \times \mathbb{R}^\mathcal{T}$  such that

$$\begin{cases} \frac{c_\mathcal{T}_0^{n+1} - c_\mathcal{T}_0^n}{\Delta t} + \text{div}_\pi^\mathcal{T}(\mathbf{u}_\mathcal{T}^n, c_\mathcal{T}^{n+1}) - \text{div}^\mathcal{T}(\nabla^\mathfrak{D} \mu_\mathcal{T}^{n+1}) = 0, & (4.13a) \\ \gamma^\mathfrak{D}(\nabla^\mathfrak{D} \mu_\mathcal{T}^{n+1}) \cdot \vec{\mathbf{n}}_\mathcal{T} = 0, & (4.13b) \end{cases}$$



with

$$\left\{ \begin{array}{l} \mu_{\mathfrak{M}}^{n+1} = -\operatorname{div}^{\mathfrak{M}}(\nabla^{\mathfrak{D}} c_{\mathcal{T}}^{n+1}) + df^b(c_{\mathfrak{M}}^n, c_{\mathfrak{M}}^{n+1}), \\ \mu_{\mathfrak{M}^*}^{n+1} = -\operatorname{div}^{\mathfrak{M}^*}(\nabla^{\mathfrak{D}} c_{\mathcal{T}}^{n+1}) + df^b(c_{\mathfrak{M}^*}^n, c_{\mathfrak{M}^*}^{n+1}), \\ m_{\mathcal{K}^*} \mu_{\mathcal{K}^*}^{n+1} = - \sum_{\mathfrak{D}_{\sigma, \sigma^*} \in \mathfrak{D}_{\mathcal{K}^*}} m_{\sigma^*} \nabla^{\mathfrak{D}} c_{\mathcal{T}}^{n+1} \cdot \vec{\mathbf{n}}_{\sigma^* \mathcal{K}^*} + m_{\mathcal{K}^*} df^b(c_{\mathcal{K}^*}^n, c_{\mathcal{K}^*}^{n+1}) \\ \quad + m_{\sigma_{\mathcal{F}^*}} \frac{c_{\mathcal{K}^*}^{n+1} - c_{\mathcal{K}^*}^n}{\Delta t} + m_{\sigma_{\mathcal{F}^*}} df^s(c_{\mathcal{K}^*}^n, c_{\mathcal{K}^*}^{n+1}), \quad \forall \mathcal{K}^* \in \partial \mathfrak{M}^*; \\ \frac{c_{\partial \mathfrak{M}}^{n+1} - c_{\partial \mathfrak{M}}^n}{\Delta t} + df^s(c_{\partial \mathfrak{M}}^n, c_{\partial \mathfrak{M}}^{n+1}) + \gamma^{\mathfrak{D}}(\nabla^{\mathfrak{D}} c_{\mathcal{T}}^{n+1}) \cdot \vec{\mathbf{n}}_{\mathcal{T}} = 0. \end{array} \right. \quad (4.14a)$$

$$\mu_{\mathfrak{M}^*}^{n+1} = -\operatorname{div}^{\mathfrak{M}^*}(\nabla^{\mathfrak{D}} c_{\mathcal{T}}^{n+1}) + df^b(c_{\mathfrak{M}^*}^n, c_{\mathfrak{M}^*}^{n+1}), \quad (4.14b)$$

$$m_{\mathcal{K}^*} \mu_{\mathcal{K}^*}^{n+1} = - \sum_{\mathfrak{D}_{\sigma, \sigma^*} \in \mathfrak{D}_{\mathcal{K}^*}} m_{\sigma^*} \nabla^{\mathfrak{D}} c_{\mathcal{T}}^{n+1} \cdot \vec{\mathbf{n}}_{\sigma^* \mathcal{K}^*} + m_{\mathcal{K}^*} df^b(c_{\mathcal{K}^*}^n, c_{\mathcal{K}^*}^{n+1}) \quad (4.14c)$$

$$\begin{aligned} & + m_{\sigma_{\mathcal{F}^*}} \frac{c_{\mathcal{K}^*}^{n+1} - c_{\mathcal{K}^*}^n}{\Delta t} + m_{\sigma_{\mathcal{F}^*}} df^s(c_{\mathcal{K}^*}^n, c_{\mathcal{K}^*}^{n+1}), \quad \forall \mathcal{K}^* \in \partial \mathfrak{M}^*; \\ & \frac{c_{\partial \mathfrak{M}}^{n+1} - c_{\partial \mathfrak{M}}^n}{\Delta t} + df^s(c_{\partial \mathfrak{M}}^n, c_{\partial \mathfrak{M}}^{n+1}) + \gamma^{\mathfrak{D}}(\nabla^{\mathfrak{D}} c_{\mathcal{T}}^{n+1}) \cdot \vec{\mathbf{n}}_{\mathcal{T}} = 0. \end{aligned} \quad (4.14d)$$

**Step 2.** Resolution of the Stokes problem with the capillary term computed with up-to-date approximations of  $c$  and  $\mu$ .

Let  $(c_{\mathcal{T}}^{n+1}, \mu_{\mathcal{T}}^{n+1}, \mathbf{u}_{\mathcal{T}}^n) \in \mathbb{R}^{\mathcal{T}} \times \mathbb{R}^{\mathcal{T}} \times \mathbb{E}_{\mathbf{u}_b}$  be given, find  $(\mathbf{u}_{\mathcal{T}}^{n+1}, p_{\mathfrak{D}}^{n+1}) \in \mathbb{E}_{\mathbf{u}_b} \times \mathbb{R}^{\mathfrak{D}}$  such that

$$\left\{ \begin{array}{l} \frac{\mathbf{u}_{\mathfrak{M}}^{n+1} - \mathbf{u}_{\mathfrak{M}}^n}{\Delta t} - \operatorname{div}^{\mathfrak{M}}(\nabla^{\mathfrak{D}} \mathbf{u}_{\mathcal{T}}^{n+1}) + \nabla^{\mathfrak{M}} p_{\mathfrak{D}}^{n+1} = \mathcal{G}^{\mathfrak{M}}(c_{\mathcal{T}}^{n+1}, \mu_{\mathcal{T}}^{n+1}) + \rho(c_{\mathfrak{M}}^{n+1}) \mathbf{g}, \\ \frac{\mathbf{u}_{\mathfrak{M}^*}^{n+1} - \mathbf{u}_{\mathfrak{M}^*}^n}{\Delta t} - \operatorname{div}^{\mathfrak{M}^*}(\nabla^{\mathfrak{D}} \mathbf{u}_{\mathcal{T}}^{n+1}) + \nabla^{\mathfrak{M}^*} p_{\mathfrak{D}}^{n+1} = \mathcal{G}^{\mathfrak{M}^*}(c_{\mathcal{T}}^{n+1}, \mu_{\mathcal{T}}^{n+1}) + \rho(c_{\mathfrak{M}^*}^{n+1}) \mathbf{g}, \\ \operatorname{div}^{\mathfrak{D}}(\mathbf{u}_{\mathcal{T}}^{n+1}) = 0, \\ m(p_{\mathfrak{D}}^{n+1}) = 0. \end{array} \right. \quad (4.15a)$$

$$\frac{\mathbf{u}_{\mathfrak{M}^*}^{n+1} - \mathbf{u}_{\mathfrak{M}^*}^n}{\Delta t} - \operatorname{div}^{\mathfrak{M}^*}(\nabla^{\mathfrak{D}} \mathbf{u}_{\mathcal{T}}^{n+1}) + \nabla^{\mathfrak{M}^*} p_{\mathfrak{D}}^{n+1} = \mathcal{G}^{\mathfrak{M}^*}(c_{\mathcal{T}}^{n+1}, \mu_{\mathcal{T}}^{n+1}) + \rho(c_{\mathfrak{M}^*}^{n+1}) \mathbf{g}, \quad (4.15b)$$

$$\operatorname{div}^{\mathfrak{D}}(\mathbf{u}_{\mathcal{T}}^{n+1}) = 0, \quad (4.15c)$$

$$m(p_{\mathfrak{D}}^{n+1}) = 0. \quad (4.15d)$$

Let us remark that, because of the explicit discretization of the velocity in the convected Cahn–Hilliard equation (which is mandatory to ensure that the two steps are uncoupled) we do not have cancellation between the convective term  $\operatorname{div}_{\pi}^{\mathcal{T}}(\mathbf{u}_{\mathcal{T}}^n, c_{\mathcal{T}}^{n+1})$  and the capillary term  $\mathcal{G}^{\mathcal{T}}(c_{\mathcal{T}}^{n+1}, \mu_{\mathcal{T}}^{n+1})$  despite the fact that the compatibility condition (4.5) holds. Thus, some additional work is needed to achieve a useful discrete energy estimate. Let us first compute the total *a priori* energy equality for the full discrete problem.

**Proposition 4.9** (*A priori* properties). *Let  $\mathbf{w}_{\mathcal{T}}$  be the lifting of the boundary data defined in Theorem 3.1.*

*For any  $c_{\mathcal{T}}^n \in \mathbb{R}^{\mathcal{T}}$ ,  $\mathbf{u}_{\mathcal{T}}^n \in \mathbb{E}_{\mathbf{u}_b}$ , if there exists a solution  $(c_{\mathcal{T}}^{n+1}, \mu_{\mathcal{T}}^{n+1}, \mathbf{u}_{\mathcal{T}}^{n+1}, p_{\mathfrak{D}}^{n+1}) \in \mathbb{R}^{\mathcal{T}} \times \mathbb{R}^{\mathcal{T}} \times \mathbb{E}_{\mathbf{u}_b} \times \mathbb{R}^{\mathfrak{D}}$  to the problem (4.13)–(4.15), then the following properties hold*

- *Volume conservation:*

$$M_{\mathfrak{M}}(c_{\mathcal{T}}^{n+1}) = M_{\mathfrak{M}}(c_{\mathcal{T}}^n), \quad \text{and} \quad M_{\mathfrak{M}^*}(c_{\mathcal{T}}^{n+1}) = M_{\mathfrak{M}^*}(c_{\mathcal{T}}^n), \quad (4.16)$$

- *Energy equality:*

$$\begin{aligned} & \left( \mathcal{F}_{\mathcal{T}}(c_{\mathcal{T}}^{n+1}) + \frac{1}{2} \|\mathbf{u}_{\mathcal{T}}^{n+1} - \mathbf{w}_{\mathcal{T}}\|_{\mathcal{T}}^2 \right) - \left( \mathcal{F}_{\mathcal{T}}(c_{\mathcal{T}}^n) + \frac{1}{2} \|\mathbf{u}_{\mathcal{T}}^n - \mathbf{w}_{\mathcal{T}}\|_{\mathcal{T}}^2 \right) \\ & + \Delta t \|\nabla^{\mathfrak{D}} \mu_{\mathcal{T}}^{n+1}\|_{\mathfrak{D}}^2 + \Delta t \|\nabla^{\mathfrak{D}}(\mathbf{u}_{\mathcal{T}}^{n+1} - \mathbf{w}_{\mathcal{T}})\|_{\mathfrak{D}}^2 \\ & + \frac{1}{2} \|\mathbf{u}_{\mathcal{T}}^{n+1} - \mathbf{u}_{\mathcal{T}}^n\|_{\mathcal{T}}^2 + \frac{1}{2} \|\nabla^{\mathfrak{D}}(c_{\mathcal{T}}^{n+1} - c_{\mathcal{T}}^n)\|_{\mathfrak{D}}^2 + \frac{1}{\Delta t} \|c_{\partial \mathcal{T}}^{n+1} - c_{\partial \mathcal{T}}^n\|_{\partial \mathcal{T}}^2 \\ & = \Delta t \llbracket \mathcal{G}^{\mathcal{T}}(c_{\mathcal{T}}^{n+1}, \mu_{\mathcal{T}}^{n+1}), \mathbf{u}_{\mathcal{T}}^{n+1} - \mathbf{u}_{\mathcal{T}}^n - \mathbf{w}_{\mathcal{T}} \rrbracket_{\mathcal{T}} + \Delta t \llbracket \rho(c_{\mathcal{T}}^{n+1}) \mathbf{g}, \mathbf{u}_{\mathcal{T}}^{n+1} - \mathbf{w}_{\mathcal{T}} \rrbracket_{\mathcal{T}}. \end{aligned}$$

*Proof.* The volume conservation property comes from the flux conservativity and the boundary conditions as stated in Proposition 4.1.

To prove the energy equality, we first consider the inner product in  $\mathbb{R}^{\mathcal{T}}$  between equation (4.13a) and  $\mu_{\mathcal{T}}^{n+1}$ . Thus, using the Green formula (2.5b) associated with the homogeneous Neumann boundary condition (4.13b), we get

$$\llbracket c_{\mathcal{T}}^{n+1} - c_{\mathcal{T}}^n, \mu_{\mathcal{T}}^{n+1} \rrbracket_{\mathcal{T}} + \Delta t \llbracket \operatorname{div}_{\pi}^{\mathcal{T}}(\mathbf{u}_{\mathcal{T}}^n, c_{\mathcal{T}}^{n+1}), \mu_{\mathcal{T}}^{n+1} \rrbracket_{\mathcal{T}} + \Delta t \|\nabla^{\mathfrak{D}} \mu_{\mathcal{T}}^{n+1}\|_{\mathfrak{D}}^2 = 0. \quad (4.17)$$

Then, we multiply all the equations (4.14a) on the interior primal mesh by  $\frac{m_{\mathcal{K}}}{2}(c_{\mathcal{K}}^{n+1} - c_{\mathcal{K}}^n)$ , all the equations on the interior dual mesh (4.14b) by  $\frac{m_{\mathcal{K}^*}}{2}(c_{\mathcal{K}^*}^{n+1} - c_{\mathcal{K}^*}^n)$  and all the equations on the boundary dual mesh (4.14c) by  $\frac{1}{2}(c_{\mathcal{K}^*}^{n+1} - c_{\mathcal{K}^*}^n)$ . Summing all the resulting equalities, we obtain

$$\begin{aligned} & \frac{1}{2} \sum_{\mathcal{K}^* \in \partial \mathfrak{M}^*} \sum_{\mathcal{D} \in \mathfrak{D}_{\mathcal{K}^*} \cap \mathfrak{D}_{\text{ext}}} d_{\mathcal{K}^*, \mathcal{L}} \nabla^{\mathcal{D}} c_{\mathcal{T}}^{n+1} \cdot \vec{\mathbf{n}}_{\sigma \mathcal{K}} (c_{\mathcal{K}^*}^{n+1} - c_{\mathcal{K}^*}^n) \\ & - \llbracket \text{div}^{\mathcal{T}} (\nabla^{\mathcal{D}} c_{\mathcal{T}}^{n+1}), c_{\mathcal{T}}^{n+1} - c_{\mathcal{T}}^n \rrbracket_{\mathcal{T}} + \llbracket d^{fb}(c_{\mathcal{T}}^n, c_{\mathcal{T}}^{n+1}), c_{\mathcal{T}}^{n+1} - c_{\mathcal{T}}^n \rrbracket_{\mathcal{T}} \\ & - \llbracket \mu_{\mathcal{T}}^{n+1}, c_{\mathcal{T}}^{n+1} - c_{\mathcal{T}}^n \rrbracket_{\mathcal{T}} + \frac{1}{2\Delta t} \sum_{\mathcal{K}^* \in \partial \mathfrak{M}^*} m_{\sigma \mathcal{K}^*} (c_{\mathcal{K}^*}^{n+1} - c_{\mathcal{K}^*}^n)^2 \\ & + \frac{1}{2} \sum_{\mathcal{K}^* \in \partial \mathfrak{M}^*} m_{\sigma \mathcal{K}^*} d^{fs}(c_{\mathcal{K}^*}^n, c_{\mathcal{K}^*}^{n+1})(c_{\mathcal{K}^*}^{n+1} - c_{\mathcal{K}^*}^n) = 0. \end{aligned} \tag{4.18}$$

Now, we have to take into account the dynamic boundary condition on the boundary primal mesh. To this end, we multiply all the equations on the boundary primal mesh (4.14d) by  $\frac{m_{\sigma}}{2}(c_{\mathcal{L}}^{n+1} - c_{\mathcal{L}}^n)$ . Summing up over all the boundary primal control volumes, we have

$$\begin{aligned} & \frac{1}{2\Delta t} \sum_{\mathcal{L} \in \partial \mathfrak{M}} m_{\sigma} (c_{\mathcal{L}}^{n+1} - c_{\mathcal{L}}^n)^2 + \frac{1}{2} \sum_{\mathcal{L} \in \partial \mathfrak{M}} m_{\sigma} d^{fs}(c_{\mathcal{L}}^n, c_{\mathcal{L}}^{n+1})(c_{\mathcal{L}}^{n+1} - c_{\mathcal{L}}^n) \\ & + \frac{1}{2} \sum_{\mathcal{D} \in \mathfrak{D}_{\text{ext}}} m_{\sigma} \nabla^{\mathcal{D}} c_{\mathcal{T}}^{n+1} \cdot \vec{\mathbf{n}}_{\sigma \mathcal{K}} (c_{\mathcal{L}}^{n+1} - c_{\mathcal{L}}^n) = 0. \end{aligned} \tag{4.19}$$

We observe that for any  $v_{\mathcal{T}} \in \mathbb{R}^{\mathcal{T}}$ ,  $\xi_{\mathfrak{D}} \in \mathbb{R}^{\mathfrak{D}_{\text{ext}}}$ , we have

$$\sum_{\mathcal{K}^* \in \partial \mathfrak{M}^*} \sum_{\mathcal{D} \in \mathfrak{D}_{\mathcal{K}^*} \cap \mathfrak{D}_{\text{ext}}} d_{\mathcal{K}^*, \mathcal{L}} \xi_{\mathfrak{D}} v_{\mathcal{K}^*} = \sum_{\mathcal{D} \in \mathfrak{D}_{\text{ext}}} (d_{\mathcal{K}^*, \mathcal{L}} v_{\mathcal{K}^*} + d_{\mathcal{L}^*, \mathcal{L}} v_{\mathcal{L}^*}) \xi_{\mathfrak{D}}.$$

Applying this equality to the functions  $v_{\mathcal{T}} = (c_{\mathcal{T}}^{n+1} - c_{\mathcal{T}}^n)$  and  $\xi_{\mathfrak{D}} = \gamma^{\mathfrak{D}} (\nabla^{\mathfrak{D}} c_{\mathcal{T}}^{n+1}) \cdot \vec{\mathbf{n}}_{\mathcal{T}}$  and summing equations (4.18) and (4.19), we obtain

$$\begin{aligned} & - \llbracket \text{div}^{\mathcal{T}} (\nabla^{\mathcal{D}} c_{\mathcal{T}}^{n+1}), c_{\mathcal{T}}^{n+1} - c_{\mathcal{T}}^n \rrbracket_{\mathcal{T}} + (\gamma^{\mathfrak{D}} (\nabla^{\mathfrak{D}} c_{\mathcal{T}}^{n+1}) \cdot \vec{\mathbf{n}}_{\mathcal{T}}, \gamma^{\mathcal{T}} (c_{\mathcal{T}}^{n+1} - c_{\mathcal{T}}^n))_{\partial \Omega} \\ & + \llbracket d^{fb}(c_{\mathcal{T}}^n, c_{\mathcal{T}}^{n+1}), c_{\mathcal{T}}^{n+1} - c_{\mathcal{T}}^n \rrbracket_{\mathcal{T}} - \llbracket \mu_{\mathcal{T}}^{n+1}, c_{\mathcal{T}}^{n+1} - c_{\mathcal{T}}^n \rrbracket_{\mathcal{T}} \\ & + \frac{1}{\Delta t} \|c_{\partial \mathcal{T}}^{n+1} - c_{\partial \mathcal{T}}^n\|_{\partial \mathcal{T}}^2 + \llbracket d^{fs}(c_{\partial \mathcal{T}}^n, c_{\partial \mathcal{T}}^{n+1}), c_{\partial \mathcal{T}}^{n+1} - c_{\partial \mathcal{T}}^n \rrbracket_{\partial \mathcal{T}} = 0. \end{aligned} \tag{4.20}$$

The Green formula (2.5b) gives,

$$\begin{aligned} & (\nabla^{\mathfrak{D}} c_{\mathcal{T}}^{n+1}, \nabla^{\mathfrak{D}} (c_{\mathcal{T}}^{n+1} - c_{\mathcal{T}}^n))_{\mathfrak{D}} - \llbracket \mu_{\mathcal{T}}^{n+1}, c_{\mathcal{T}}^{n+1} - c_{\mathcal{T}}^n \rrbracket_{\mathcal{T}} + \frac{1}{\Delta t} \|c_{\partial \mathcal{T}}^{n+1} - c_{\partial \mathcal{T}}^n\|_{\partial \mathcal{T}}^2 \\ & = - \llbracket d^{fb}(c_{\mathcal{T}}^n, c_{\mathcal{T}}^{n+1}), c_{\mathcal{T}}^{n+1} - c_{\mathcal{T}}^n \rrbracket_{\mathcal{T}} - \llbracket d^{fs}(c_{\partial \mathcal{T}}^n, c_{\partial \mathcal{T}}^{n+1}), c_{\partial \mathcal{T}}^{n+1} - c_{\partial \mathcal{T}}^n \rrbracket_{\partial \mathcal{T}}. \end{aligned} \tag{4.21}$$

Summing equations (4.17) and (4.21), using the relation  $2a(a - b) = a^2 - b^2 + (a - b)^2$  and the definition (3.7) of the nonlinear terms  $d^{fb}$  and  $d^{fs}$  we deduce

$$\begin{aligned} & \mathcal{F}_{\mathcal{T}}(c_{\mathcal{T}}^{n+1}) - \mathcal{F}_{\mathcal{T}}(c_{\mathcal{T}}^n) + \Delta t \|\nabla^{\mathfrak{D}} \mu_{\mathcal{T}}^{n+1}\|_{\mathfrak{D}}^2 \\ & + \frac{1}{2} \|\nabla^{\mathfrak{D}} (c_{\mathcal{T}}^{n+1} - c_{\mathcal{T}}^n)\|_{\mathfrak{D}}^2 + \frac{1}{\Delta t} \|c_{\partial \mathcal{T}}^{n+1} - c_{\partial \mathcal{T}}^n\|_{\partial \mathcal{T}}^2 + \Delta t \llbracket \text{div}_{\pi}^{\mathcal{T}}(\mathbf{u}_{\mathcal{T}}^n, c_{\mathcal{T}}^{n+1}), \mu_{\mathcal{T}}^{n+1} \rrbracket_{\mathcal{T}} = 0. \end{aligned} \tag{4.22}$$

We concentrate now on the Stokes part of the system. We multiply the mass balance equation in the interior primal cells (4.15a) by  $m_{\mathcal{K}}(\mathbf{u}_{\mathcal{K}}^{n+1} - \mathbf{w}_{\mathcal{K}})$  and we sum up over all the interior primal control volumes. Then we multiply all the equations in the interior dual cells (4.15b) by  $m_{\mathcal{K}^*}(\mathbf{u}_{\mathcal{K}^*}^{n+1} - \mathbf{w}_{\mathcal{K}^*})$  and we sum up over all

the interior dual control volumes. Summing these two equations and noting that by definition of the lifting  $\mathbf{w}_\mathcal{T}$  we have  $\mathbf{u}_\mathcal{T}^{n+1} - \mathbf{w}_\mathcal{T} \in \mathbb{E}_0$  we obtain,

$$\begin{aligned} & \llbracket \mathbf{u}_\mathcal{T}^{n+1} - \mathbf{u}_\mathcal{T}^n, \mathbf{u}_\mathcal{T}^{n+1} - \mathbf{w}_\mathcal{T} \rrbracket_\mathcal{T} - \Delta t \llbracket \mathbf{div}^\mathcal{T}(\nabla^\mathfrak{D} \mathbf{u}_\mathcal{T}^{n+1}), \mathbf{u}_\mathcal{T}^{n+1} - \mathbf{w}_\mathcal{T} \rrbracket_\mathcal{T} + \Delta t \llbracket \nabla^\mathcal{T} p_\mathfrak{D}^{n+1}, \mathbf{u}_\mathcal{T}^{n+1} - \mathbf{w}_\mathcal{T} \rrbracket_\mathcal{T} \\ & = \Delta t \llbracket \mathcal{G}^\mathcal{T}(c_\mathcal{T}^{n+1}, \mu_\mathcal{T}^{n+1}), \mathbf{u}_\mathcal{T}^{n+1} - \mathbf{w}_\mathcal{T} \rrbracket_\mathcal{T} + \Delta t \llbracket \rho(c_\mathcal{T}^{n+1})\mathbf{g}, \mathbf{u}_\mathcal{T}^{n+1} - \mathbf{w}_\mathcal{T} \rrbracket_\mathcal{T}. \end{aligned} \quad (4.23)$$

Since  $(\mathbf{w}_\mathcal{T}, q_\mathfrak{D})$  is solution to discrete Stokes problem (3.4), we get:

$$\begin{aligned} & - \llbracket \mathbf{div}^\mathcal{T}(\nabla^\mathfrak{D} \mathbf{u}_\mathcal{T}^{n+1}), \mathbf{u}_\mathcal{T}^{n+1} - \mathbf{w}_\mathcal{T} \rrbracket_\mathcal{T} + \llbracket \nabla^\mathcal{T} p_\mathfrak{D}^{n+1}, \mathbf{u}_\mathcal{T}^{n+1} - \mathbf{w}_\mathcal{T} \rrbracket_\mathcal{T} \\ & = - \llbracket \mathbf{div}^\mathcal{T}(\nabla^\mathfrak{D}(\mathbf{u}_\mathcal{T}^{n+1} - \mathbf{w}_\mathcal{T})), \mathbf{u}_\mathcal{T}^{n+1} - \mathbf{w}_\mathcal{T} \rrbracket_\mathcal{T} + \llbracket \nabla^\mathcal{T}(p_\mathfrak{D}^{n+1} - q_\mathfrak{D}), \mathbf{u}_\mathcal{T}^{n+1} - \mathbf{w}_\mathcal{T} \rrbracket_\mathcal{T}. \end{aligned}$$

Using again that  $\mathbf{u}_\mathcal{T}^{n+1} - \mathbf{w}_\mathcal{T} \in \mathbb{E}_0$  and that  $\operatorname{div}^\mathfrak{D} \mathbf{u}_\mathcal{T}^{n+1} = \operatorname{div}^\mathfrak{D} \mathbf{w}_\mathcal{T} = 0$ , the Stokes formula (2.5a) gives

$$- \llbracket \mathbf{div}^\mathcal{T}(\nabla^\mathfrak{D}(\mathbf{u}_\mathcal{T}^{n+1} - \mathbf{w}_\mathcal{T})), \mathbf{u}_\mathcal{T}^{n+1} - \mathbf{w}_\mathcal{T} \rrbracket_\mathcal{T} = \|\nabla^\mathfrak{D}(\mathbf{u}_\mathcal{T}^{n+1} - \mathbf{w}_\mathcal{T})\|_\mathfrak{D}^2$$

and

$$\llbracket \nabla^\mathcal{T}(p_\mathfrak{D}^{n+1} - q_\mathfrak{D}), \mathbf{u}_\mathcal{T}^{n+1} - \mathbf{w}_\mathcal{T} \rrbracket_\mathcal{T} = - \left( \operatorname{div}^\mathfrak{D}(\mathbf{u}_\mathcal{T}^{n+1} - \mathbf{w}_\mathcal{T}), p_\mathfrak{D}^{n+1} - q_\mathfrak{D} \right)_\mathfrak{D} = 0.$$

Finally, writing  $\mathbf{u}_\mathcal{T}^{n+1} - \mathbf{u}_\mathcal{T}^n = (\mathbf{u}_\mathcal{T}^{n+1} - \mathbf{w}_\mathcal{T}) - (\mathbf{u}_\mathcal{T}^n - \mathbf{w}_\mathcal{T})$ , equation (4.23) leads to

$$\begin{aligned} & \frac{1}{2} \|\mathbf{u}_\mathcal{T}^{n+1} - \mathbf{w}_\mathcal{T}\|_\mathcal{T}^2 - \frac{1}{2} \|\mathbf{u}_\mathcal{T}^n - \mathbf{w}_\mathcal{T}\|_\mathcal{T}^2 + \frac{1}{2} \|\mathbf{u}_\mathcal{T}^{n+1} - \mathbf{u}_\mathcal{T}^n\|_\mathcal{T}^2 + \Delta t \|\nabla^\mathfrak{D}(\mathbf{u}_\mathcal{T}^{n+1} - \mathbf{w}_\mathcal{T})\|_\mathfrak{D}^2 \\ & = \Delta t \llbracket \mathcal{G}^\mathcal{T}(c_\mathcal{T}^{n+1}, \mu_\mathcal{T}^{n+1}), \mathbf{u}_\mathcal{T}^{n+1} - \mathbf{w}_\mathcal{T} \rrbracket_\mathcal{T} + \Delta t \llbracket \rho(c_\mathcal{T}^{n+1})\mathbf{g}, \mathbf{u}_\mathcal{T}^{n+1} - \mathbf{w}_\mathcal{T} \rrbracket_\mathcal{T}. \end{aligned} \quad (4.24)$$

Thanks to the compatibility condition (4.5) we sum equations (4.22) and (4.24) to conclude the proof.  $\square$

**Lemma 4.10** (Initial data). *Let  $\mathbf{u}_0 \in (L^2(\Omega))^2$ ,  $c^0 \in H^1(\Omega)$ . For any DDFV mesh  $\mathcal{T}$  on  $\Omega$ , we set*

$$c_\mathcal{T}^0 := \mathbb{P}_\mathbf{m}^\mathcal{T} c_0 \in \mathbb{R}^\mathcal{T}, \quad \mathbf{u}_\mathcal{T}^0 := (\mathbb{P}_\mathbf{m}^\mathfrak{m} \mathbf{u}_0, 0, \mathbb{P}_\mathbf{m}^{\mathfrak{m}^*} \mathbf{u}_0, 0) \in (\mathbb{R}^2)^\mathcal{T}.$$

*Then, for some  $C_{13} > 0$  depending only on  $\operatorname{reg}(\mathcal{T})$ ,  $f_b$  and  $f_s$ , we have*

$$\begin{aligned} \mathcal{F}_\mathcal{T}(c_\mathcal{T}^0) & \leq C_{13}(1 + \|c_0\|_{H^1(\Omega)}^{p+1}), \quad \text{and} \quad \|\mathbf{u}_\mathcal{T}^0\|_\mathcal{T} \leq C_{13} \|\mathbf{u}_0\|_{L^2(\Omega)}, \\ |M_{\mathfrak{m}}(c_\mathcal{T}^0)| + |M_{\mathfrak{m}^*}(c_\mathcal{T}^0)| & \leq C_{13} \|c_0\|_{H^1(\Omega)}. \end{aligned}$$

Observe that the boundary values for the discrete initial velocity are taken to be 0 here even though we consider non-homogeneous boundary data for the velocity. Actually, it can be checked that those values are not used in our scheme.

*Proof.* Thanks to definition (3.9) of the discrete energy  $\mathcal{F}_\mathcal{T}$  and growth assumption (1.4) we have,

$$\mathcal{F}_\mathcal{T}(c_\mathcal{T}) \leq \frac{1}{2} \|\nabla^\mathfrak{D} c_\mathcal{T}^0\|_\mathfrak{D}^2 + C \left( |\Omega| + \|c_\mathcal{T}^0\|_{p+1, \mathcal{T}}^{p+1} \right) + C \left( |\Gamma| + \|c_{\partial\mathcal{T}}^0\|_{p+1, \partial\mathcal{T}}^{p+1} \right).$$

Proposition 2.14 gives the bound on the discrete  $H^1$  semi-norm of  $c_\mathcal{T}^0$  and for any  $q \geq 1$  definition of  $c_\mathcal{T}^0$ , the Jensen inequality and the trace inequality get

$$\begin{aligned} \|c_\mathcal{T}^0\|_{q, \mathcal{T}}^q & \leq \|c_\mathcal{T}^0\|_{L^q(\Omega)}^q + C(\operatorname{reg}(\mathcal{T}))\operatorname{size}(\mathcal{T}) \|c_\mathcal{T}^0\|_{L^q(\Gamma)}^q \\ & \leq \|c_\mathcal{T}^0\|_{L^q(\Omega)}^q + C(\operatorname{reg}(\mathcal{T}))\operatorname{size}(\mathcal{T}) \|c_\mathcal{T}^0\|_{H^1(\Omega)}^q, \end{aligned}$$

that gives the bound on  $\|c_\mathcal{T}^0\|_{p+1, \mathcal{T}}$  and on the mean-value of  $c_\mathcal{T}^0$ . Similarly we obtain the bound on  $\|c_{\partial\mathcal{T}}^0\|_{p+1, \partial\mathcal{T}}$  and so the bound on the discrete initial energy.

Finally in the same way, definition of  $\mathbf{u}_\mathcal{T}^0$  and especially the fact that  $\mathbf{u}_\mathcal{T}^0$  is chosen equal to 0 on the boundary mesh  $\partial\mathcal{T}$  and the Jensen inequality give the bound on the velocity.  $\square$

**Theorem 4.11** (Existence of a family of solutions and energy inequality). *Let  $\mathcal{T}$  be a DDFV mesh associated with  $\Omega$ ,  $c^0 \in H^1(\Omega)$ ,  $\mathbf{u}_0 \in (L^2(\Omega))^2$  and  $\alpha > 0$ .*

*There exists  $\gamma > 0$  depending only on  $\text{reg}_{\text{unif}}(\mathcal{T})$ ,  $\beta_{\mathcal{T}}$ ,  $\alpha$ , and on the data of the problem such that for any  $\Delta t \leq \gamma \text{size}(\mathcal{T})^\alpha$  there exists a solution*

$$((c_{\mathcal{T}}^n)_{1 \leq n \leq N}, (\mu_{\mathcal{T}}^n)_{1 \leq n \leq N}, (\mathbf{u}_{\mathcal{T}}^n)_{1 \leq n \leq N}, (p_{\mathcal{D}}^n)_{1 \leq n \leq N}) \in (\mathbb{R}^{\mathcal{T}})^N \times (\mathbb{R}^{\mathcal{T}})^N \times (\mathbb{E}_{\mathbf{u}_b})^N \times (\mathbb{R}^{\mathcal{D}})^N$$

to the problem (4.13)–(4.15) associated with the discretization of the initial data  $c_{\mathcal{T}}^0$ ,  $\mathbf{u}_{\mathcal{T}}^0$  as introduced in Lemma 4.10.

Moreover, for some  $M_0 > 0$  depending only on  $\text{reg}_{\text{unif}}(\mathcal{T})$ ,  $\beta_{\mathcal{T}}$ ,  $\alpha$  and the data, we can choose such a solution so that the following bounds are satisfied

$$\sum_{n=0}^{N-1} \Delta t \left( \|\mu_{\mathcal{T}}^{n+1}\|_{\mathcal{T}}^2 + \|\nabla^{\mathcal{D}} \mu_{\mathcal{T}}^{n+1}\|_{\mathcal{D}}^2 + \|\nabla^{\mathcal{D}} \mathbf{u}_{\mathcal{T}}^{n+1}\|_{\mathcal{D}}^2 \right) \leq M_0, \tag{4.25a}$$

$$\sup_{n \leq N} \left( \|c_{\mathcal{T}}^n\|_{\mathcal{T}}^2 + \|\nabla^{\mathcal{D}} c_{\mathcal{T}}^n\|_{\mathcal{D}}^2 \right) \leq M_0, \tag{4.25b}$$

$$\sup_{n \leq N} \|\mathbf{u}_{\mathcal{T}}^n\|_{\mathcal{T}}^2 \leq M_0, \tag{4.25c}$$

and

$$\sum_{n=0}^{N-1} \Delta t \left\| \frac{c_{\partial\mathcal{T}}^{n+1} - c_{\partial\mathcal{T}}^n}{\Delta t} \right\|_{\partial\mathcal{T}}^2 \leq M_0. \tag{4.25d}$$

**Remark 4.12.** Observe that, on a quasi-uniform mesh family and provided that the time step is suitably chosen, this theorem gives uniform bounds on :

- the discrete  $L^\infty(0, T; H^1(\Omega))$  norm of the order parameter  $c$ ,
- the discrete  $L^2(0, T; H^1(\Omega))$  norm of the chemical potential  $\mu$ ,
- the discrete  $L^\infty(0, T; L^2(\Omega)) \cap L^2(0, T; H^1(\Omega))$  norm of the velocity field  $\mathbf{u}$ ,
- the discrete  $L^2(]0, T[ \times \Gamma)$  norm of the time derivative of the trace of  $c$ .

Those bounds correspond to the natural energy space *a priori* estimates for the PDE system (1.1) we are interested in.

At least for a linear dynamic boundary condition, those estimates are sufficient (along with compactness) arguments to prove the convergence, up to a subsequence, of the approximate solutions towards a solution of (1.1). We do not give the details here and we refer for instance to [13, 37].

*Proof of Theorem 4.11.* In this proof, all the constants  $M_i$ ,  $i = 0, \dots$  are supposed to depend only on  $\text{reg}_{\text{unif}}(\mathcal{T})$ ,  $\beta_{\mathcal{T}}$ ,  $c_0$ ,  $\mathbf{u}_0$ , and  $\alpha$ .

For any  $\delta \in [0, 1]$ , we denote by  $(\mathcal{P}_\delta)$  the same problem as (4.13)–(4.15) where we added a factor  $\delta$  in front of the nonlinear terms, namely:

- in front of  $\text{div}_{\pi}^{\mathcal{T}}$  in (4.13a),
- in front of  $d^{f_b}$  in (4.14a), (4.14b) and (4.14c),
- in front of  $d^{f_s}$  in (4.14c) and (4.14d),
- in front of  $\mathcal{G}^{\mathcal{T}}$  and  $\rho \mathbf{g}$  in (4.15a) and (4.15b).

The total discrete free energy naturally associated with the modified problem  $(\mathcal{P}_\delta)$  is then defined as follows

$$\mathcal{F}_{\mathcal{T}}^\delta(c_{\mathcal{T}}) := \frac{1}{2} \|\nabla^{\mathcal{D}} c_{\mathcal{T}}\|_{\mathcal{D}}^2 + \delta \llbracket f_b(c_{\mathcal{T}}), 1_{\mathcal{T}} \rrbracket_{\mathcal{T}} + \delta \llbracket f_s(c_{\partial\mathcal{T}}), 1_{\partial\mathcal{T}} \rrbracket_{\partial\mathcal{T}}, \quad \forall c_{\mathcal{T}} \in \mathbb{R}^{\mathcal{T}}. \tag{4.26}$$

Using a same computations as in Proposition 4.9 we get that any solution of  $(\mathcal{P}_\delta)$  satisfies the following energy equality

$$\begin{aligned} & \left( \mathcal{F}_\tau^\delta(c_\tau^{n+1}) + \frac{1}{2} \|\mathbf{u}_\tau^{n+1} - \mathbf{w}_\tau\|_\tau^2 \right) - \left( \mathcal{F}_\tau^\delta(c_\tau^n) + \frac{1}{2} \|\mathbf{u}_\tau^n - \mathbf{w}_\tau\|_\tau^2 \right) + \Delta t \|\nabla^\mathfrak{D} \mu_\tau^{n+1}\|_\mathfrak{D}^2 \\ & + \Delta t \|\nabla^\mathfrak{D}(\mathbf{u}_\tau^{n+1} - \mathbf{w}_\tau)\|_\mathfrak{D}^2 + \frac{1}{2} \|\mathbf{u}_\tau^{n+1} - \mathbf{u}_\tau^n\|_\tau^2 + \frac{1}{2} \|\nabla^\mathfrak{D}(c_\tau^{n+1} - c_\tau^n)\|_\mathfrak{D}^2 + \frac{1}{\Delta t} \|c_{\partial\tau}^{n+1} - c_{\partial\tau}^n\|_{\partial\tau}^2 \\ & = \Delta t \delta \llbracket \mathcal{G}^\tau(c_\tau^{n+1}, \mu_\tau^{n+1}), \mathbf{u}_\tau^{n+1} - \mathbf{u}_\tau^n - \mathbf{w}_\tau \rrbracket_\tau + \Delta t \delta \llbracket \rho(c_\tau^{n+1})\mathbf{g}, \mathbf{u}_\tau^{n+1} - \mathbf{w}_\tau \rrbracket_\tau. \end{aligned} \tag{4.27}$$

For  $M_0 > 0$  and  $C_{\tau, \Delta t} > 0$  given (to be determined later), we introduce the following *a priori* bound on the pressure

$$\sup_{n \leq N} \|p_\mathfrak{D}^n\|_\mathfrak{D}^2 \leq C_{\tau, \Delta t}, \tag{4.28}$$

and the set

$$K = \left\{ ((c_\tau^n)_n, (\mu_\tau^n)_n, (\mathbf{u}_\tau^n)_n, (p_\mathfrak{D}^n)_n) \in (\mathbb{R}^\tau)^N \times (\mathbb{R}^\tau)^N \times (\mathbb{E}_{\mathbf{u}_b})^N \times (\mathbb{R}^\mathfrak{D})^N, \right. \\ \left. \text{that satisfy the estimates (4.25) and (4.28)} \right\}.$$

The set of equations  $(\mathcal{P}_\delta)_\delta$  forms a continuous map with respect to all the variables - including  $\delta$  - and the problem we initially want to solve is simply  $(\mathcal{P}_1)$ .

The Brouwer degree theory will let us conclude to the existence of at least one solution of our initial problem in  $K$  if we manage to prove that

- (a) For  $\delta = 0$ , the linear problem  $(P_0)$  has a unique solution in  $K$ .
- (b) For any  $\delta \in [0, 1]$ ,  $(\mathcal{P}_\delta)$  has no solution on  $\partial K$ .

Observe first that if  $\delta = 0$ ,  $\mathbf{u}_b = 0$ ,  $c_\tau^0 = 0$ ,  $\mathbf{u}_0 = 0$ , then (4.27) implies that  $c_\tau^n = \mu_\tau^n = 0$  and  $\mathbf{u}_\tau^n = 0$  for all  $n$ . It follows that  $\nabla^\mathfrak{D} p_\mathfrak{D}^n = 0$  and thus  $p_\mathfrak{D}^n = 0$  for any  $n$ . As a consequence, the only solution of the homogeneous linear problem associated with  $(\mathcal{P}_0)$  is zero; this proves that  $(\mathcal{P}_0)$  is well-posed. The estimates given below will clearly show that its solution belongs to  $K$  and thus the property (a) is proved.

Let  $\delta \in [0, 1]$ . Let us assume that there is a solution of  $(P_\delta)$  in  $K$ . We are going to show that (for a suitable choice of  $M_0$  and  $C_{\tau, \Delta t}$ ) this solution necessarily satisfies the same estimates as (4.25) and (4.28) but with strict inequalities. This will obviously imply the property (b).

We begin with the study of the first term in the right hand side of (4.27)

$$\begin{aligned} \delta \Delta t \llbracket \mathcal{G}^\tau(c_\tau^{n+1}, \mu_\tau^{n+1}), \mathbf{u}_\tau^{n+1} - \mathbf{u}_\tau^n - \mathbf{w}_\tau \rrbracket_\tau \\ = \delta \Delta t \llbracket \mathcal{G}^\tau(c_\tau^{n+1}, \mu_\tau^{n+1}), \mathbf{u}_\tau^{n+1} - \mathbf{u}_\tau^n \rrbracket_\tau - \delta \Delta t \llbracket \mathcal{G}^\tau(c_\tau^{n+1}, \mu_\tau^{n+1}), \mathbf{w}_\tau \rrbracket_\tau. \end{aligned} \tag{4.29}$$

Thanks to Lemma 4.5, the Young inequality and since  $\delta \leq 1$  the first term in (4.29) satisfies,

$$\delta \Delta t \llbracket \mathcal{G}^\tau(c_\tau^{n+1}, \mu_\tau^{n+1}), \mathbf{u}_\tau^{n+1} - \mathbf{u}_\tau^n \rrbracket_\tau \leq \frac{1}{4} \|\mathbf{u}_\tau^{n+1} - \mathbf{u}_\tau^n\|_\tau^2 + \Delta t^2 \left\| \mathcal{G}^\tau(c_\tau^{n+1}, \widetilde{\mu_\tau^{n+1}}) \right\|_\tau^2$$

where  $\widetilde{\mu_\tau^{n+1}}$  is defined by (4.12) in such a way that  $M_{\text{opt}}(\widetilde{\mu_\tau^{n+1}}) = M_{\text{opt}^*}(\widetilde{\mu_\tau^{n+1}}) = 0$ .

Applying Corollary 4.7 (with  $\alpha/2$  instead of  $\alpha$ ) and using bound (4.25b) we get

$$\begin{aligned} \Delta t^2 \left\| \mathcal{G}^\tau(c_\tau^{n+1}, \widetilde{\mu_\tau^{n+1}}) \right\|_\tau^2 & \leq \frac{C_{11}^2 \Delta t^2}{\text{size}(\mathcal{T})^\alpha} \|\nabla^\mathfrak{D} c_\tau^{n+1}\|_\mathfrak{D}^2 \|\nabla^\mathfrak{D} \widetilde{\mu_\tau^{n+1}}\|_\mathfrak{D}^2 \\ & \leq \frac{C_{11}^2 M_0 \Delta t^2}{\text{size}(\mathcal{T})^\alpha} \|\nabla^\mathfrak{D} \widetilde{\mu_\tau^{n+1}}\|_\mathfrak{D}^2. \end{aligned}$$

Thus, if  $\Delta t \leq \Delta t_1 := \frac{\text{size}(\mathcal{T})^\alpha}{4C_{11}^2 M_0}$ , noting that  $\|\nabla^{\mathfrak{D}} \widetilde{\mu_{\mathcal{T}}^{n+1}}\|_{\mathfrak{D}} = \|\nabla^{\mathfrak{D}} \mu_{\mathcal{T}}^{n+1}\|_{\mathfrak{D}}$ , we obtain

$$\delta \Delta t \llbracket \mathcal{G}^{\mathcal{T}}(c_{\mathcal{T}}^{n+1}, \mu_{\mathcal{T}}^{n+1}), \mathbf{u}_{\mathcal{T}}^{n+1} - \mathbf{u}_{\mathcal{T}}^n \rrbracket_{\mathcal{T}} \leq \frac{1}{4} \|\mathbf{u}_{\mathcal{T}}^{n+1} - \mathbf{u}_{\mathcal{T}}^n\|_{\mathcal{T}}^2 + \frac{\Delta t}{4} \|\nabla^{\mathfrak{D}} \mu_{\mathcal{T}}^{n+1}\|_{\mathfrak{D}}^2. \quad (4.30)$$

As far as the second term in (4.29) is concerned, we use Lemma 4.5, the Hölder inequality and Proposition 4.6 to obtain,

$$\begin{aligned} \llbracket \mathcal{G}^{\mathcal{T}}(c_{\mathcal{T}}^{n+1}, \mu_{\mathcal{T}}^{n+1}), \mathbf{w}_{\mathcal{T}} \rrbracket_{\mathcal{T}} &\leq \|\mathcal{G}^{\mathcal{T}}(c_{\mathcal{T}}^{n+1}, \mu_{\mathcal{T}}^{n+1})\|_{4/3, \mathcal{T}} \|\mathbf{w}_{\mathcal{T}}\|_{4, \mathcal{T}} \\ &\leq C_{10} \|\nabla^{\mathfrak{D}} c_{\mathcal{T}}^{n+1}\|_{\mathfrak{D}} \|\widetilde{\mu_{\mathcal{T}}^{n+1}}\|_{4, \mathcal{T}} \|\mathbf{w}_{\mathcal{T}}\|_{4, \mathcal{T}}. \end{aligned}$$

Thus thanks to Theorems 2.8, 2.12 and 3.1 we have

$$\llbracket \mathcal{G}^{\mathcal{T}}(c_{\mathcal{T}}^{n+1}, \mu_{\mathcal{T}}^{n+1}), \mathbf{w}_{\mathcal{T}} \rrbracket_{\mathcal{T}} \leq 2C_2 C_5 C_9 C_{10} \|\mathbf{u}_{\mathbf{b}}\|_{H^{1/2}(\Gamma)} \|\nabla^{\mathfrak{D}} c_{\mathcal{T}}^{n+1}\|_{\mathfrak{D}} \|\nabla^{\mathfrak{D}} \mu_{\mathcal{T}}^{n+1}\|_{\mathfrak{D}}.$$

Using the Young inequality, we deduce

$$\Delta t \llbracket \mathcal{G}^{\mathcal{T}}(c_{\mathcal{T}}^{n+1}, \mu_{\mathcal{T}}^{n+1}), \mathbf{w}_{\mathcal{T}} \rrbracket_{\mathcal{T}} \leq \frac{\Delta t}{4} \|\nabla^{\mathfrak{D}} \mu_{\mathcal{T}}^{n+1}\|_{\mathfrak{D}}^2 + 4\Delta t C_2^2 C_5^2 C_9^2 C_{10}^2 \|\mathbf{u}_{\mathbf{b}}\|_{H^{1/2}(\Gamma)}^2 \|\nabla^{\mathfrak{D}} c_{\mathcal{T}}^{n+1}\|_{\mathfrak{D}}^2.$$

Let us set  $C_{14} := 4C_2^2 C_5^2 C_9^2 C_{10}^2$ , if we choose  $\Delta t \leq \Delta t_2 := \frac{1}{8C_{14} \|\mathbf{u}_{\mathbf{b}}\|_{H^{1/2}(\Gamma)}^2}$  we have,

$$\begin{aligned} \Delta t \delta \llbracket \mathcal{G}^{\mathcal{T}}(c_{\mathcal{T}}^{n+1}, \mu_{\mathcal{T}}^{n+1}), \mathbf{w}_{\mathcal{T}} \rrbracket_{\mathcal{T}} &\leq \frac{\Delta t}{4} \|\nabla^{\mathfrak{D}} \mu_{\mathcal{T}}^{n+1}\|_{\mathfrak{D}}^2 + \frac{1}{4} \|\nabla^{\mathfrak{D}}(c_{\mathcal{T}}^{n+1} - c_{\mathcal{T}}^n)\|_{\mathfrak{D}}^2 \\ &\quad + 2C_{14} \|\mathbf{u}_{\mathbf{b}}\|_{H^{1/2}(\Gamma)}^2 \Delta t \|\nabla^{\mathfrak{D}} c_{\mathcal{T}}^n\|_{\mathfrak{D}}^2. \end{aligned} \quad (4.31)$$

Finally, since  $\mathbf{u}_{\mathcal{T}}^{n+1} - \mathbf{w}_{\mathcal{T}} \in \mathbb{E}_0$  we can use the Poincaré inequality and the Young inequality, so that the last term in the right hand side of (4.27) satisfies

$$\delta \Delta t \llbracket \rho(c_{\mathcal{T}}^{n+1}) \mathbf{g}, \mathbf{u}_{\mathcal{T}}^{n+1} - \mathbf{w}_{\mathcal{T}} \rrbracket_{\mathcal{T}} \leq \frac{\Delta t}{2} \|\nabla^{\mathfrak{D}}(\mathbf{u}_{\mathcal{T}}^{n+1} - \mathbf{w}_{\mathcal{T}})\|_{\mathfrak{D}}^2 + \Delta t \frac{C_3^2}{2} \|\rho\|_{L^\infty}^2 |\mathbf{g}|^2. \quad (4.32)$$

Gathering estimates (4.27)–(4.32) and assuming that  $\Delta t \leq \min(\Delta t_1, \Delta t_2)$ , we have obtained

$$\begin{aligned} &\left( \mathcal{F}_{\mathcal{T}}^\delta(c_{\mathcal{T}}^{n+1}) + \frac{1}{2} \|\mathbf{u}_{\mathcal{T}}^{n+1} - \mathbf{w}_{\mathcal{T}}\|_{\mathcal{T}}^2 \right) - \left( \mathcal{F}_{\mathcal{T}}^\delta(c_{\mathcal{T}}^n) + \frac{1}{2} \|\mathbf{u}_{\mathcal{T}}^n - \mathbf{w}_{\mathcal{T}}\|_{\mathcal{T}}^2 \right) \\ &\quad + \frac{\Delta t}{2} \|\nabla^{\mathfrak{D}} \mu_{\mathcal{T}}^{n+1}\|_{\mathfrak{D}}^2 + \frac{\Delta t}{2} \|\nabla^{\mathfrak{D}}(\mathbf{u}_{\mathcal{T}}^{n+1} - \mathbf{w}_{\mathcal{T}})\|_{\mathfrak{D}}^2 + \frac{1}{4} \|\mathbf{u}_{\mathcal{T}}^{n+1} - \mathbf{u}_{\mathcal{T}}^n\|_{\mathcal{T}}^2 \\ &\quad + \frac{1}{4} \|\nabla^{\mathfrak{D}}(c_{\mathcal{T}}^{n+1} - c_{\mathcal{T}}^n)\|_{\mathfrak{D}}^2 + \frac{1}{\Delta t} \|c_{\partial \mathcal{T}}^{n+1} - c_{\partial \mathcal{T}}^n\|_{\partial \mathcal{T}}^2 \\ &\leq \Delta t \frac{C_3^2}{2} \|\rho\|_{L^\infty}^2 |\mathbf{g}|^2 + 2C_{14}^2 \|\mathbf{u}_{\mathbf{b}}\|_{H^{1/2}(\Gamma)}^2 \Delta t \|\nabla^{\mathfrak{D}} c_{\mathcal{T}}^n\|_{\mathfrak{D}}^2. \end{aligned} \quad (4.33)$$

Setting  $E^n = \mathcal{F}_{\mathcal{T}}^\delta(c_{\mathcal{T}}^n) + \frac{1}{2} \|\mathbf{u}_{\mathcal{T}}^n - \mathbf{w}_{\mathcal{T}}\|_{\mathcal{T}}^2$ , and using (1.5), we have proved that

$$E^{n+1} - E^n \leq \Delta t \frac{C_3^2}{2} \|\rho\|_{L^\infty}^2 |\mathbf{g}|^2 + 4C_{14}^2 \|\mathbf{u}_{\mathbf{b}}\|_{H^{1/2}(\Gamma)}^2 \Delta t E^n.$$

From the discrete Gronwall lemma, we deduce that, for all  $n$ ,

$$E^n \leq \left( E^0 + T \frac{C_3^2}{2} \|\rho\|_{L^\infty}^2 |\mathbf{g}|^2 \right) e^{4C_{14}^2 \|\mathbf{u}_{\mathbf{b}}\|_{H^{1/2}(\Gamma)}^2 T}.$$

By Lemma 4.10 and Theorem 3.1, we have

$$E^0 \leq C_{13}(1 + \|c_0\|_{H^1(\Omega)}^{p+1}) + C_{13}^2 \|\mathbf{u}_0\|_{L^2(\Omega)}^2 + C_9^2 \|\mathbf{u}_b\|_{H^{1/2}(\Gamma)}^2.$$

All these estimates show that, for some  $M_1 > 0$ , we have

$$\sup_{n \leq N} \left( \|\nabla^{\mathcal{D}} c_{\mathcal{T}}^n\|_{\mathfrak{D}}^2 + \|\mathbf{u}_{\mathcal{T}}^n\|_{\mathcal{T}}^2 \right) \leq M_1. \quad (4.34)$$

Coming back to (4.33), we find that for some  $M_2 > 0$ , we have

$$\sum_{n=0}^{N-1} \left( \Delta t \|\nabla^{\mathcal{D}} \mu_{\mathcal{T}}^{n+1}\|_{\mathfrak{D}}^2 + \Delta t \|\nabla^{\mathcal{D}} \mathbf{u}_{\mathcal{T}}^{n+1}\|_{\mathfrak{D}}^2 + \Delta t \left\| \frac{c_{\partial\mathcal{T}}^{n+1} - c_{\partial\mathcal{T}}^n}{\Delta t} \right\|_{\partial\mathcal{T}}^2 \right) \leq M_2. \quad (4.35)$$

Observe next that the volume conservation property (4.16) still holds for the problem  $(\mathcal{P}_\delta)$ , so that with Lemma 4.10 we obtain that

$$\sup_{n \leq N} \left( |M_{\mathfrak{M}}(c_{\mathcal{T}}^n)| + |M_{\overline{\mathfrak{M}}^*}(c_{\mathcal{T}}^n)| \right) \leq C_{13} \|c_0\|_{H^1(\Omega)}.$$

Therefore, we can deduce from Theorem 2.12 that, for a suitable  $M_3 > 0$ ,

$$\sup_{n \leq N} \|c_{\mathcal{T}}^n\|_{\mathcal{T}}^2 \leq M_3. \quad (4.36)$$

We shall now estimate the primal and dual mean values of the chemical potential. By summing the equations (4.14a)–(4.14d) of the problem  $(\mathcal{P}_\delta)$  with suitable weights that are respectively the measures of the primal edges and the measures of the boundary primal edges, we obtain

$$M_{\mathfrak{M}}(\mu_{\mathcal{T}}^{n+1}) = \delta M_{\mathfrak{M}}(d^{fb}(c_{\mathfrak{M}}^n, c_{\mathfrak{M}}^{n+1})) + \delta M_{\partial\mathfrak{M}}(d^{fs}(c_{\partial\mathfrak{M}}^n, c_{\partial\mathfrak{M}}^{n+1})) + M_{\partial\mathfrak{M}} \left( \frac{c_{\partial\mathfrak{M}}^{n+1} - c_{\partial\mathfrak{M}}^n}{\Delta t} \right).$$

Similarly, by summing the equations (4.14b) and (4.14c) with the corresponding weights, we get

$$M_{\overline{\mathfrak{M}}^*}(\mu_{\mathcal{T}}^{n+1}) = \delta M_{\overline{\mathfrak{M}}^*}(d^{fb}(c_{\overline{\mathfrak{M}}^*}^n, c_{\overline{\mathfrak{M}}^*}^{n+1})) + \delta M_{\partial\overline{\mathfrak{M}}^*}(d^{fs}(c_{\partial\overline{\mathfrak{M}}^*}^n, c_{\partial\overline{\mathfrak{M}}^*}^{n+1})) + M_{\partial\overline{\mathfrak{M}}^*} \left( \frac{c_{\partial\overline{\mathfrak{M}}^*}^{n+1} - c_{\partial\overline{\mathfrak{M}}^*}^n}{\Delta t} \right).$$

Using the Cauchy–Schwarz inequality, the property (3.8), the trace theorem 2.13, and the bounds (4.34), (4.35), (4.36), we deduce that, for some  $M_4 > 0$ , we have

$$\sum_{n=0}^{N-1} \Delta t (|M_{\mathfrak{M}}(\mu_{\mathcal{T}}^{n+1})|^2 + |M_{\overline{\mathfrak{M}}^*}(\mu_{\mathcal{T}}^{n+1})|^2) \leq M_4. \quad (4.37)$$

With (4.35), (4.37) and the Poincaré–Wirtinger inequality given in Theorem 2.12, we finally obtain for some  $M_5 > 0$ , that

$$\sum_{n=0}^{N-1} \Delta t \|\mu_{\mathcal{T}}^{n+1}\|_{\mathcal{T}}^2 \leq M_5.$$

Finally, for any  $\mathbf{v}_{\mathcal{T}} \in \mathbb{E}_0$ , we deduce from the momentum equation, that

$$\begin{aligned} \llbracket \nabla^{\mathcal{D}} p_{\mathfrak{D}}^{n+1}, \mathbf{v}_{\mathcal{T}} \rrbracket_{\mathcal{T}} &= -\frac{1}{\Delta t} \llbracket \mathbf{u}_{\mathcal{T}}^{n+1} - \mathbf{u}_{\mathcal{T}}^n, \mathbf{v}_{\mathcal{T}} \rrbracket_{\mathcal{T}} - (\nabla^{\mathcal{D}} \mathbf{u}_{\mathcal{T}}^{n+1} : \nabla^{\mathcal{D}} \mathbf{v}_{\mathcal{T}})_{\mathfrak{D}} \\ &\quad + \delta \llbracket \mathcal{G}^{\mathcal{T}}(c_{\mathcal{T}}^{n+1}, \mu_{\mathcal{T}}^{n+1}), \mathbf{v}_{\mathcal{T}} \rrbracket_{\mathcal{T}} + \delta \llbracket \rho(c_{\mathcal{T}}^{n+1}) \mathbf{g}, \mathbf{v}_{\mathcal{T}} \rrbracket_{\mathcal{T}} \\ &\leq \left( \frac{2\sqrt{M_1}}{\Delta t} + \frac{C_{11}}{\sqrt{\Delta t \text{size}(\mathcal{T})^{2/q}}} \sqrt{M_1 M_2} + \|\rho\|_{\infty} |\mathbf{g}| \right) \|\mathbf{v}_{\mathcal{T}}\|_{\mathcal{T}} + \frac{\sqrt{M_2}}{\sqrt{\Delta t}} \|\nabla^{\mathcal{D}} \mathbf{v}_{\mathcal{T}}\|_{\mathfrak{D}}. \end{aligned}$$

Using that  $m(p_{\mathfrak{D}}^{n+1}) = 0$ , the Poincaré inequality (Thm. 2.9), and the inf-sup inequality (3.3), we obtain the bound (4.28) with a strict inequality, provided that  $C_{\mathcal{T}, \Delta t}$  is chosen large enough.

To conclude the proof, it is enough to choose a  $M_0$  satisfying

$$M_0 > \max(M_1 + M_3, M_2 + M_5). \quad \square$$

TABLE 1. Physical parameters (common to all simulations).

$\sigma_b$	$\mathcal{R}_e$	$\rho_{c=0} = \rho^*$	$\mathbf{g}$
24.5	100	1000	$-0.98 \mathbf{e}_y$

TABLE 2. Parameters for the droplet spreading simulations.

	$\Gamma_b$	$\varepsilon$	$D_s$	$\theta_s$	$\rho_{c=1}/\rho_{c=0}$
Case 1 (Fig. 10)	$10^{-5}$	0.05	0.05	$\frac{\pi}{3}$ or $\frac{2\pi}{3}$	1
Case 2 (Fig. 11)	$10^{-5}$	0.05	0.05	$\frac{\pi}{3}$ or $\frac{2\pi}{3}$	0.1

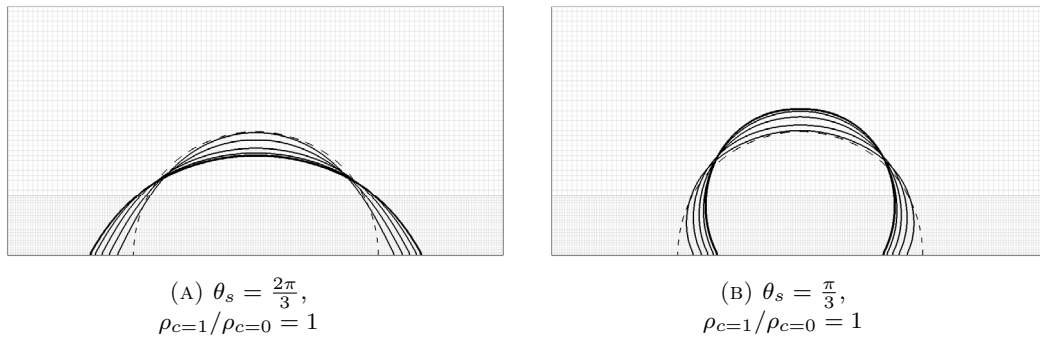


FIGURE 10. Case 1: Comparison of two different static contact angles; no buoyancy effects.

## 5. NUMERICAL RESULTS

We present now three families of numerical simulations obtained by means of the presented numerical method for our phase-field model with nonlinear dynamic boundary condition.

For all the simulations below, we consider a set of parameters taken from the benchmark proposed in [24] and that we summarise in Table 1. The other parameters will vary from one test to another and will be precised in each subsection.

### 5.1. Droplet spreading

We aim at simulating the spreading of a droplet on a solid surface so as to observe the influence of the wetting parameters as well as the influence of buoyancy effects.

The computational domain  $\Omega$  is the rectangle  $]0, 2[\times] - 0.5, 0.5[$ . We consider the homogeneous Dirichlet boundary condition for the velocity, namely  $\mathbf{u}_b = 0$  and at time  $t = 0$  the velocity is zero. The initial shape of the droplet is a half-circle whose center is at  $(1, -0.5)$  (see the dashed line in Figs. 10 and 11). In order to be more accurate near the contact point and to illustrate the robustness of our numerical method on general grids, the simulation is computed on a non-conforming Cartesian mesh (the bottom quarter of the domain is refined). The primal cells size for the coarse grid is 0.028 and 0.014 in the fine grid, and the time step is  $\Delta t = 10^{-3}$ .

On each figure, in order to visualise the time evolution of the droplet, we plot the isolines  $c = 0.5$  are various times  $t = 0$  (dashed line),  $t = 1, 2, 3, 4$  (thin solid lines) and the final time  $t = 5$  (thick solid line). The physical parameters used are those given in Table 1 and in Table 2.



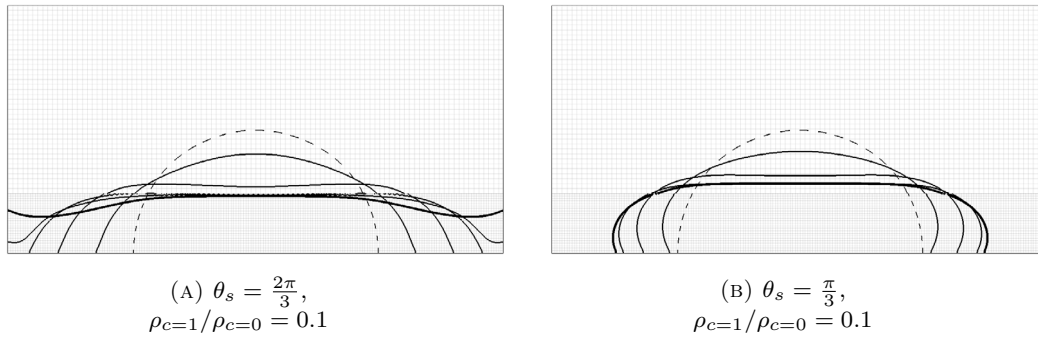


FIGURE 11. Case 2: Comparison of two different static contact angles; with buoyancy effects.

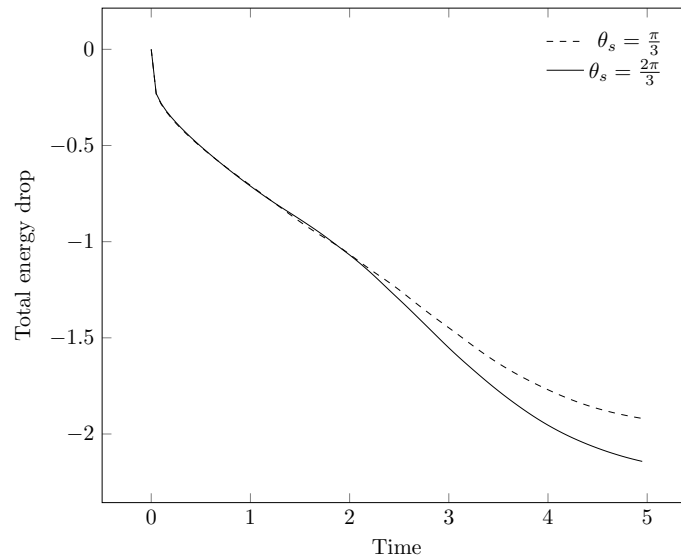


FIGURE 12. Case 1: Evolution of the energy drop as a function of time.

- In Case 1, the densities of the two phases are the same, so that there is no buoyancy effects. We observe the dynamics of the interface for the two values of the static contact angle  $\theta_s$ . When  $\theta_s = \frac{2\pi}{3}$  the droplet is wetting whereas when  $\theta_s = \frac{\pi}{3}$  it is non wetting.
- In Case 2, the density ratio between the two phases is 0.1, and we can observe the influence of buoyancy effects on the dynamics of the interface compared to the Case 1. Due to the gravity, the spreading of the droplet is increased and the shape of the interface is no more circular at the equilibrium.

The results are qualitatively similar to those reported in the literature (see [42,43] for example and the references therein).

Moreover, in Case 1 we can observe that the numerical method actually dissipates the total energy. To this end, we plot in Figure 12 the evolution of the energy drop (that is the difference between the total energy at time  $t$  and the initial total energy) as a function of time. In Case 2 a similar plot is not relevant since the energy may locally increase due to the power of buoyancy forces.

TABLE 3. Parameters for the inclined plane simulation, see Figures 13 and 14.

$\Gamma_b$	$\varepsilon$	$D_s$	$\theta_s$	$\rho_{c=1}/\rho_{c=0}$
$10^{-4}$	0.05	0.05 or 5	$\frac{\pi}{3}$ or $\frac{2\pi}{3}$	0.1

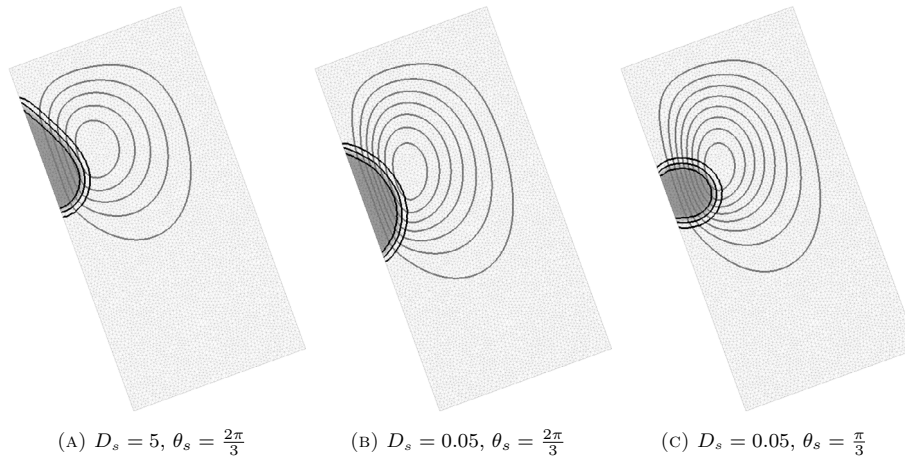


FIGURE 13. Falling drop simulations at time  $t = 3$ .

### 5.2. Falling drop on an inclined plane

We would like now to illustrate the influence of the relaxation parameter  $D_s$  on the dynamics of the contact angle. To this end we propose a simulation of a droplet that falls under the effect of gravity alongside an inclined plane.

The computational domain  $\Omega$  is the rectangle  $] - 0.5, 0.5[ \times ] 0, 2[$  that we incline with the angle  $\alpha = 70^\circ$  with respect to the horizontal axis. The primal mesh is made of conforming triangles whose maximal diameter is around 0.03 and the time step is  $\Delta t = 10^{-3}$ . We consider the homogeneous Dirichlet boundary condition for the velocity:  $\mathbf{u}_b = 0$ .

At time  $t = 0$  the velocity is zero and the initial interface is a half-circle of radius  $R = 0.25$  centered at  $(x_0, y_0) = (0.35, -0.5)$ . More precisely, the initial concentration  $c_0$  we used is given by the formula

$$c_0(x, y) := \frac{1}{2} \left( 1 + \tanh \left( \frac{\sqrt{(x - x_0)^2 + (y - y_0)^2} - R}{0.01\sqrt{2}} \right) \right).$$

We represent the solution, for various values of the parameters  $D_s$  and  $\theta_s$ , at times  $t = 3$  (in Fig. 13) and  $t = 10$  (in Fig. 14) by using the following visualisation rules:

- We plot the three isolines  $c \in \{0.1, 0.5, 0.9\}$  of the order parameter with black lines to represent the interface position and its actual thickness;
- The zone where  $c = 0$  is filled in gray, whereas the zone where  $c = 1$  is left in white;
- We plot uniformly distributed isolines of the stream function with thin grey lines.

We can make the following observations:

- For a fixed static contact-angle ( $\theta_s = \frac{2\pi}{3}$  here), when  $D_s = 5$  (see Figs. 13a and 14a) the falling velocity of the droplet is lower than for  $D_s = 0.05$  (see Figs. 13b and 14b).

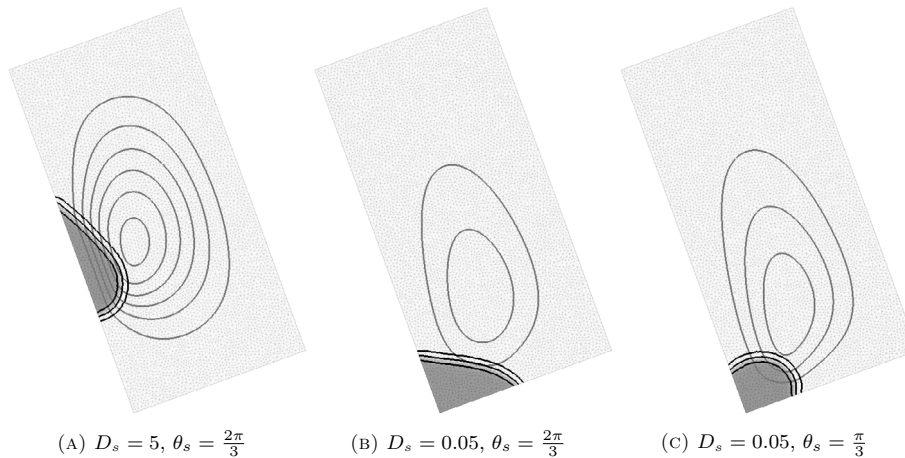
FIGURE 14. Falling drop simulations at time  $t = 10$ .

TABLE 4. Parameters for driven cavity simulations, see Figures 16 and 17.

$\Gamma_b$	$\varepsilon$	$D_s$	$\theta_s$	$\rho_{c=1}/\rho_{c=0}$
$10^{-4}$	0.04	0.2	$\frac{\pi}{3}$ or $\frac{2\pi}{3}$	1

This phenomenon is the one expected for the chosen dynamic boundary condition. Indeed, in the asymptotics  $D_s \rightarrow +\infty$ , the boundary condition becomes  $\partial_t c_{\Gamma} = 0$  on  $\Gamma$  and thus, the values of the order parameter on the boundary should not depend on time. This would imply, in this limit, that the interface do not move.

- For the same fixed static contact-angle, when  $D_s = 0.05$  (see Figs. 13b and 14b) we observe that the actual contact-angle between the wall and the interface is established almost instantaneously at both contact points to the given value of the static contact angle. This is in accordance with the mathematical structure of the dynamic boundary condition. Indeed, in the limit  $D_s \rightarrow 0$  the boundary condition becomes  $\partial_n c = -f'_s(c_{\Gamma})$ , which is built so as to impose at each given time  $t$  the contact angle to the prescribed static value. By contrast, in the case where  $D_s = 5$  (see Figs. 13a and 14a) we observe different that the actual contact angles are different at the front and at the back of the droplet, and they are not equal to the fixed static contact angle  $\theta_s$ . Moreover, those actual contact angles evolve during time until they achieve the prescribed static value once a steady state is achieved.

### 5.3. Driven cavity

Here the computational domain  $\Omega$  is the unit square  $]0, 1[^2$  and the simulation is performed on a non-conforming Cartesian mesh (see Fig. 15a). The cells size for the coarse grid is 0.028 and 0.014 in the fine grid, and the time step is  $10^{-3}$ . The other parameters used are summarised in Table 4. We perform two different simulations with two different values of the static contact angle, so that in one case the wetting phase is either the one represented by  $c = 0$  or the one represented by  $c = 1$ .

The non-homogeneous Dirichlet boundary condition chosen for the velocity (which generates the flow) is  $\mathbf{u}_b = (4, 0)$  on the top side of the cavity and  $\mathbf{u}_b = (0, 0)$  elsewhere. Due to the singularity of this boundary data at the top corners of the cavity (it does not satisfy (1.2)) we decided to refine the mesh near those singular points.

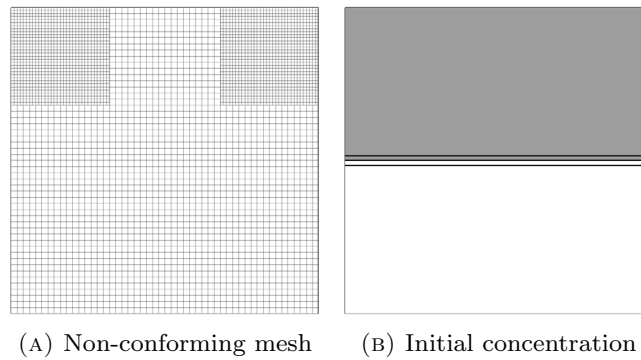


FIGURE 15. Primal mesh  $\mathfrak{M}$  and initial data for the driven cavity simulations.

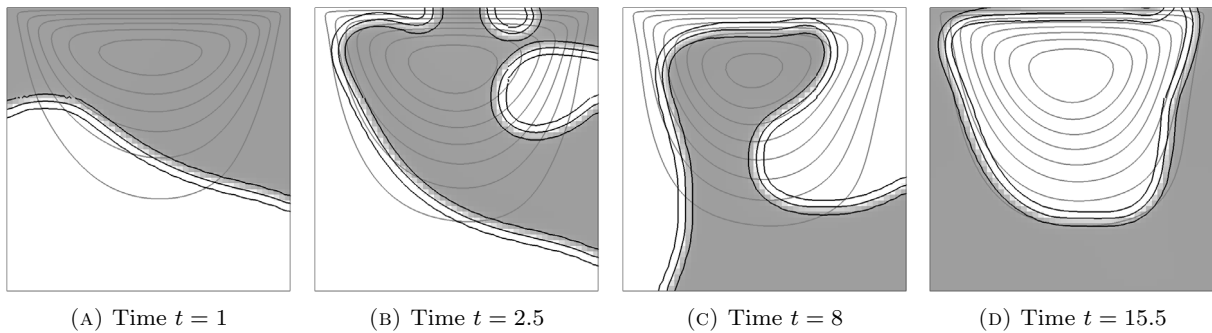


FIGURE 16. Evolution of the driven cavity for a static contact-angle  $\theta_s = \frac{2\pi}{3}$ .

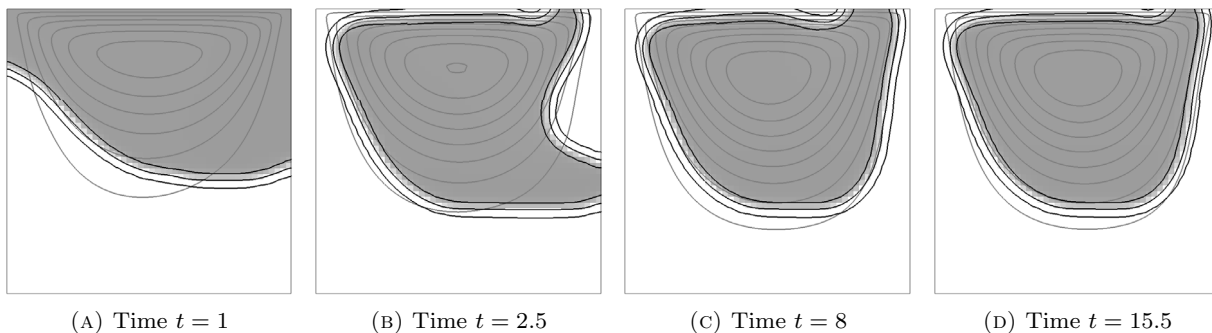


FIGURE 17. Evolution of the driven cavity for a static contact-angle  $\theta_s = \frac{\pi}{3}$ .

We observe that, from the very beginning of the simulation (see Figs. 16a and 17a), the solution advances in such a way to satisfy the prescribed contact-angle, since  $D_s$  is small. Then, the solution evolves very differently depending on which of the two phases is wetting:

- When the phase  $c = 0$  is wetting (that is, with our convention,  $\theta_s = \frac{2\pi}{3}$ , see Fig. 16), there is a competition between the effects of the rotating flow and the fact that the gray phase is preferred by the wall.
- When the phase  $c = 1$  is wetting ( $\theta_s = \frac{\pi}{3}$ , see Fig. 17), there is no more competition.

In both cases the steady-states achieved are similar (with of course the phases  $c = 0$  and  $c = 1$  that are exchanged so that the wetting phase is in contact with the boundary) but the dynamics is rather different.

## APPENDIX A. THE DDFV METHOD FOR THE NON-HOMOGENEOUS STOKES PROBLEM

We gather in this appendix the main results concerning the DDFV approximation of the non-homogeneous Stokes problem. In particular, we aim at proving the lifting Theorem 3.1.

**Lemma A.1.** *Let  $\mathbf{u}_b$  satisfying (1.2) and  $\mathbf{v}_T \in \mathbb{E}_{\mathbf{u}_b}$ , then  $m(\operatorname{div}^{\mathfrak{D}} \mathbf{v}_T) = 0$ .*

*Proof.* By the Definition 2.3, we have

$$2|\Omega|m(\operatorname{div}^{\mathfrak{D}} \mathbf{v}_T) = \sum_{\mathfrak{D} \in \mathfrak{D}} [m_{\sigma}(\mathbf{v}_{\mathcal{L}} - \mathbf{v}_{\mathcal{K}}) \cdot \vec{\mathbf{n}}_{\sigma\mathcal{K}} + m_{\sigma^*}(\mathbf{v}_{\mathcal{L}^*} - \mathbf{v}_{\mathcal{K}^*}) \cdot \vec{\mathbf{n}}_{\sigma^*\mathcal{K}^*}].$$

We can rewrite this quantity as sums over the primal and dual unknowns as follows

$$\begin{aligned} 2|\Omega|m(\operatorname{div}^{\mathfrak{D}} \mathbf{v}_T) = & - \sum_{\mathcal{K} \in \mathfrak{M}} \mathbf{v}_{\mathcal{K}} \cdot \left( \sum_{\sigma \in \mathcal{E}_{\mathcal{K}}} m_{\sigma} \vec{\mathbf{n}}_{\sigma\mathcal{K}} \right) + \sum_{\mathcal{L} \in \partial\mathfrak{M}} m_{\sigma} \mathbf{v}_{\mathcal{L}} \cdot \vec{\mathbf{n}}_{\sigma\mathcal{L}} \\ & - \sum_{\mathcal{K}^* \in \mathfrak{M}^*} \mathbf{v}_{\mathcal{K}^*} \cdot \left( \sum_{\sigma^* \in \mathcal{E}_{\mathcal{K}^*}} m_{\sigma^*} \vec{\mathbf{n}}_{\sigma^*\mathcal{K}^*} \right) - \sum_{\mathcal{K}^* \in \partial\mathfrak{M}^*} \mathbf{v}_{\mathcal{K}^*} \cdot \left( \sum_{\sigma^* \in \mathcal{E}_{\mathcal{K}^*}} m_{\sigma^*} \vec{\mathbf{n}}_{\sigma^*\mathcal{K}^*} \right). \end{aligned}$$

Observe in particular in this formula that the boundary primal unknowns appear in the contribution of one single diamond cell whereas the boundary dual unknowns may appear in the contribution of several diamond cells (see for instance Fig. A.1 where the unknown  $\mathbf{v}_{\mathcal{K}^*}$  is concerned with three diamond cells).

We now claim that we have

$$\begin{aligned} \sum_{\sigma \in \mathcal{E}_{\mathcal{K}}} m_{\sigma} \vec{\mathbf{n}}_{\sigma\mathcal{K}} &= \int_{\partial\mathcal{K}} \operatorname{Id} \cdot \vec{\mathbf{n}} = \int_{\mathcal{K}} \operatorname{div}(\operatorname{Id}) = 0, \quad \forall \mathcal{K} \in \mathfrak{M}, \\ \sum_{\sigma^* \in \mathcal{E}_{\mathcal{K}^*}} m_{\sigma^*} \vec{\mathbf{n}}_{\sigma^*\mathcal{K}^*} &= \int_{\partial\mathcal{K}^*} \operatorname{Id} \cdot \vec{\mathbf{n}} = \int_{\mathcal{K}^*} \operatorname{div}(\operatorname{Id}) = 0, \quad \forall \mathcal{K}^* \in \mathfrak{M}^*. \end{aligned}$$

Moreover, since  $\mathbf{v}_T \in \mathbb{E}_{\mathbf{u}_b}$ , and by the Definition 2.1 of the projection  $\tilde{\mathbb{P}}_m^T$  and (1.2), we see that

$$\mathbf{v}_{\mathcal{L}} \cdot \vec{\mathbf{n}}_{\sigma\mathcal{L}} = \frac{1}{m_{\sigma}} \int_{\sigma} \mathbf{u}_b \cdot \vec{\mathbf{n}}_{\sigma\mathcal{L}} = 0, \quad \forall \mathcal{L} \in \partial\mathfrak{M}.$$

At this point we have shown that

$$2|\Omega|m(\operatorname{div}^{\mathfrak{D}} \mathbf{v}_T) = \sum_{\mathcal{K}^* \in \partial\mathfrak{M}^*} \mathbf{v}_{\mathcal{K}^*} \cdot \left( \sum_{\sigma^* \in \mathcal{E}_{\mathcal{K}^*}} m_{\sigma^*} \vec{\mathbf{n}}_{\sigma^*\mathcal{K}^*} \right), \quad (\text{A.1})$$

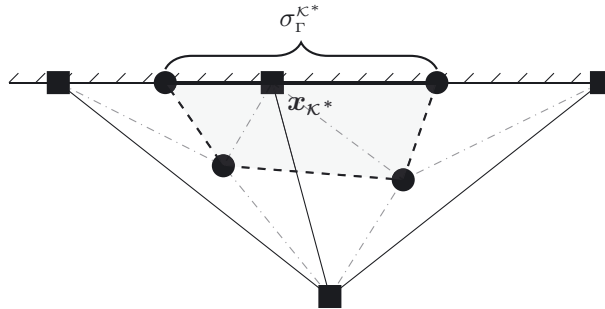


FIGURE A.1. The case of boundary dual unknowns.

and it remains to evaluate the contribution of the boundary dual unknowns. By Definition 2.1, such a boundary unknown is zero if  $x_{\mathcal{K}^*}$  is a corner of  $\partial\Omega$ . Hence, we assume that  $x_{\mathcal{K}^*}$  is not a corner of  $\partial\Omega$ . The difference with interior dual control volumes stands in the fact that the boundary of the cell  $\partial\mathcal{K}^*$  is not the union of the dual edges in  $\mathcal{E}_{\mathcal{K}^*}$  since we also need to take into account the “edge”  $\sigma_{\Gamma}^{\mathcal{K}^*}$ , as shown in Figure A.1 for instance. Thus, we can write

$$0 = \int_{\mathcal{K}^*} \operatorname{div}(\operatorname{Id}) = \int_{\partial\mathcal{K}^*} \operatorname{Id} \cdot \vec{\mathbf{n}} = \sum_{\sigma^* \in \mathcal{E}_{\mathcal{K}^*}} m_{\sigma^*} \vec{\mathbf{n}}_{\sigma^* \mathcal{K}^*} + m_{\sigma_{\Gamma}^{\mathcal{K}^*}} \vec{\mathbf{n}}_{\sigma_{\Gamma} \mathcal{K}^*}.$$

The contribution of  $\mathbf{v}_{\mathcal{K}^*}$  in (A.1) can thus be rewritten as follows

$$\mathbf{v}_{\mathcal{K}^*} \cdot \left( \sum_{\sigma^* \in \mathcal{E}_{\mathcal{K}^*}} m_{\sigma^*} \vec{\mathbf{n}}_{\sigma^* \mathcal{K}^*} \right) = -m_{\sigma_{\Gamma}^{\mathcal{K}^*}} \mathbf{v}_{\mathcal{K}^*} \cdot \vec{\mathbf{n}}_{\sigma_{\Gamma} \mathcal{K}^*} = - \int_{\sigma_{\Gamma}^{\mathcal{K}^*}} \mathbf{u}_{\mathbf{b}} \cdot \vec{\mathbf{n}}_{\sigma_{\Gamma} \mathcal{K}^*},$$

and this term is equal to zero by (1.2). The proof is complete. □

**Remark A.2.** In particular, the previous lemma gives that for any  $\mathbf{v}_{\mathcal{T}} \in \mathbb{E}_0$ , we have  $m(\operatorname{div}^{\mathfrak{D}} \mathbf{v}_{\mathcal{T}}) = 0$ .

**Theorem A.3.** *Let  $f_{\mathfrak{D}} \in (\mathcal{M}_2(\mathbb{R}))^{\mathfrak{D}}$ ,  $\mathbf{f}_{\mathcal{T}} \in (\mathbb{R}^2)^{\mathcal{T}}$ , and  $g_{\mathfrak{D}} \in \mathbb{R}^{\mathfrak{D}}$  such that  $m(g_{\mathfrak{D}}) = 0$ , then there exists a unique  $(\mathbf{v}_{\mathcal{T}}, p_{\mathfrak{D}}) \in \mathbb{E}_0 \times \mathbb{R}^{\mathfrak{D}}$  solution to the following Stokes problem:*

$$\begin{cases} \operatorname{div}^{\mathfrak{M}}(-\nabla^{\mathfrak{D}} \mathbf{v}_{\mathcal{T}} + p_{\mathfrak{D}} \operatorname{Id}) = \operatorname{div}^{\mathfrak{M}}(f_{\mathfrak{D}}) + \mathbf{f}_{\mathfrak{M}}, \\ \operatorname{div}^{\mathfrak{M}^*}(-\nabla^{\mathfrak{D}} \mathbf{v}_{\mathcal{T}} + p_{\mathfrak{D}} \operatorname{Id}) = \operatorname{div}^{\mathfrak{M}^*}(f_{\mathfrak{D}}) + \mathbf{f}_{\mathfrak{M}^*}, \\ \operatorname{div}^{\mathfrak{D}} \mathbf{v}_{\mathcal{T}} = g_{\mathfrak{D}}, \\ m(p_{\mathfrak{D}}) = 0. \end{cases} \tag{A.2}$$

Moreover, for some  $C_{15} > 0$  depending only on  $\operatorname{reg}(\mathcal{T})$  and  $\beta_{\mathcal{T}}$ , we have

$$\|\nabla^{\mathfrak{D}} \mathbf{v}_{\mathcal{T}}\|_{\mathfrak{D}} + \|p_{\mathfrak{D}}\|_{\mathfrak{D}} \leq C_{15} (\|f_{\mathfrak{D}}\|_{\mathfrak{D}} + \|g_{\mathfrak{D}}\|_{\mathfrak{D}} + \|\mathbf{f}_{\mathcal{T}}\|_{\mathcal{T}}). \tag{A.3}$$

*Proof.* Observe first that solving the system (A.2) is equivalent to solving the following one

$$\begin{cases} \operatorname{div}^{\mathfrak{M}}(-\nabla^{\mathfrak{D}} \mathbf{v}_{\mathcal{T}} + p_{\mathfrak{D}} \operatorname{Id}) = \operatorname{div}^{\mathfrak{M}}(f_{\mathfrak{D}}) + \mathbf{f}_{\mathfrak{M}}, \\ \operatorname{div}^{\mathfrak{M}^*}(-\nabla^{\mathfrak{D}} \mathbf{v}_{\mathcal{T}} + p_{\mathfrak{D}} \operatorname{Id}) = \operatorname{div}^{\mathfrak{M}^*}(f_{\mathfrak{D}}) + \mathbf{f}_{\mathfrak{M}^*}, \\ \operatorname{div}^{\mathfrak{D}} \mathbf{v}_{\mathcal{T}} + m(p_{\mathfrak{D}}) = g_{\mathfrak{D}}. \end{cases} \tag{A.4}$$

Indeed, using that  $m(g_{\mathfrak{D}}) = 0$  and that  $m(\operatorname{div}^{\mathfrak{D}} \mathbf{v}_{\mathcal{T}}) = 0$  for any  $\mathbf{v}_{\mathcal{T}} \in \mathbb{E}_0$  (see Lem. A.1 and Rem. A.2), we observe that any solution of (A.4) necessarily satisfies  $m(p_{\mathfrak{D}}) = 0$  and is thus a solution of (A.2). Since (A.4) is a linear system with as many unknowns as equations, it is enough to prove that any possible solution  $(\mathbf{v}_{\mathcal{T}}, p_{\mathfrak{D}}) \in \mathbb{E}_0 \times \mathbb{R}^{\mathfrak{D}}$  satisfies the estimate (A.3).

- For any  $\mathbf{w}_{\mathcal{T}} \in \mathbb{E}_0$ , the first two equations in (A.4) lead to

$$- \llbracket \operatorname{div}^{\mathcal{T}}(\nabla^{\mathfrak{D}} \mathbf{v}_{\mathcal{T}}), \mathbf{w}_{\mathcal{T}} \rrbracket_{\mathcal{T}} + \llbracket \nabla^{\mathcal{T}} p_{\mathfrak{D}}, \mathbf{w}_{\mathcal{T}} \rrbracket_{\mathcal{T}} = \llbracket \operatorname{div}^{\mathcal{T}}(f_{\mathfrak{D}}), \mathbf{w}_{\mathcal{T}} \rrbracket_{\mathcal{T}} + \llbracket \mathbf{f}_{\mathcal{T}}, \mathbf{w}_{\mathcal{T}} \rrbracket_{\mathcal{T}}, \tag{A.5}$$

so that, using the Green formulas (Thm. 2.7), the Cauchy–Schwarz inequality and the Poincaré inequality 2.9, we obtain

$$\left( p_{\mathfrak{D}}, \operatorname{div}^{\mathfrak{D}} \mathbf{w}_{\mathcal{T}} \right)_{\mathfrak{D}} \leq (\|\nabla^{\mathfrak{D}} \mathbf{v}_{\mathcal{T}}\|_{\mathfrak{D}} + \|f_{\mathfrak{D}}\|_{\mathfrak{D}} + C_3 \|\mathbf{f}_{\mathcal{T}}\|_{\mathcal{T}}) \|\nabla^{\mathfrak{D}} \mathbf{w}_{\mathcal{T}}\|_{\mathfrak{D}}.$$

By definition of the inf-sup constant (3.3) we deduce

$$\|p_{\mathfrak{D}} - m(p_{\mathfrak{D}})\|_{\mathfrak{D}} \leq \frac{1}{\beta_{\mathcal{T}}} (\|\nabla^{\mathfrak{D}} \mathbf{v}_{\mathcal{T}}\|_{\mathfrak{D}} + \|f_{\mathfrak{D}}\|_{\mathfrak{D}} + C_3 \|\mathbf{f}_{\mathcal{T}}\|_{\mathcal{T}}). \tag{A.6}$$

- Taking  $\mathbf{w}_\mathcal{T} = \mathbf{v}_\mathcal{T}$  in (A.5), the Green formula (since  $\mathbf{v}_\mathcal{T} \in \mathbb{E}_0$ ) and the mass conservation equation, we obtain

$$\begin{aligned} \|\nabla^\mathfrak{D} \mathbf{v}_\mathcal{T}\|_\mathfrak{D}^2 + |\Omega|(m(p_\mathfrak{D}))^2 &= (g_\mathfrak{D}, p_\mathfrak{D})_\mathfrak{D} + \llbracket \mathbf{div}^\mathfrak{T}(f_\mathfrak{D}), \mathbf{v}_\mathcal{T} \rrbracket_\mathfrak{T} + \llbracket \mathbf{f}_\mathcal{T}, \mathbf{v}_\mathcal{T} \rrbracket_\mathfrak{T} \\ &\leq \|g_\mathfrak{D}\|_\mathfrak{D} \|p_\mathfrak{D}\|_\mathfrak{D} + (\|f_\mathfrak{D}\|_\mathfrak{D} + C_3 \|\mathbf{f}_\mathcal{T}\|_\mathfrak{T}) \|\nabla^\mathfrak{D} \mathbf{v}_\mathcal{T}\|_\mathfrak{D}. \end{aligned}$$

Using the Young inequality, we obtain

$$\|\nabla^\mathfrak{D} \mathbf{v}_\mathcal{T}\|_\mathfrak{D}^2 + |\Omega|(m(p_\mathfrak{D}))^2 \leq \left(1 + \frac{3}{\beta_\mathfrak{T}^2}\right) \|g_\mathfrak{D}\|_\mathfrak{D}^2 + 3(\|f_\mathfrak{D}\|_\mathfrak{D} + C_3 \|\mathbf{f}_\mathcal{T}\|_\mathfrak{T})^2. \tag{A.7}$$

- The two previous estimates (A.6) and (A.7) give the required *a priori* estimate and conclude the proof.  $\square$

To build the lifting  $\mathbf{w}_\mathcal{T}$  as in Theorem 3.1 we first need to define a lifting of the boundary data (which is not necessarily divergence free) and which satisfies a suitable discrete  $H^1$ -bound.

**Proposition A.4.** *Let  $\mathbf{u}_\mathbf{b}$  satisfying (1.2). There exists a discrete vector field  $\mathbf{G}_\mathcal{T} \in \mathbb{E}_{\mathbf{u}_\mathbf{b}}$  such that there exists  $C_{16} > 0$  only depending on  $\text{reg}(\mathcal{T})$  and on  $\Omega$  satisfying*

$$\|\mathbf{G}_\mathcal{T}\|_\mathfrak{T} + \|\nabla^\mathfrak{D} \mathbf{G}_\mathcal{T}\|_\mathfrak{D} \leq C_{16} \|\mathbf{u}_\mathbf{b}\|_{H^{1/2}(\Gamma)}. \tag{A.8}$$

*Proof.* Let  $\mathbf{U}_\mathbf{b} \in (H^1(\mathbb{R}^2))^2$  be a lifting of the function  $\mathbf{u}_\mathbf{b} \in (H^{1/2}(\Gamma))^2$  (that is  $\mathbf{U}_{\mathbf{b},\Gamma} = \mathbf{u}_\mathbf{b}$ ) and such that, for some  $C_{17} > 0$  depending only on  $\Omega$ , we have

$$\|\mathbf{U}_\mathbf{b}\|_{H^1(\mathbb{R}^2)} \leq C_{17} \|\mathbf{u}_\mathbf{b}\|_{H^{1/2}(\Gamma)}. \tag{A.9}$$

We set  $\mathbf{G}_\mathcal{T} = \tilde{\mathbb{P}}_m^\mathfrak{T} \mathbf{U}_\mathbf{b}$  (see Def. 2.1) and the claim simply follows from the stability estimate of Proposition 2.14.  $\square$

We can now deduce the

*Proof of Theorem 3.1.* Let  $\mathbf{G}_\mathcal{T} \in \mathbb{E}_{\mathbf{u}_\mathbf{b}}$  given by Proposition A.4. We set  $f_\mathfrak{D} = \nabla^\mathfrak{D} \mathbf{G}_\mathcal{T}$ ,  $\mathbf{f}_\mathcal{T} = 0$  and  $g_\mathfrak{D} = -\text{div}^\mathfrak{D} \mathbf{G}_\mathcal{T}$  and we observe that Lemma A.1 gives  $m(g_\mathfrak{D}) = 0$ .

Thus, we can apply Theorem A.3 and obtain a solution  $(\mathbf{v}_\mathcal{T}, p_\mathfrak{D}) \in \mathbb{E}_0 \times \mathbb{R}^\mathfrak{D}$  to

$$\begin{cases} \mathbf{div}^{\mathfrak{m}}(-\nabla^\mathfrak{D} \mathbf{v}_\mathcal{T} + p_\mathfrak{D} \text{Id}) = \mathbf{div}^{\mathfrak{m}}(\nabla^\mathfrak{D} \mathbf{G}_\mathcal{T}), \\ \mathbf{div}^{\mathfrak{m}^*}(-\nabla^\mathfrak{D} \mathbf{v}_\mathcal{T} + p_\mathfrak{D} \text{Id}) = \mathbf{div}^{\mathfrak{m}^*}(\nabla^\mathfrak{D} \mathbf{G}_\mathcal{T}), \\ \text{div}^\mathfrak{D} \mathbf{v}_\mathcal{T} = -\text{div}^\mathfrak{D} \mathbf{G}_\mathcal{T}, \\ m(p_\mathfrak{D}) = 0, \end{cases}$$

that satisfies the estimates (A.3). We easily deduce that  $\mathbf{w}_\mathcal{T} = \mathbf{v}_\mathcal{T} + \mathbf{G}_\mathcal{T}$  belongs to  $\mathbb{E}_{\mathbf{u}_\mathbf{b}}$  and satisfies the required properties (with  $q_\mathfrak{D} = p_\mathfrak{D}$ ).  $\square$

## REFERENCES

- [1] H. Abels, On a diffuse interface model for two-phase flows of viscous, incompressible fluids with matched densities. *Arch. Ration. Mech. Anal.* **194** (2009) 463–506.
- [2] H. Abels and E. Feireisl, On a diffuse interface model for a two-phase flow of compressible viscous fluids. *Indiana Univ. Math. J.* **57** (2008) 659–698.
- [3] H. Abels, H. Garcke and G. Grün, Thermodynamically consistent, frame indifferent diffuse interface models for incompressible two-phase flows with different densities. *Math. Models Methods Appl. Sci.* **22** (2012) 1150013, 40.
- [4] B. Andreianov, M. Bendahmane, F. Hubert and S. Krell, On 3D DDFV discretization of gradient and divergence operators. I. meshing, operators and discrete duality. *IMA J. Numer. Anal.* **32** (2012) 1574–1603.



- [5] B. Andreianov, F. Boyer and F. Hubert, Discrete duality finite volume schemes for Leray-Lions-type elliptic problems on general 2D meshes. *Numer. Methods Partial Differ. Equ.* **23** (2007) 145–195.
- [6] M. Bessemoulin-Chatard, C. Chainais-Hillairet and F. Filbet. On discrete functional inequalities for some finite volume schemes. *IMA J. Numer. Anal.* **35** (2015) 1125–1149.
- [7] F. Boyer, A theoretical and numerical model for the study of incompressible mixture flows. *Comput. Fluids* **31** (2002) 41–68.
- [8] F. Boyer, F. Hubert and S. Krell, Nonoverlapping Schwarz algorithm for solving two-dimensional m-DDFV schemes. *IMA J. Numer. Anal.* **30** (2010) 1062–1100.
- [9] F. Boyer, S. Krell and F. Nabet, Inf-sup stability of the discrete duality finite volume method for the 2D stokes problem. *Math. Comput.* **84** (2015) 2705–2742.
- [10] F. Boyer, C. Lapuerta, S. Minjeaud, B. Piar and M. Quintard, Cahn–Hilliard/Navier–Stokes model for the simulation of three-phase flows. *Trans. Porous Media* **82** (2010) 463–483.
- [11] F. Boyer and S. Minjeaud, Numerical schemes for a three component Cahn–Hilliard model. *ESAIM: M2AN* **45** (2011) 697–738.
- [12] A. Carlson, M. Do Quang and G. Amberg, Dissipation in rapid dynamic wetting. *J. Fluid Mech.* **682** (2011) 213–240.
- [13] L. Cherfils, M. Petcu and M. Pierre, A numerical analysis of the Cahn–Hilliard equation with dynamic boundary conditions. *Discrete Contin. Dyn. Syst.* **27** (2010) 1511–1533.
- [14] R. Chill, E. Fašangová and J. Prüss, Convergence to steady state of solutions of the Cahn–Hilliard and Caginalp equations with dynamic boundary conditions. *Math. Nachr.* **279** (2006) 1448–1462.
- [15] K. Domelevo and P. Omnes. A finite volume method for the Laplace equation on almost arbitrary two-dimensional grids. *M2AN: M2AN* **39** (2005) 1203–1249.
- [16] S. Dong, On imposing dynamic contact-angle boundary conditions for wall-bounded liquid-gas flows. *Comput. Methods Appl. Mech. Engrg.* **247/248** (2012) 179–200.
- [17] S. Dong, An outflow boundary condition and algorithm for incompressible two-phase flows with phase field approach. *J. Comput. Phys.* **266** (2014) 47–73.
- [18] R. Eymard, T. Gallouët and R. Herbin, Finite volume methods. In *Handbook of numerical analysis*, Vol. VII. Edited by Ph. Ciarlet and J.L. Lions. North-Holland, Amsterdam (2000) 715–1022.
- [19] R. Eymard, G. Henry, R. Herbin, F. Hubert, R. Kloforn and G. Manzini, 3d benchmark on discretization schemes for anisotropic diffusion problems on general grids. In *Proc. of Finite Volumes for Complex Applications*, Vol. VI. Springer (2011) 895–930.
- [20] H.P. Fischer, P. Maass and W. Dieterich, Novel surface modes in spinodal decomposition. *Phys. Rev. Lett.* **79** (1997) 893–896.
- [21] H.P. Fischer, P. Maass and W. Dieterich, Diverging time and length scales of spinodal decomposition modes in thin films. *EPL Europhys. Lett.* **42** (1998) 49–54.
- [22] T. Goudon and S. Krell, A DDFV Scheme for Incompressible Navier–Stokes equations with variable density. In *Proc. of Finite Volumes for Complex Applications VII*, edited by J. Fuhrmann, M. Ohlberger and C. Rohde. In Vol. 77 and 78. *Springer Proceedings in Mathematics and Statistics*. Springer, Berlin, Allemagne (2014).
- [23] R. Herbin and F. Hubert, Benchmark on discretization schemes for anisotropic diffusion problems on general grids. In *Proc. of Finite Volumes for Complex Applications V*, Aussois, France. Edited by R. Eymard and J.M. Herard. Hermès (2008).
- [24] S. Hysing, S. Turek, D. Kuzmin, N. Parolini, E. Burman, S. Ganesan and L. Tobiska, Quantitative benchmark computations of two-dimensional bubble dynamics. *Int. J. Numer. Methods Fluids* **60** (2009) 1259–1288.
- [25] D. Jacqmin, Calculation of two-phase Navier–Stokes flows using phase-field modeling. *J. Comput. Phys.* **155** (1999) 96–127.
- [26] D. Jacqmin, Contact-line dynamics of a diffuse fluid interface. *J. Fluid Mech.* **402** (2000) 57–88.
- [27] D. Kay, V. Styles and R. Welford, Finite element approximation of a Cahn–Hilliard–Navier–Stokes system. *Interfaces Free Bound.* **10** (2008) 15–43.
- [28] R. Kenzler, F. Eurich, P. Maass, B. Rinn, J. Schropp, E. Bohl and W. Dieterich, Phase separation in confined geometries: Solving the Cahn–Hilliard equation with generic boundary conditions. *Comput. Phys. Commun.* **133** (2001) 139–157.
- [29] S. Krell, Stabilized DDFV schemes for Stokes problem with variable viscosity on general 2D meshes. *Numer. Methods Partial Differ. Equ.* **27** (2011) 1666–1706.
- [30] S. Krell and G. Manzini, The discrete duality finite volume method for stokes equations on three-dimensional polyhedral meshes. *SIAM J. Numer. Anal.* **50** (2012) 808–837.
- [31] C. Liu and J. Shen, A phase field model for the mixture of two incompressible fluids and its approximation by a Fourier-spectral method. *Physica D* **179** (2003) 211–228.
- [32] S. Metzger, On numerical schemes for phase-field models for electrowetting with electrolyte solutions. *Proc. Appl. Math. Mech.* **15** (2015) 715–718.
- [33] S. Minjeaud, An adaptive pressure correction method without spurious velocities for diffuse-interface models of incompressible flows. *J. Comput. Phys.* **236** (2013) 143–156.
- [34] S. Minjeaud, An unconditionally stable uncoupled scheme for a triphasic Cahn–Hilliard/Navier–Stokes model. *Numer. Methods Partial Differ. Equ.* **29** (2013) 584–618.
- [35] A. Miranville and S. Zelik, Exponential attractors for the Cahn–Hilliard equation with dynamic boundary conditions. *Math. Methods Appl. Sci.* **28** (2005) 709–735.
- [36] F. Nabet, *Schémas volumes finis pour des problèmes multiphasiques*. Ph.D. thesis, Aix-Marseille université (2014).
- [37] F. Nabet, Convergence of a finite-volume scheme for the cahn–hilliard equation with dynamic boundary conditions. *IMA J. Numer. Anal.* **36** (2015) 1898–1942.



- [38] F. Nabet, An error estimate for a finite-volume scheme for the Cahn–Hilliard equation with dynamic boundary conditions (2016). Preprint [hal-01273945](https://hal.archives-ouvertes.fr/hal-01273945) (2016).
- [39] J. Prüss, R. Racke and S. Zheng, Maximal regularity and asymptotic behavior of solutions for the Cahn–Hilliard equation with dynamic boundary conditions. *Ann. Mat. Pura Appl.* **185** (2006) 627–648.
- [40] T. Qian, X.-P. Wang and P. Sheng, A variational approach to moving contact line hydrodynamics. *J. Fluid Mech.* **564** (2006) 333.
- [41] R. Racke and S. Zheng, The Cahn–Hilliard equation with dynamic boundary conditions. *Adv. Differ. Equ.* **8** (2003) 83–110.
- [42] A.J. Salgado, A diffuse interface fractional time-stepping technique for incompressible two-phase flows with moving contact lines. *ESAIM: M2AN* **47** (2013) 743–769, 5.
- [43] J. Shen, X. Yang and H. Yu, Efficient energy stable numerical schemes for a phase field moving contact line model. *J. Comput. Phys.* **284** (2015) 617–630.
- [44] X.-P. Wang, T. Qian and P. Sheng, Moving contact line on chemically patterned surfaces. *J. Fluid Mech.* **605** (2008) 59–78.
- [45] H. Wu and S. Zheng, Convergence to equilibrium for the Cahn–Hilliard equation with dynamic boundary conditions. *J. Differ. Equ.* **204** (2004) 511–531.